Bioaugmentation with Sidestream Granular Sludge for Nitrification in Activated Sludge Wastewater Treatment: Pilot-Scale Investigation

John Andrews Carter

A Thesis

submitted in partial fulfillment of the

requirements for the degree of

Master of Science

University of Washington

2020

Committee:

H David Stensel, Chair

Mari-Karoliina H. Winkler

Program Authorized to Offer Degree:

Civil and Environmental Engineering

University of Washington

Abstract

Bioaugmentation with Sidestream Granular Sludge for Nitrification in Activated Sludge Wastewater Treatment: Pilot-Scale Investigation

John Andrews Carter

Chair of the Supervisory Committee:

H David Stensel

Department of Civil and Environmental Engineering

Stricter effluent permits and growing metropolitan areas have contributed to a move towards the intensification of biological treatment processes for water resource recovery facilities (WRRFs). Process intensification with aerobic granular sludge (AGS) has the potential to increase the treatment capacity of WRRFs and enable or increase biological nutrient removal without increasing footprint. Growth of AGS in continuous flow activated sludge (CFAS) facilities has yet to be fully realized, despite the success of AGS wastewater treatment in sequencing batch reactors (SBRs). Sidestream growth and bioaugmentation of AGS aim to take advantage of the selection pressures for growth of granular sludge in SBRs to increase the treatment and nutrient removal capacity of a CFAS system. A sidestream SBR fed acetate and anaerobic digestion

centrate diluted with final effluent was used to grow AGS enriched with ammonia oxidizing bacteria (AOB) and polyphosphate accumulating organisms (PAOs) to evaluate the effect of sidestream AGS bioaugmentation on a low solids retention time (SRT) non-nitrifying CFAS system in a pilot plant study. The CFAS system had a hydraulic separator unit for the purpose of uncoupling the SRTs of granular and flocculent sludge to enhance the impact of bioaugmentation.

The sidestream SBR was operated for a 6.5-month period at an NH_3-N loading of 0.31 ± 0.04 g/L-d, an SRT of 25-30 days, and a mixed liquor suspended solids (MLSS) concentration between 8.6 and 14.4 g/L. The sidestream NH_3-N loading averaged 21% of the mainstream NH_3-N loading, to represent a typical proportion for full-scale treatment systems with anaerobic sludge digestion. Specific nitrification rates (SNRs) varied between 1.2 and 1.4 mg NH_3-N/g VSS-hr. A low DO:NH_3-N concentration ratio of 0.06 mg/mg or less during the aeration phase resulted in suppression of nitrite oxidizing bacteria (NOB) growth and thus shortcut nitrogen removal with over 89% simultaneous nitrification/denitrification. NOB suppression was evident because of an effluent NO2-:/NO3-N ratio of greater than 1.0 and a qPCR AOB to NOB ratio of between 3 and 4. A high COD:N removed ratio of 6.0 – 7.0 resulted in PAOs to be in the granule outer aerobic layers besides the inner core to thus compete with AOBs for space and dissolved oxygen, which would limit AOB activity causing a lower SNR than expected based on prior operation with the same reactor.

The mainstream pilot was seeded with return activated sludge from a local WRRF and operated at two different time periods: Phase 1 and Phase 2. Phase 1 provided initial operating experience

for the CFAS system but was shut down for pilot plant repairs and modifications before bioaugmentation could be started.

Phase 2 lasted 56 days with 3 operating conditions: 1) 16 days for baseline flocculent sludge operation, 2) a spike of sidestream AGS and operation for 20 days, and 3) 20 days with continual sidestream bioaugmentation. After bioaugmentation the separator only captured 40-50% of the granular sludge, which limited the fraction of granules in the MLSS from 17.1 to 40.5%, the granular to floc SRT ratio to an average of 1.5, and the nitrification efficiency to increase by 20 to 30%.

Acknowledgements

I would like to express my sincere gratitude towards:

Professor Stensel and Professor Winkler for their countless guidance, patience, and the fantastic opportunity to work on this project.

Bob Bucher, Pardi Sukapanpotharam, and Eron Jacobson for their assistance, patience, and hard work in orchestrating this project.

Maxwell Armenta and Bryce Figdore for their work preceding this study.

Annie Dubner and Renjie Song for their assistance with lab work.

Bao Ngyuen Quoc for his qPCR and FISH work for this study.

The Winkler Lab for their friendliness and support in making learning and working in the lab an absolute pleasure.

This work was supported by the King County (Seattle, Washington, USA) Department of Natural Resources Wastewater Technology Evaluation Program Graduate Student Research Fellowship, the National Science Foundation (GOALI 1603707), and the Water Research Foundation (Project TIRR3C15).

Table of Contents

List of Figures

List of Tables

List of Acronyms

AGS	aerobic granular sludge
AN	anaerobic
AO	anoxic
AOB	ammonia oxidizing bacteria
BOD	biological oxygen demand (5-day)
CAS	conventional activated sludge
CFAS	continuous flow activated sludge
COD	chemical oxygen demand
DO	dissolved oxygen
EBPR	enhanced biological phosphorus removal
FISH	fluorescence in situ hybridization
GAO	glycogen accumulating organisms
HRT	hydraulic retention time
ISO	International Organization for Standardization
KC	King County
MLSS	mixed liquor suspended solids
MLVSS	mixed liquor volatile suspended solids
NDN	nitrifying and denitrifying
NOB	nitrite oxidizing bacteria
NRT	nominal retention time
PAO	polyphosphate accumulating organism

pH	negative $\log_{10}c$, where c is the hydrogen ion concentration in moles per liter
PHA	Polyhydroxyalkanoate
PVC	polyvinyl chloride
qPCR	quantitative polymerase chain reaction
RAS	return activated sludge
SBR	sequencing batch reactor
SM	Standard Methods for Examination of Water and Wastewater
SNR	specific nitrification rate
SP	South Plant
SRT	solids retention time
SVI	sludge volume index
VER	volume exchange ratio
VSS	volatile suspended solids
TIN	total inorganic nitrogen
TKN	total Kjeldahl nitrogen
TSS	total suspended solids
WPTP	West Point Treatment Plant
WRRF	water resource recovery facility

List of Units and Symbols

%	percent
°C	degrees Celsius

d	day(s)
ft	foot/feet
gal	gallon(s)
gpm	gallons per minutes
Hp	horsepower
hr	hour
in	inch(es)
L	liter(s)
m	meter(s)
min	minute(s)
rpm	rotations per minute
scfm	standard cubic feet per minute

1 Introduction and Objectives

As environmental awareness spreads, there is an increasing desire for the expansive cities we live in to exist in harmony with the earth. To bring our cities closer to environmental neutrality our waste must be effectively treated to minimize negative impact on the ecosystem. This goal has driven greater restrictions on nutrient effluent limits from water resource recovery facilities (WRRFs), to prevent eutrophication of the surrounding waters. A move towards intensification of biological wastewater treatment to provide greater treatment capacity in existing tankage without increasing footprint has led to interest and research into aerobic granular sludge (AGS). AGS has the potential to increase the capacity and biological nutrient removal capability of existing continuous flow activated sludge (CFAS) WRRFs.

The use of AGS may be able to mitigate the high cost and construction complexity associated with upgrading existing CFAS systems for nutrient removal. Many existing systems may require additional tank volume for nitrogen removal because the autotrophic bacteria required that oxidize ammonia (NH_3) to nitrite (NO_2^-) and nitrate (NO_3^-) (nitrification) are slow growers and require solid retention times (SRTs) that are 2-3 times longer than that for BOD removal. Longer SRTs require greater tank volume and associated costs which may be difficult to achieve in WRRFs that exist in well-established residential and industrial areas with limited space. Growing nitrifying AGS in sidestream treatment of anaerobic digester sludge dewatering centrate and feeding the nitrifying AGS into an existing low-SRT CFAS process could enable or increase nitrogen removal with little or no additional tank volume. The process described above is referred to as bioaugmentation and has been demonstrated at full scale for a flocculent sludge system with nitrifying bacteria grown in an aerobic sidestream reactor treating anaerobic

digestion centrate with the flocculent sludge produced fed to the mainstream activated sludge process (Bowden et al., 2016). Flocculent sludge bioaugmentation however, has provided a limited improvement in nitrification because the bioaugmented flocculent sludge has the same SRT as the CFAS system.

The physical characteristics of AGS provide a number of possible improvements for nutrient removal with activated sludge treatment. The dense spherical morphology of AGS results in a much higher settling velocity than that of flocculent sludge, and thus AGS has the potential for decoupling the SRT of bioaugmented granules and mainstream flocculent sludge. Under appropriate conditions, it is possible to separate bioaugmented AGS from the AGS/flocculent sludge mixed liquors. AGS consists of deep dense biofilms, which result in oxygen and substrate gradients from aerobic conditions at the surface to anoxic and anaerobic conditions further in the biofilm. The different redox conditions with depth allow nitrification, denitrification, and enhanced biological phosphorus removal (EBPR) to be performed within a single granule. The improved settling and thickening ability of AGS allows systems to carry a higher mixed liquor suspended solids (MLSS) concentration and thus greater treatment capacity and nutrient removal from AGS bioaugmentation.

Growth and nutrient removal by AGS with nitrification, denitrification, and EBPR by polyphosphate accumulating organisms (PAOs) (referred to as PAO-NDN granules) in a bench-scale sequencing batch reactor (SBR) was demonstrated by Figdore et al. (2018a). Additionally, short-cut nitrogen removal and EBPR were demonstrated by AGS bioaugmentation in a low SRT non-nitrifying flocculent sludge SBR from granules grown in a sidestream SBR treating digester

centrate. Short-cut nitrogen removal refers to NO_2^- being converted directly to N_2 gas, instead of being converted to NO_3^- first. The findings by Figdore et al. (2018a) confirmed the potential of bioaugmentation with decoupled SRTs. However, the simulated mainstream system was an SBR fed synthetic wastewater. Further research was needed to evaluate the feasibility of AGS bioaugmentation treating real wastewater in a CFAS system.

To-date AGS has found success in full-scale SBRs, namely Nereda®, but there is much interest in applying the technology in the more commonly used CFAS systems (Pronk et al., 2015; Kent et al., 2018). The technologies that have been applied to mainstream sludge densification, which were summarized by Kent et al. (2018), are hydrocyclones, sieves, and hydraulic designs for gravity separation. Additionally, AGS growth and treatment was demonstrated in a pilot scale aerobic-only plug-flow reactor system with a batch separator to selectively retain granules, by Sun et al. (2019). However, there has been no pilot or full-scale research into the sidestream bioaugmentation of a CFAS system.

This thesis follows a series of research work started by Bryce Figdore and continued by Maxwell Armenta aimed at developing a sidestream AGS system with nitrification bioaugmentation to a mainstream CFAS system with low SRT flocculent sludge and long SRT AGS mixed liquor. At laboratory scale Figdore (2018a) found that PAO-NDN granules, could be grown on West Point Treatment Plant (WPTP) centrate and be sustained with effective nitrification in an SBR treating synthetic wastewater. Armenta (2019) found that sidestream granule PAO-NDN growth could be sustained for over 1.5 years in a pilot plant SBR treating WPTP centrate with shortcut nitrogen

removal. The work presented in this thesis and in Armenta (2019) was supported by microbial work done by Bao Ngyuen Quoc, a UW PhD candidate.

The major objective of this research was to continue the sidestream reactor operation and investigate the ability for sidestream AGS bioaugmentation to enhance nitrification and nitrogen removal in a low SRT flocculent sludge mainstream system. The scheme of the mainstream and sidestream pilot plants is illustrated below in Figure 1-1. The mainstream pilot consisted of an anoxic reactor, two anaerobic reactors, an aerobic zone, a hydraulic upflow separator, and a secondary clarifier. The anaerobic zone functions to select for PAOs in the granules, to encourage granule growth and EBPR. The hydraulic upflow separator was intended to take advantage of the difference in settling velocities of granular and flocculent sludge, allowing for the granular sludge to settle out to the bottom and be returned to the anaerobic zone, while the flocculent sludge exits in the separator overflow to the secondary clarifier. The secondary clarifier underflow return activated sludge (RAS) is directed to the aerobic zone.

The sidestream pilot SBR functioned to grow PAO-NDN granules with anaerobic and aerobic periods to favor PAO and ammonia oxidizing bacteria (AOB) growth. Acetate was fed during the anerobic phase to foster PAO growth, and the WPTP final effluent dilution water and centrate were fed at the start of the aerobic phase to grow nitrifiers at close to mainstream temperature. The WPTP final effluent is after chlorination and dichlorination of secondary effluent from a BOD-removal only high purity oxygen activated sludge system.

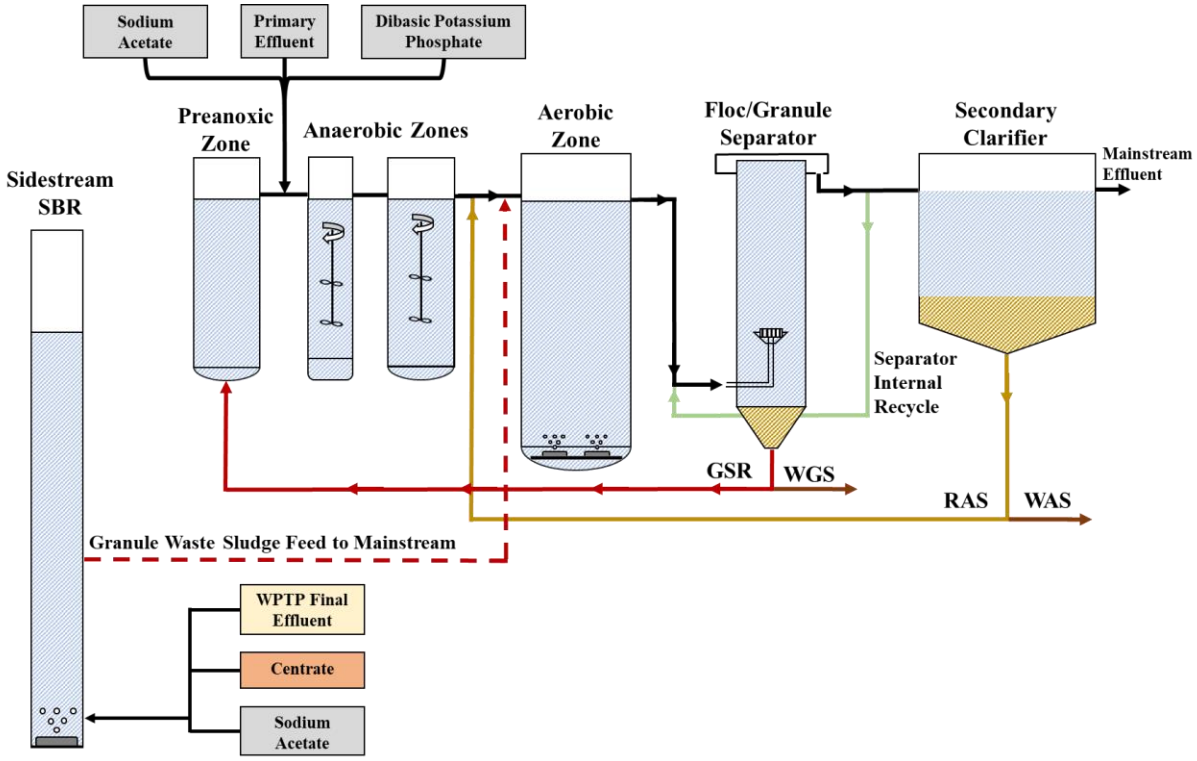

Figure 1-1. Flow scheme for the sidestream aerobic nitrifying granular sludge bioaugmentation pilot plant. Granules grown in a sequencing batch reactor (SBR) are fed into the mainstream CFAS system. Preanoxic, anaerobic, and aerobic zones precede a hydraulic separator and secondary clarifier. The separator underflow is primarily granular sludge (GSR), while the clarifier return is primarily flocculent sludge (RAS). Separate waste granular sludge (WGS) and waste activated sludge (WAS) lines allow for uncoupled SRT control.

The main goals of the sidestream pilot plant investigation were presented by Armenta (2019). However, as this investigation was concluded, the objectives for the sidestream pilot plant changed to focus on steady operation at a fixed loading and granule production for bioaugmentation. The specific goals were as follows:

1. Continue sidestream operation at an NH_3-N loading of 0.35 g/L-d and a 25-day SRT, to represent the typical proportion of plant N treated in the sidestream.
2. Maintain shortcut N removal and evaluate the COD:N ratio needed.
3. Investigate acetate utilization kinetics.

4. Continue to evaluate SNR and granule size characteristics.
5. Evaluate the microbial characteristics of the sidestream reactor granules using molecular methods.

The specific goals of the mainstream pilot plant were as follows:

1. Investigate sidestream bioaugmentation with PAO-NDN granules on a low SRT non-nitrifying continuous flow conventional activated sludge system, with selective retention of the granular sludge.
2. Determine the nitrification biokinetics of the pilot plant mainstream mixed liquor, flocculent sludge, and granular sludge.
3. Investigate the persistence and size of bioaugmented granules and the ability to grow granules in the mainstream, through examination of changes in granule total suspended solids (TSS), size distribution, and morphology.
4. Evaluate the impact of sidestream AGS bioaugmentation on the mainstream nitrification efficiency.
5. Evaluate the microbial composition and nitrifying bacteria concentration of the mainstream activated sludge flocs and granules using molecular methods.

2 Background

Mainstream and sidestream pilot operation, monitoring, and goals during this period were informed by research done by Figdore et al. (2018a, b, c) and Armenta (2019). There were three publications by Figdore et al. which drove the sidestream and mainstream pilot design and research. The first publication evaluated three different types of AGS for their bioaugmentation potential (Figdore et al., 2018b). The granules tested were, 1) nitrification only (NIT granules), 2) nitrification and denitrification with ordinary heterotrophic organisms (NDN-OHO granules), and 3) nitrification, denitrification, and enhanced biological phosphorus removal (PAO-NDN granules). The three granules were tested in lab scale SBRs fed with media emulating digester dewatering centrate and evaluated on four criteria, 1) treatment performance, 2) granule physical characteristics, 3) growth and production rates of granular mass, and 4) nitrification capacity. After each granule had undergone a thorough testing period, it was determined that the PAO-NDN granules performed the best on each criterion (Figdore et al., 2018b). However, NIT granules also showed good potential for bioaugmentation, performing similarly to the PAO-NDN granules on treatment performance and nitrification capacity. Following these results, both NIT and PAO-NDN granules were tested as bioaugmentation material at the lab-scale (Figdore et al., 2018a, c). Both tests were done in 2.5-day aerobic SRT flocculent sludge SBRs using sidestream granules grown in SBRs fed WPTP centrate. Figdore et al. (2018c) showed that NIT granules could be effectively used for bioaugmentation. Effluent NH_3-N was less than 1 mg/L for a 30-day bioaugmentation period and nitrification disappeared once the granules were removed from the system (Figdore et al., 2018c). Additionally, it was shown that the nitrifiers stayed attached to the granules, with few leeching into the flocculent sludge. After testing NIT granules, the

PAO-NDN granules were evaluated by with a 40-day bioaugmentation period. During the period, it was shown that PAO-NDN granules are effective for bioaugmentation, producing an effluent NH_3-N of 0.6 to 1.7 mg/L (Figdore et al., 2018a). Like the first test, nitrification vanished once the granules were removed and it was confirmed that most of the nitrifiers stayed on the granules with minimal nitrifiers in the flocculent sludge. As both bioaugmentation systems were successful, PAO-NDN granules were chosen to be tested on the pilot scale, due to their faster growth and ability to denitrify and remove phosphorus. The pilot scale sidestream SBR was built and operated for a 10.5-month period described by Maxwell Armenta in his master's thesis (Armenta, 2019). During this period, PAO-NDN granules were successfully grown and maintained while being fed WPTP centrate and final effluent dilution water. The sidestream SBR was operated with a high NH_3-N loading rate, 0.38 ± 0.07 g/L-d, and good NH_3-N and total inorganic nitrogen (TIN) removal performance, 95% and 85% respectively. Furthermore, sustained shortcut nitrogen removal was demonstrated.

2.1 PAO-NDN Granules

PAO-NDN granules accomplish simultaneous nitrification, denitrification, and EBPR by taking advantage of the various redox zones inherent to the granular structure. These different conditions within the biofilm are caused by diffusion limiting oxygen penetration and an anaerobic feed, allowing for a substrate rich anoxic layer (De Kreuk et al., 2007). As illustrated below on the right side of Figure 2-1, AOB and nitrite oxidizing bacteria (NOB) within the aerobic zone of the granule convert NH_3 to NO_2^- and NO_2^- to NO_3^- respectively. In the anoxic zone of the granule, PAOs and glycogen accumulating organisms (GAOs) utilize polyhydroxyalkanoate (PHA) stored within their cells to reduce NO_2^- and NO_3^- to nitrogen gas.

Both nitrification and denitrification occur during the aerobic phase, in a process referred to as simultaneous nitrification-denitrification (SND). During the anaerobic phase, illustrated on the left side of Figure 2-1, volatile fatty acids (VFAs) are fed to the system and taken up by PAOs and GAOs and turned into storage produces, like PHA. Although PAOs and GAOs can both denitrify, it is advantageous to select for PAOs to achieve EBPR and better settling granules (Winkler et al., 2011). The PAO-NDN granules used in this project were grown in the sidestream pilot SBR using a cycle compounded of an anaerobic and aerobic phase.

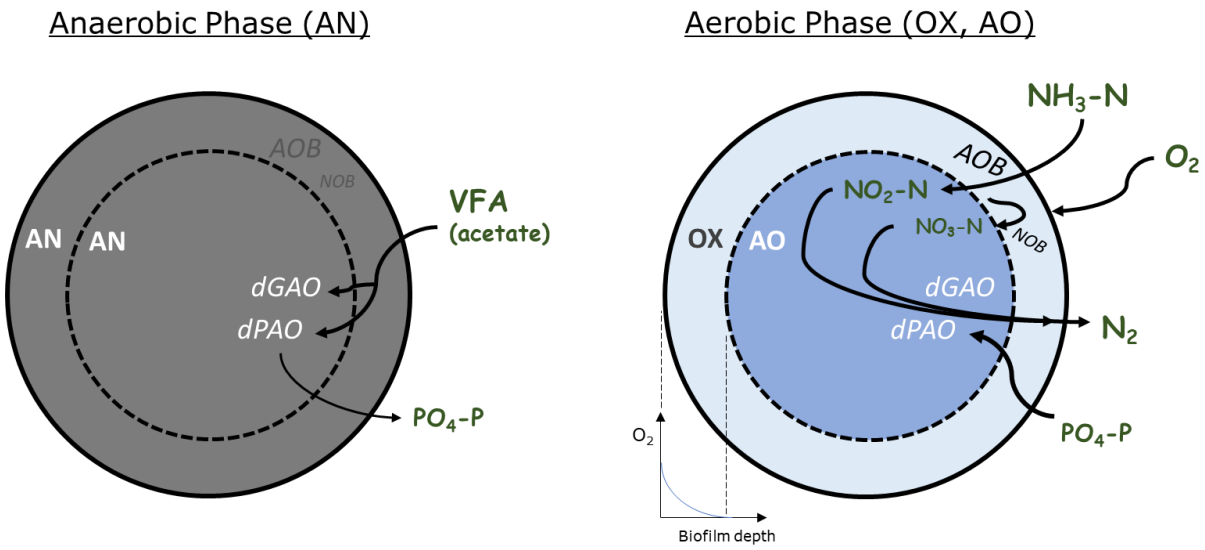

Figure 2-1. Anaerobic (AN) and aerobic (OX) phases for anaerobic COD removal, SND, and orthophosphate (PO_4^{3-}) removal by aerobic granular sludge. Diffusion resistance, DO concentration, and oxygen uptake on outer granule layers creates conditions for an anoxic (AO) zone within granules for denitrification to occur in an aerated reactor. Chemical pathways are simplified, and spatial representation of microbial populations is ideal. (Armenta, 2019)

2.2 Granule PAO and GAO Populations

PAO and GAO populations in AGS tend to be quite diverse, however Candidatus Accumulibacter phosphatis (*Accumulibacter*) and *Dechloromonas* tend to be the best documented PAOs, while Candidatus Competibacter phosphatis (*Competibacter*) is the best

documented GAO (Oehmen et al., 2010). *Dechloromonas*-related organisms have been shown to exhibit characteristics of PAOs (Zong et al., 2007) and GAOs (Ahn et al., 2007). However, *Dechloromonas* is usually referred to as a PAO. *Accumulibacter* is known to have two distinct types (type I and type II), which contain clades IA-IC and clades IIA-IIF, respectively (Nielsen et al., 2019; He et al., 2007). Additionally, *Competibacter* contains sub-groups 1-7 (Oehmen et al., 2010). Oehmen et al. (2010) detailed the denitrification capacity of the different types of *Accumulibacter* and sub-groups of *Competibacter*. However, later research illustrated the likely sub-clade diversity of PAOs (Section 2.4).

Microbial characterization of PAO-NDN granules by Figdore et al. (2018a, b) and Armenta (2019) revealed that *Accumulibacter*, *Dechloromonas*, and *Competibacter* were the dominant PAOs and GAOs. The first bench scale SBR tests by Figdore et al. (2018b) found that *Dechloromonas* was dominant, with an abundance of 28%. Secondly, Figdore et al., (2018a) discovered *Accumlibacter* and *Competibacter* to be the dominant PAO and GAO, respectively, with relative abundances of greater than 10% each. Armenta (2019) found that *Accumlibacter* and *Dechloromonas* were dominant in the sidestream SBR used to grow PAO-NDN granules for bioaugmentation in September 2018, with a combined relative abundance greater than 20%.

2.3 Granule Nitrifier Populations

Nitrification in municipal WRRFs is primarily conducted by AOBs and NOBs. AOB populations are predominantly reported in WRRFs as being from the *Nitrosomonas* and *Nitrosospira* genus. Between the two, *Nitrosospira* are generally reported to be more abundant. However, *Nitrosomonas* has been reported as more abundant in PAO-NDN granules by both Figdore

(2018b) and Armenta (2019), with relative abundances of greater than 99% and 65%, respectively.

Among NOB populations, *Nitrobacter* and *Nitrospira* are the most reported genera in municipal WRRFs. *Nitrotoga* was reported to be the dominant NOB genus in PAO-NDN granules by Fidgore (2018b), although only at a relative abundance of 0.4%. NOB genera tend to be much more diverse than AOB in municipal WRRFs. Contrary to the findings by Figdore et al (2018b), Armenta (2019) found that *Nitrospira* were the most dominant NOB genus in the PAO-NDN sidestream SBR pilot, with over 80% relative abundance.

2.4 Denitrifying Polyphosphate and Glycogen Accumulating Organisms

Although PAOs have been historically used in anaerobic-aerobic systems, to utilize O_2 as the primary electron acceptor, both PAOs and GAOs have been shown to contain groups capable of reducing NO_3^- and NO_2^- to oxidize PHA. The groups capable of denitrification are termed denitrifying polyphosphate accumulating organisms (dPAOs) and denitrifying glycogen accumulating organisms (dGAOs). Meinhold et al. (1999) showed that there were two unique groups of PAOs, dPAOs and non-denitrifying PAOs. Furthermore, Zeng et al. (2003) demonstrated the existence of dGAOs and their ability to anoxically reduce NO_3^- and NO_2^-. *Accumlibacter* clade I was documented to denitrify with NO_3^- by both Oehmen et al. (2010) and Flowers et al. (2009). Additionally, both studies determined that *Accumlibacter* clade II could not denitrify with NO_3^-. Furthermore, Flowers et al. (2009) found that *Accumlibacter* clade II contained genes enabling NO_2^- reduction. These results were supported by Lanham et al. (2011), who found that *Accumlibacter* clade I could reduce NO_3^- and NO_2^-. On the contrary,

Accumlibacter clades I, IA, IC, IIC, and IIF were reported to be unable to reduce NO_3^-, instead relying on NO_3^- reducers, like *Dechloromonas* and *Competibacter*, to provide NO_2^- (Kim et al., 2013; Rubio-Rincón et al., 2017; Saad et al., 2016).

2.5 Simultaneous Nitrification and Denitrification

SND has proven to be effective within flocculent sludge (Munch et al., 1996), biofilm (Helmer and Kunst, 1998), granular sludge (De Kreuk et al., 2005), and hybrid reactors (Jianlong et al., 2008). All these systems rely upon DO concentration gradients resulting from biomass diffusion limitations to create aerobic and anoxic zones in the biomass for nitrification and denitrification, respectively (Figure 2-1). These conditions are achieved in flocculent sludge by the optimization of three parameters, 1) bulk liquid DO, 2) floc size, and 3) readily biodegradable COD (rbCOD) addition (Pochana and Keller, 1999). Munch et al. (1996) showed that nitrification rate increased with greater DO, while denitrification rate decreased, in anaerobic-aerobic bench-scale SBRs. Within their reactors, a DO concentration of 0.5 mg/L led to equal nitrification and denitrification rates, allowing for complete SND. The low DO concentrations necessary for SND in a flocculent sludge provide opportunities for operation cost savings. Bertanza (1997) described upgrading existing WRRFs to conduct up to 90% N removal, without adding anoxic zones, by using DO and ORP measurements to actively control aeration. Because of the dispersed structure of flocculent sludge, active DO control has proved useful to ensure adequate anoxic volume for SND. Zhao et al. (1999) utilized a two-stage process, an anaerobic zone followed by an intermittent aeration zone, to achieve SND efficiencies of up to 50% by maintaining a low DO (less than 0.6 mg/L) with ORP control. Additionally, Guo et al. (2009) showed up to 45% SND with DO concentrations between 0.4 and 0.8 mg/L in a lab-scale SBR.

SND within aerobic granules is fundamentally the same as for flocculent sludge, but granule size and density increase oxygen diffusion limitation and provide more anoxic volume at higher DO concentrations when compared with flocculent sludge. AGS is generally grown in SBRs, allowing for anaerobic feeding to favor PAOs and GAOs. De Kruek et al. (2005) showed up to 94% N removal efficiency at a DO of 1.8 mg/L, resulting from dPAO populations inside the granules. They also illustrated the reliance of SND efficiency on bulk liquid DO concentration, detailing 35% and 56% N removal efficiency at concentrations of 9.1 and 3.6 mgDO/L, respectively. This result was supported by Bassin et al. (2012), who maintained greater than 80% N removal at bulk liquid DO concentrations of less than 2.0 mg/L. Bassin et al., however, observed that dGAO were primarily responsible for the reduction of NO_3^- to NO_2^-. To try to optimize cost, Yuan and Gao (2010) suggested a DO concentration of 2.5 mg/L was optimal for aerobic granular sludge SBRs, based on reaction duration and aeration and mixing costs. Overall, the dense biofilm structure of aerobic granules allows for SND to occur with higher DO concentration than with flocculent sludge, which allows for increased nitrification rates.

2.6 Exogenous Carbon used for Denitrification

To achieve full N removal, many biological nitrogen removal WRRFs must add supplemental carbon to their influent wastewaters to reach the COD:N ratio necessary for denitrification. The carbon consumed per NO_x removed ratio is dependent on the oxygen equivalent of the species reduced and the synthesis yield achieved with the carbon source (Tchobanoglous et al., 2014b). Because of the favorability of using O_2 as an electron acceptor, NO_2^-/NO_3^- are only utilized in anoxic conditions. The oxygen equivalent of NO_3^- is greater than that of NO_2^-, which are 2.86 and 1.71 g O_2/g NO_x^--N removed, respectively (Tchobanoglous et al., 2014b; Bowden et al.,

2016). This means that the carbon consumption ratio is 40% lower for NO_2^- than NO_3^-. The COD consumption ratio can be estimated with Equation 2-1.

$$COD_{CR} = \frac{OEq}{1 - 1.42 \cdot Y_H} \quad (2\text{-}1)$$

where: COD_{CR} = COD consumption ratio, g COD-used/g NO_X-N-removed

OEq = oxygen equivalent, 2.86 g O_2/g NO_3^--N or 1.71 g O_2/g NO_2^--N-removed

Y_H = synthesis yield, g VSS/ g COD

The above model is difficult to utilize to estimate the COD:N in the sidestream or the mainstream pilot because it only pertains to the immediate uptake of a COD source and the denitrifying synthesis yield. The effective yield is lower due to the long SRT and SND aeration time, with carbon released due to endogenous decay. Furthermore, the COD fed is not directly used for cell synthesis and denitrification, instead, COD is anaerobically converted to PHA for storage by PAOs and GAOs. Krasnits et al. (2013) detailed that greater than 80% of fed acetate COD was converted to PHA in GAOs and PAOs, accounting for glycogen used in substrate uptake. Thus, a reduced amount of COD fed is available for usage in synthesis and denitrification.

2.7 Shortcut Nitrogen Removal

Shortcut nitrogen removal, or denitrification using NO_2^- instead of NO_3^-, offers significant operations cost savings, by reducing the carbon and oxygen required for N removal by up to 40% and 25%, respectively (Bowden et al., 2016). AOB activity combined with NOB suppression

drives shortcut nitrogen removal, by stopping the oxidation of NO_2^- to NO_3^- and allowing for full nitritation and denitritation.

2.7.1 Repression of NOB in Flocculent Sludge

Bowden et al. (2016) summarized four flocculent sludge NOB inhibition strategies, 1) selective NOB washout using temperature and SRT control, 2) low DO concentration, 3) intermittent aeration, and 4) free ammonia (FA) and free nitrous acid (FNA) concentration. An SRT of less than 2-3 days at a temperature above 20°C is reported to cause selective washout. Furthermore, low DO or intermittent aeration at DO concentrations between 0.3 and 2.0 mg/L cause inhibition of NOB (Bowden et al., 2016). AOB and NOB are both inhibited by high FA and FNA concentrations, AOB inhibition has been reported at 7.0 mg/L FA and 0.065 to 0.83 mg/L FNA (Tchobanoglous et al., 2014a; Anthonsien et al., 1976) while NOB inhibition has been reported at 0.04 to 50 mg/L FA and 0.01 to 1.0 mg/L FNA (Blackburne et al., 2007). Blackburne et al. (2007) reported inhibition of *Nitrospira* and *Nitrobacter* NOBs at 0.04 to 0.08 mg/L FA and about 50 mg/L FA, respectively. However, Tchobanoglous et al., (2014a) summarized inhibition of NOB in the range of 0.1 to 8.9 mg/L FA. The large range in FA inhibition concentrations for AOB and NOB points to FA inhibition concentration as being species dependent. Both AOB and NOB have been shown to acclimate to higher FA concentrations when exposed to long term high concentrations (Tchobanoglous et al., 2014a; Kouba et al., 2014).

2.7.2 Repression of NOB in Granular Sludge

The low SRT for selective NOB washout is difficult to apply to AGS reactors, which generally require an SRT of 10 to 50 days. Instead, the stratification of AOB and NOB in granules is relied

on to suppress NOB activity by limiting oxygen penetration depth. Stratification is created using high residual ammonia concentrations to favor AOB growth on the outer layer of the granule. Once established, AOB on the granule surface will consume most of the oxygen, repressing NOBs located in the inner granule layers (Poot et al., 2016). These granule characteristics allow for the usage of reactor DO:NH_3-N ratio to suppress NOB activity. Conceptually, a lower DO:NH_3-N corresponds to greater NOB inhibition. NOB inhibitions based on various DO:NH_3-N ratios in airlift granular sludge lab reactors are outlined in Table 2-1.

Table 2-1. Lab-scale studies of NOB suppression using DO:NH_3-N ratio, with airlift granular sludge reactors.

DO, mgO_2/L	Effluent NH_3-N, mgN/L	Temp, °C	DO:NH_3-N Ratio, mgO_2/mgN	NH_3-N to NO_2-N, %	NH_3-N to NO_3-N, %	NOB Inhibition, %	Reference
7	20	30	0.35	1	98		Bartrolí et al., 2010
5-7	20-40	30	0.17-0.25	96-98	1		Bartrolí et al., 2010
1	40	12.5	0.05			100	Isanta et al., 2015
1-2	40	10	0.04			100	Reino et al., 2016
2.0-3.6	0.8-1.8	20	2-2.5			55-60	Poot et al., 2016*
2.7	27	20	0.1			80	Poot et al., 2016*
2.9	7	20	0.41			97	Soler-Jofra et al., 2019**
2.4	19	15	0.13			90	Soler-Jofra et al., 2019**

*DO:NH_3-N ratio and NOB inhibition are estimates based on influent, effluent, and specific rates given.

**Batch tests using granular sludge to evaluate DO:NH_3-N ratio for NOB inhibition

Variations of NOB inhibition at similar conditions implies that the DO:NH_3-N ratio isn't the only important factor to consider for NOB inhibition in granular sludge. Kent et al. (2019) suggested that FA concentration and DO limitation in combination with AOB and NOB stratification must be considered for complete NOB suppression. Furthermore, they observed that NOB inhibition

from FA concentration was most effective with smaller granules, while bulk liquid DO concentration and nitrifier stratification was more crucial with larger diameter granules.

2.8 Mainstream Systems with Granular Activated Sludge

2.8.1 Full-Scale Sequencing Batch Reactors with Activated Granular Sludge

Nereda® AGS SBRs have found success treating domestic sewage since 2009, the first full-scale installation operations data was documented in 2013 with a MLSS and a sludge volume index (SVI_5) in the range of 8 g/L and 45 mL/g, respectively (Pronk et al., 2015). Furthermore, the SBR was reported to easily reach effluent requirements of 7 mgN/L and 1 mgP/L in summer and winter conditions. Pronk et al. (2015) also showed a significant degree of granulation, with 80% and 60% of the biomass greater than 0.2 and 1.0 mm, respectively. Li et al., (2014b) also reported the effective startup and operation of a full-scale AGS SBR, which obtained an average SVI_{30} and granule diameter of 47.1 mL/g and 0.5 mm, respectively. Effective ammonia removal of about 96% was achieved, although the TN removal efficiency was about 60%. AGS has proved to be effective for reducing footprint and energy costs, while maintaining effective COD and nutrient removal using SBRs (Pronk et al., 2015; Li et al., 2014b). However, SBRs can be difficult to install because flow equalization tanks are needed to maintain consistent flow to a batch process.

2.8.2 Continuous Flow Applications of Activated Granular Sludge

Despite the success of AGS in SBR processes, it has been complicated to apply the technology to continuous flow systems. Continuous flow systems provide three general benefits over SBR processes, as summarized by Kent et al. (2018), 1) ease of operation, 2) treatment volume and

consistency, and 3) current infrastructure. Airlift reactors, hydraulic separators (both internal and external), bubble columns, baffles, sieves, and other selection pressure strategies have been tested to cultivate continuous flow aerobic granules (Table 2-2). Bubble columns and airlift reactors have been favored in continuous flow granulation research because of their similarities to SBRs in shape. Using these technologies, average granule diameters up to 3 mm have been achieved. However, their similarities to SBRs in shape make them more difficult to apply to the CFAS systems commonly used. Sajjad et al. (2016) used an SBR to grow granules, so that they could be seeded into an MBR pilot facility. After seeding with granules there was a decrease in membrane fouling and an improvement in particle size and SVI_5, from 200 to 625 µm and 145 to 45 mL/g, respectively. Wei et al. (2019) documented between 0.5 to 80.2 percent granules in the MLSS of 17 CFAS treatment facilities. They also detailed a correlation between high percent granules and the treatment plants resemblance to a plug-flow system with a high F/M ratio, with the usage of two or more anaerobic selector stages. The granules observed were mostly small, with diameters between 212 and 600 µm. Sun et al. (2019) tested a pilot-scale plug-flow reactor with in-line separators for selective granule retention and achieved an average granule diameter of 3.4 mm within 90 days of operation. Furthermore, Downing et al. (2017) documented granulation (average diameters between 0.30 and 0.75 mm) in a full-scale CFAS system using a selector with a plug-flow conditions allowing for a high F/M in the selector, relative to the rest of the process. Although a full-scale AGS continuous flow system has yet to be realized, various selection strategies have been researched, documenting the levels of success of numerous novel designs to create mainstream continuous flow granulation.

Table 2-2. Summary of reported continuous flow aerobic granular sludge cultivation strategies and time spans for granule formation. The stable phase is defined as the period after granule formation where structure and performance were maintained. (Adapted from Kent et al., 2018)

Granulation Strategy	Reactor Type	Reactor Liquid Volume (L)	Formation / acclimation phase (days)	Stable phase (days)	Inoculum/ diameter (mm)	Average Granule Diameter (mm)	SRT (day)	Loading Rate (gCOD or N /L-d)	DO (mg/L)	Temperature (°C)	HRT (hr)	Reference
Adjustable baffles for settling large particles	Modified oxidation ditch	60	13	107	Anaerobic & aerobic sludge / < 0.05	0.6	-	0.53 - 1.1	-	18 - 30	3	Li et al., 2014
Size-based selection pressure with sieve	Bubble column	7.5	7	48	Activated sludge	1.0 - 3.0	-	1.07	3.0 - 6.0	20	9	Liu et al., 2014
Reactor with novel settling tank; stepwise reduction in settling time	Bubble column system	6, 9	16	180	P-removal / 0.98	0.93	—	1.2 [I]	2.0 - 5.0 [II]	22	6 [I]	Li et al., 2016
Three-phase separator; hydrodynamic shear force	ALR	—	11	36	Activated sludge	0.51	—	1.2 - 1.8	5.8 - 7.6	20	1.8 - 2.0	Zhou et al., 2014
N/A [III]	ALR	5	—	23	—	1.5 - 2.6	—	—	4	—	—	Yulianto et al., 2017
ALR with settling tank; MBR with sieve	ALR + MBR system	29, 24	30	45	Aerobic granules / 1.0 - 6.0	0.1 - 1.0	—	0.18 - 0.74	2.0 - 3.0	20	13	Liu et al., 2012
Three-phase separator + external separator; temporary inorganic carriers provide nucleation sites for biomass attachment	ALR	112	—	300	Nitrifying granules [IV]	0.7 - 0.9	—	0.75 - 6.1	5 - 7	30	—	Bartrolí et al., 2010
Internal settling tank	Upflow reactor	10	—	70	Aerobic granules	—	—	3.1 - 5.6	—	—	10	Bumbac et al., 2015
Inclined tube settler + external settling tank	Upflow reactor	12, 12	18	—	Activated sludge + aerobic granules	1.2	—	6	—	10 - 20	4	Long et al., 2015

Table 2-2. (continued)

Two-zone sedimentation tank + micropowder with metal ions	CFR	27	61	94	Activated sludge	0.1	—	0.11 - 0.21	—	20-30	18	Zou et al., 2018
Mixed sedimentation tank for selective wasting	CFR	65	—	—	Activated sludge	0.1 - 0.2	18	1.3 - 1.5	1.5 - 2.5	20	6	Devlin et al., 2018
Settling zone; gradually reducing HRT to increase EPSs	Aerated CSTR	1.5	—	145	Nitritation granules / 0.9	1.2	33 - 56	1.5 - 3.3	0.8 - 1.5	28	0.9 - 2	Qian et al., 2017
Two external separators + feast-famine conditions	PFR	128	51	69	Activated sludge	3.4	4	1.2	>3	10 - 22.5	6.5	Sun et al., 2019
Hydraulically-induced biomass collisions and filamentous entanglement [V]	CMAS	Lab	21	70	Sludge from secondary clarifier	0.18 - 1.25	18	1.35	4.2	25 - 27	8	Chen et al., 2015
Internal settling tank; intermittent inoculation from SBR [VI]	MBR	14000	40	80	Aerobic granules	0.625	—	0.6 - 1.2	—	—	8	Sajjad et al., 2016
Feast-famine conditions	CFR	— [VII]	—	—	Activated sludge	0.30 - 0.75	—	0.002	—	—	—	Downing et al., 2017

[I] Based on combined HRT from both aerobic and anaerobic tanks

[II] Corresponding only to the aerobic tank in the system

[III] It is not clear whether a means for selection pressure is present or not.

[IV] Biofilm was grown around activated carbon carriers, then the carriers were removed, leading seeded granules

[V] Lack of or insufficient means for selection pressure

[VI] Data only from stage II or the experiment, where intermittent seeding from an SBR occurred

[VII] Full scale facility with capacity of 164 mgd

ALR, airlift reactor, CFR, continuous flow reactor, CMAS, completed mixed activated sludge, MBR, membrane bioreactor, PFR, plug-flow reactor

3 Methods

3.1 Sidestream Reactor Description

The sidestream SBR (Figure 3-1) had a volume of 176 L and was a 10-ft tall, 12-in diameter tinted schedule 40 PVC tube. The main steps in the SBR operation were mixed anaerobic with acetate addition, aeration with centrate and dilution water feeding, settling, and decanting. Supplemental information regarding the fabrication of the pilot plant is given in Appendix A.

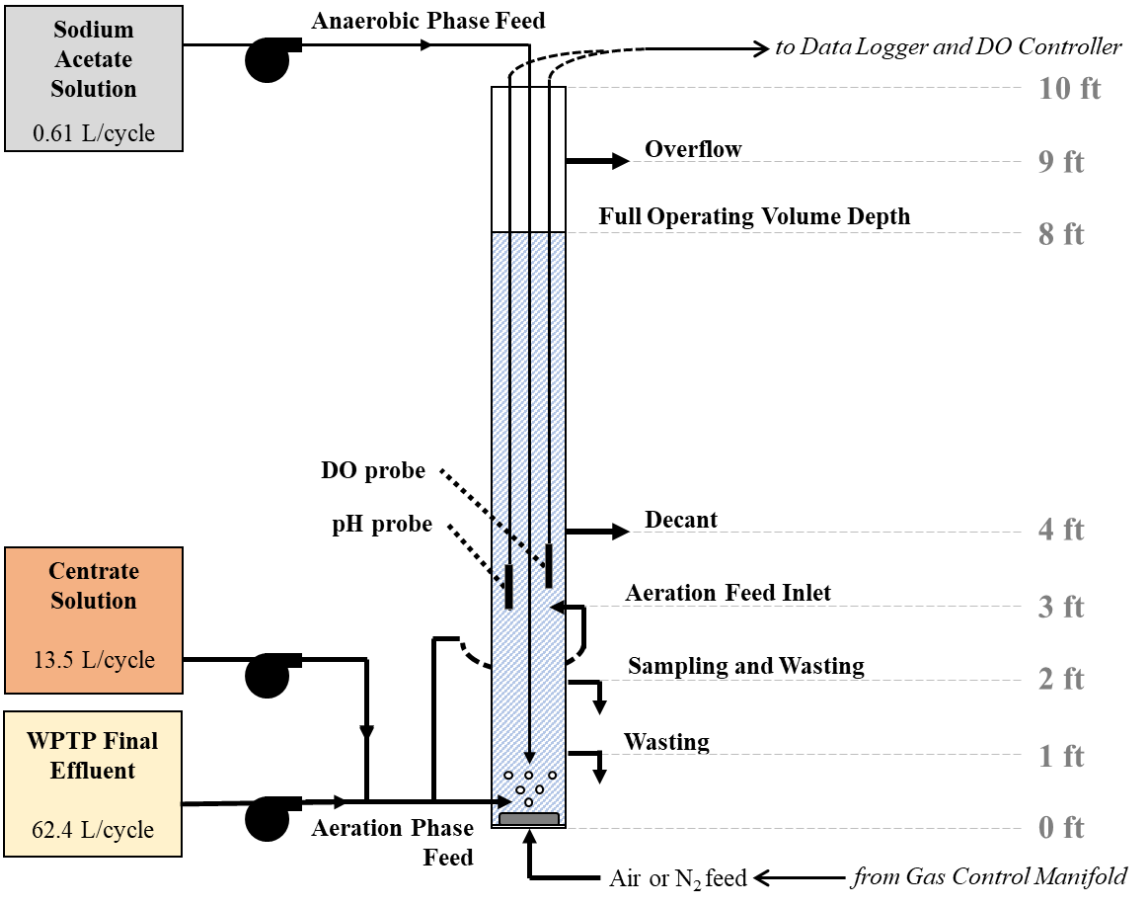

Figure 3-1. Sidestream sequencing batch reactor including 1) feed sources and volumes fed per cycle, 2) DO and pH probes, and 3) decant, sampling, and sludge working depth. (Adapted from Armenta, 2019)

As shown in Figure 3-1, the reactor overflow was located 9 ft above the bottom of the reactor. The reactor full liquid level operating volume (176 L) was controlled by a float switch at a height of 8 ft. When the float switch was triggered, it shut off the WPTP final effluent feed pump. The decant line was located at a depth of 4 ft so that half of the reactor volume (88 L) was discharged each cycle, setting the volume exchange ratio (VER) at 0.5. The decant drained by gravity through a line with a solenoid valve that was actuated to control the discharge time. Reactor sampling and sludge wasting were normally from the 2 ft tap, but wasting was sometimes done at the 1 ft tap to try to waste larger granules. Aeration feed was through two taps simultaneously, using the tap at 3 ft and a tap below the 1 ft wasting tap. The sodium acetate COD feed line was discharged at 1 ft above the bottom of the reactor. The DO and pH probes and the COD feed line were mounted to a Unistrut™ channel at the top of the reactor. A 9-in diameter Environmental Dynamics International (EDI) FlexAir™ membrane disc diffuser was mounted in the center of the bottom of the reactor. The diffuser orientation and layout are illustrated in Figure 3-2 (Environmental Dynamics International, Columbia, Missouri, USA).

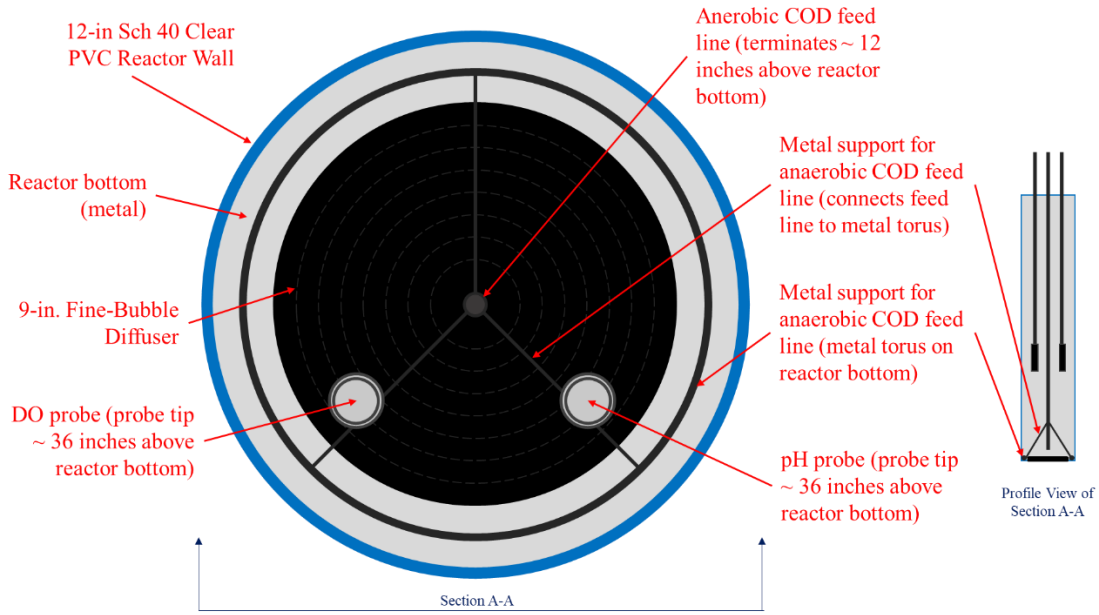

Figure 3-2. Sketch of fine bubble membrane diffuser and the relative orientation of the DO and pH probes and the COD feed line. (Adapted from Armenta, 2019)

3.1.1 Sidestream Reactor Feed System

The sidestream reactor received three feed solutions, 1) a sodium acetate feed to provide COD for PAO uptake and growth, 2) a screened anaerobic digestion dewatering centrate diluted with tap water to control NH_3-N concentration and loading, and 3) WPTP final effluent dilution water to produce a temperature closer to the mainstream. During mainstream operation, the WPTP effluent to centrate feed volume ratio was approximately 4.6. The typical cycle feed volumes were 610 mL for the sodium acetate solution, 13.6 L for the diluted centrate, and 62.4 L for the WPTP effluent. These feed solutions were supplied through a combination of flexible plastic and stainless-steel tubing by three separate Masterflex® L/S® Series peristaltic pumps (Cole-Parmer® Instrument Company, Vernon Hills, Illinois, USA). The peristaltic pumps were calibrated periodically, and the Masterflex® peristaltic tubing was replaced when necessary.

All the feed solutions were batched and managed by KC staff. The sodium acetate solution was batched every one-to-four days in a 5-gal plastic container, by dissolving $NaC_2H_3O_2$ into tap water. To prevent biofilm growth, multiple 5-gal containers were used and periodically swapped out so that the container not in use could be held at a 1-4-day contact time with a sodium hypochlorite solution. The soak solution was prepared by pouring approximately one liter of bleach into the 5-gal container and filling with tap water. The pH of the solution was between 8.5 and 9.

The centrate feed solution was batched every 1 to 7 days. The centrate was carried from the WPTP dewatering building to the pilot area and allowed to settle for 10 to 60 min and then screened using a 425µm sieve, before being added to the 100-gal plastic feed tank. Tap water was added to the feed tank to dilute the centrate to the desired NH_3-N concentration. The centrate feed tank was mechanically mixed for 1 min after batch feeding. The centrate feed tank was periodically drained and cleaned to prevent high solids accumulation at the bottom.

The WPTP final effluent dilution water was available from a plant reuse water line in the pilot plant building. The water was pumped to the sidestream reactor from a tap at the bottom of a 100-gal plastic tank. The tank was fed at the top from a valve in the water line that was controlled by a float switch to maintain the tank liquid level. The float switch closed the valve when the liquid level returned to the 100-gal volume. Similar to the centrate feed tank, the WPTP effluent feed tank was cleaned periodically to control biofilm growth.

3.1.2 Sidestream Reactor Aeration, Anaerobic Mixing, and DO Control

Nitrogen gas for mixing in the anaerobic phase and air for the aeration phase were provided through the diffuser at the bottom of the SBR and regulated by a gas control manifold. The manifold consisted of pressure regulators followed by Gilmont™ glass float rotameters (Vernon Hills, Illinois, USA). The rotameters have a flow rate capacity of 86.95 L/min at standard conditions (1.0 atm and 70°F, or 21.1°C). The anaerobic N_2 and baseline aeration mixing intensity is described below in Table 3-1. Additional aeration was regulated to maintain the DO setpoint.

Table 3-1. Anaerobic N_2 mixing and baseline air mixing rates, sparge rates, and gas superficial upflow velocities.

Mixing Type	SBR Phase	Flow Rate (L/min)	Sparge Rate (scfm/ft^2)	Superficial Upflow Velocity (m/hr)
N_2	Anaerobic	7.8	3.3	6.4
Baseline Air	Aerobic	4-6	1.7-2.5	3.3-4.9

As previously mentioned, additional aeration was provided intermittently to maintain the DO setpoint. This was done through PID control using a Moore Controller (Moore Industries, North Hills, California, USA) until September 23, 2019 and then using a Hach® sc1000 module for the remainder of the project (Loveland, Colorado, USA). Both controllers utilized 60-sec-moving-average DO from the in-situ probes as the bulk liquid DO concentration. The aeration rate was changed in proportion to the bulk liquid DO concentration and the DO concentration setpoint.

3.2 Mainstream Reactor Description

The mainstream pilot plant (Figure 3-3) consists of a 1) preanoxic tank that receives return sludge from the separator underflow, 2) two anaerobic tanks with the first receiving the primary effluent feed and the preanoxic overflow, 3) an aeration tank, 4) a hydraulic upflow separator with overflow to the secondary clarifier and underflow return sludge to the preanoxic tank, and 5) a secondary clarifier with return activated sludge (RAS) to the aeration tank. The RAS line had a tap for sludge wasting for SRT control. The RAS line was intended to go to the aerobic tank, but it could also be directed to the first anaerobic tank. The volumes and HRTs of the reactors at an influent flow of 1.5 gpm are shown in Table 3-2.

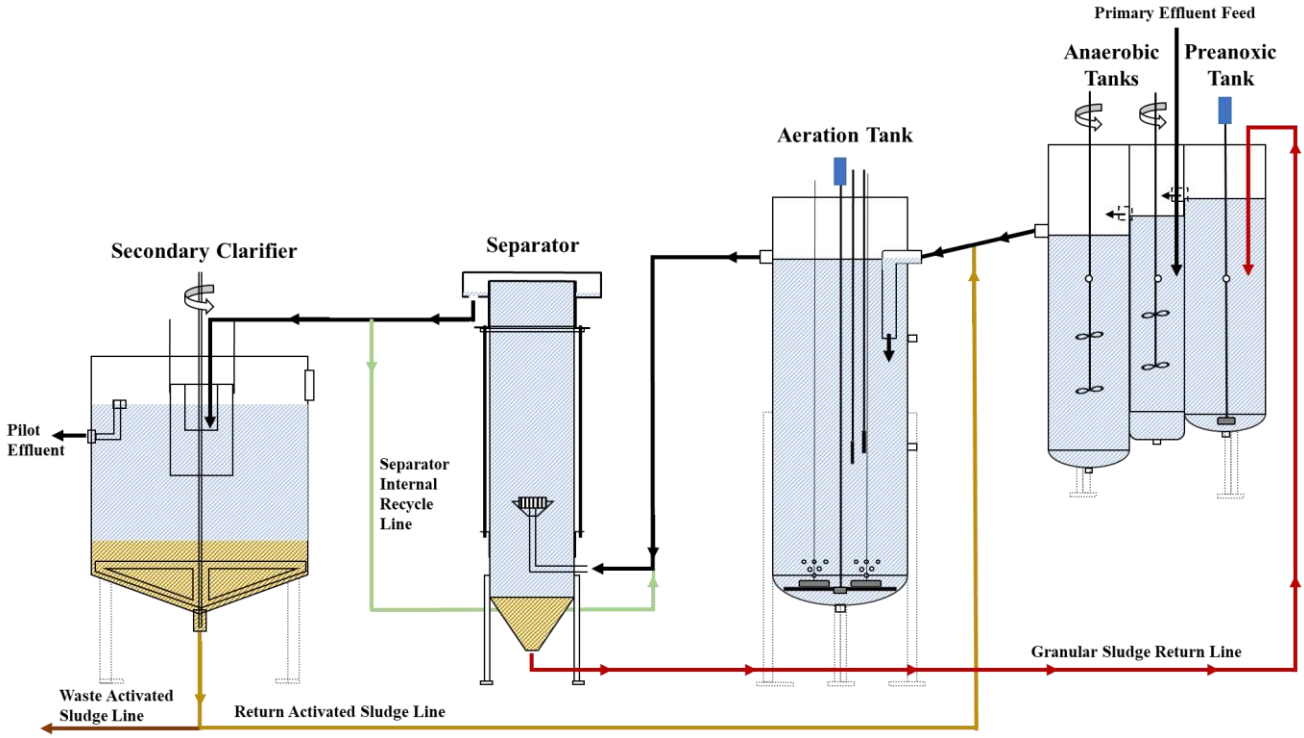

Figure 3-3. Sketch of mainstream pilot system, illustrating influent, effluent, and the internal flow scheme. From left to right, the preanoxic, anaerobic 1, anaerobic 2, and aeration reactors, the granular separator, and the secondary clarifier.

Table 3-2. Mainstream tank volume and hydraulic retention time (HRT). The HRT of the preanoxic tank is based on a separator RAS rate of 0.75 gpm, while the anaerobic 1, 2, and aerobic HRTs are based on a primary effluent flow of 1.5 gpm.

Tank	Volume	HRT	
	gal	hrs	min
Preanoxic	52	1.16	
Anaerobic 1	24		16.0
Anaerobic 2	52		34.7
Aeration	214	2.38	

3.2.1 Preanoxic/Anaerobic/Anaerobic Reactor Description

The preanoxic and the two anaerobic tanks were built in tandem using a stainless-steel frame across the tops of the reactors (Figure 3-4). The three reactors were built from schedule 10s stainless-steel pipe, and had diameters of 18 in, 12.75 in, and 18 in, respectively. The preanoxic tank was mixed using a Pulsair Systems big bubble Drum-Stick® diffuser (Kirkland, Washington, USA). The ORP probe and the Pulsair mixer were mounted to a section of Unistrut™ channel at the top of the preanoxic reactor. The Hach® P/N DRS5 ORP probe data was logged using a Hach® sc1000 module until November 6, 2019, and then a Hach sc1500 controller for the remainder of the project (Loveland, Colorado, USA). The Pulsair mixer was located approximately 2 in from the bottom of the reactor and activated one out of every ten minutes. The preanoxic tank was fed through a 1-in PVC pipe at 0.5-0.75 gpm, using a Keco Pumps Rotho® peristaltic pump (San Diego, California, USA). The Pulsair mixer, probe, and feed lines of the preanoxic tank and first anaerobic tank are also illustrated in Figure 3-4.

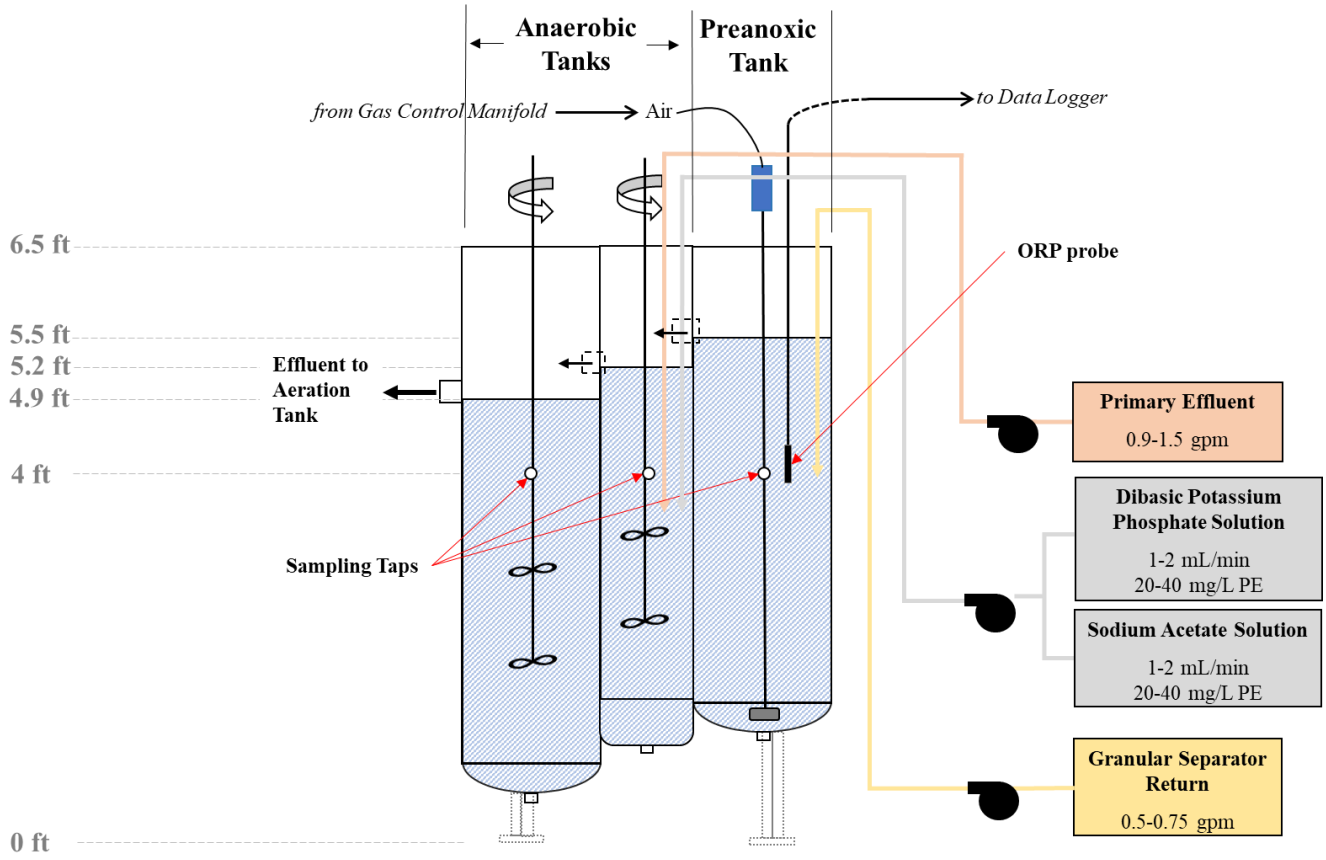

Figure 3-4. Schematic of the preanoxic and anaerobic reactor tanks, mixing equipment, and feed sources. The concentrations displayed for the sodium acetate and dibasic potassium phosphate are shown as mg per liter of primary effluent.

The preanoxic tank had a liquid level of 5.5 ft and the granular separator return sludge line inlet was 18 in below the liquid level. The ORP probe was also at the 18-in depth. The sampling taps for the anoxic and two anaerobic tanks, were located at liquid depths of 18 in, 14 in, and 9 in, respectively. All the tanks had a bottom tap for draining.

Primary effluent was fed to the first anaerobic reactor at 1.5 gpm during the initial operation using a SoloTech ST23® peristaltic pump made by Graco (Minneapolis, Minnesota, USA). The feed rate was monitored using a magnetic flowmeter made by Krohne (Frankfort, Illinois, USA).

The phosphate and acetate feed solutions were pumped at between 1 and 2 mL/min using a Masterflex® L/S® Series peristaltic pump (Cole-Parmer® Instrument Company, Vernon Hills, Illinois, USA). These two feed solutions were used to provide a more typical municipal wastewater strength by offsetting the more dilute wastewater due to wet weather higher flow conditions at the WRRF. The sodium acetate solution and dibasic potassium phosphate solution were batched every one-to-seven days by KC staff in 5-gal plastic containers, by dissolving $NaC_2H_3O_2$ or K_2HPO_4, respectively, into tap water. The used 5-gal containers were periodically swapped out so that each container could be cleaned with a 1-4-day sodium hypochlorite solution soak.

Both anaerobic reactors were mechanically mixed using Indco Inc. HS-VS Gear Clamp Mixers® (New Albany, Indiana, USA). As their title implies, the mixers were clamped onto the top edge of each reactor and the mixer shafts were tilted into the reactors. Each mixer was equipped with two 5-inch hydrofoil propellers, with the lower one at the end of the shaft and the second one 12 inches above that (Figure 3-4). The two differences between the mixers in the first and second anaerobic tanks were the mixer shaft length and the mixing frequency. The mixer shaft going into the second reactor is longer, at 66 in, compared to 61 in the first anaerobic reactor, to account for the difference in liquid level between the two reactors. Mixing frequency was set visually to minimize rotations per minute (rpm) while maintaining a well-mixed reactor. The first anaerobic reactor mixer rotational speed was estimated by KC at 60 rpm and the second reactor at 30 rpm.

3.2.2 Aerobic Reactor Description

The aerobic reactor liquid volume was 214 gal and was built from schedule 10s stainless steel pipe, at a height of 84 in and a 30-in diameter (Figure 3-5). The influent was submerged at 18 inches below the liquid surface. The operating liquid depth was 6 ft and the DO and pH probes were located at a liquid level of about 2.5 ft, as was the commonly used mixed liquor sampling tap. The upper sampling tap was located at a liquid level of 4.5 ft. A drain valve was installed at the bottom of the reactor. To prevent the reactor from overflowing if the effluent line became backed up, the reactor was designed with about 14 in of freeboard. Two fine bubble diffusers and a pulse air unit were installed towards the bottom of the aeration tank to regulate DO and provide adequate mixing. The location of the probes, the diffusers, and the Pulsair mixer are shown in Figures 3-5 and 3-6.

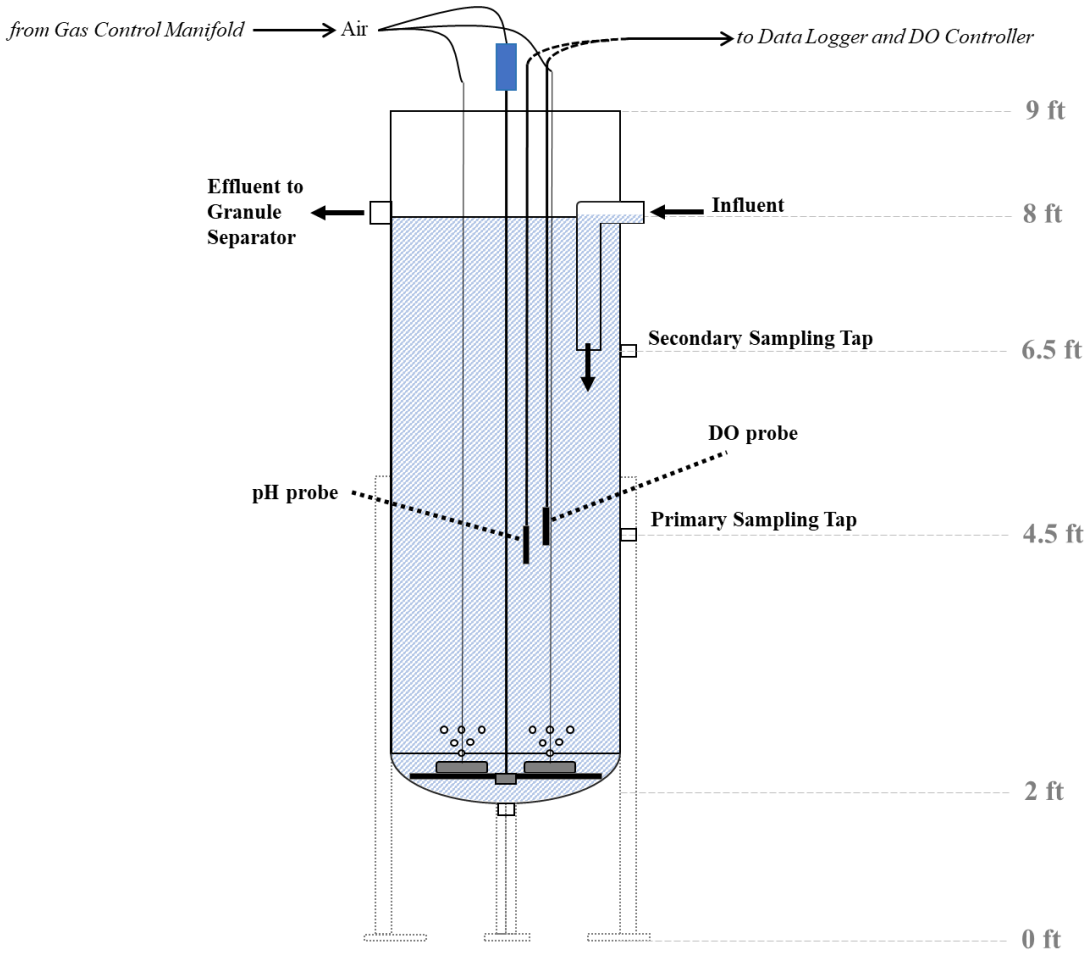

Figure 3-5. Mainstream aerobic reactor. The probes and diffusers are shown in the center of the figure, while the tap, their function, and the influent pipe are shown on the right.

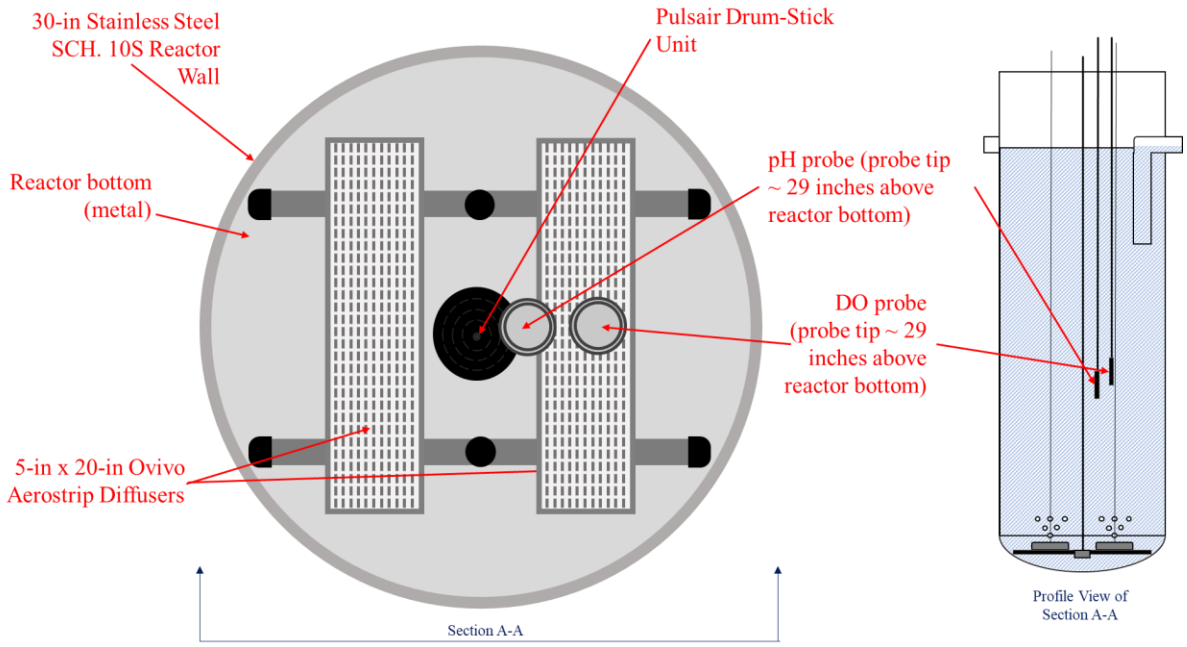

Figure 3-6. Sketch of fine bubble diffuser array and the relative orientation of the DO and pH probes.

The two-fine bubble Aerostrip diffusers were model T0.5-15, made by Ovivo (Salt Lake City, Utah, USA). They were rated for at an air supply rate between 0 and 5 standard cubic feet per minute (scfm) each. The Pulsair unit was secured to the top of the reactor alongside the DO and pH probes and was suspended about 2 in from the bottom of the reactor.

The DO and pH probes were Hach® models P/N 9020000 and P/N DPD2P1, respectively. Data logging was done by the sc1000 and sc1500 modules. The Hach® sc1000 module was used, with PID control, to maintain the DO setpoint (Loveland, Colorado, USA). The DO control and aeration was done in the same way as that for the sidestream except for no baseline aeration. The constant oxygen demand was normally sufficiency with PID control to have enough air for mixing. Additional mixing was provided to the aeration tank, from the initial seeding (October 17, 2019) during the first operational period until November 18, 2019, by a Pulsair Drum-Stick

unit, identical to the one used in the preanoxic reactor (Kirkland, Washington, USA). While it was being utilized, the Pulsair unit provided large bubble mixing to the aeration tank at a frequency of 1 min per 10 min. Compressed air was provided to the diffusers from the same gas control manifold used to provide air and N_2 to the sidestream. The aeration to the mainstream aerobic reactor was controlled using a modulating air value made by Emerson Process (51000 NPS with Baumann 16 Actuator, and Fisher™ 3660 Pneumatic Positioner) (Monterey, California, USA). The aeration intensity was measured using a Kurz air flow meter, Series 504 FTB, which operated between 0 and 10 scfm. After the first start up, the pulse air mixing was not used because it caused variation in flow to the separator due to the increased liquid depth when aeration was increased.

3.2.3 Granular Separator Description

The separator was an 18-inch diameter, 80-gal cylinder made of clear acrylic above a painted steel 45° cone base that connected at the bottom to the underflow recycle line. The height of the separator from below the effluent launder to the bottom of the cone-shaped base was 7 ft 2 in. The granular upflow separator had a special inlet nozzle located at a 4 ft liquid depth to provide a uniform radial discharge of the feed mixed liquor. The resultant superficial upflow velocity was selected to be high enough to carry out slower settling floc and allow the faster settling granules to move to the separator bottom for discharge to the granular sludge return line to the preanoxic reactor. After the first operational period, the acrylic effluent launder was modified by expanding it to the full separator inner diameter to provide a more uniform upward flow pattern. A schematic of the separator design is shown in Figure 3-7a, b.

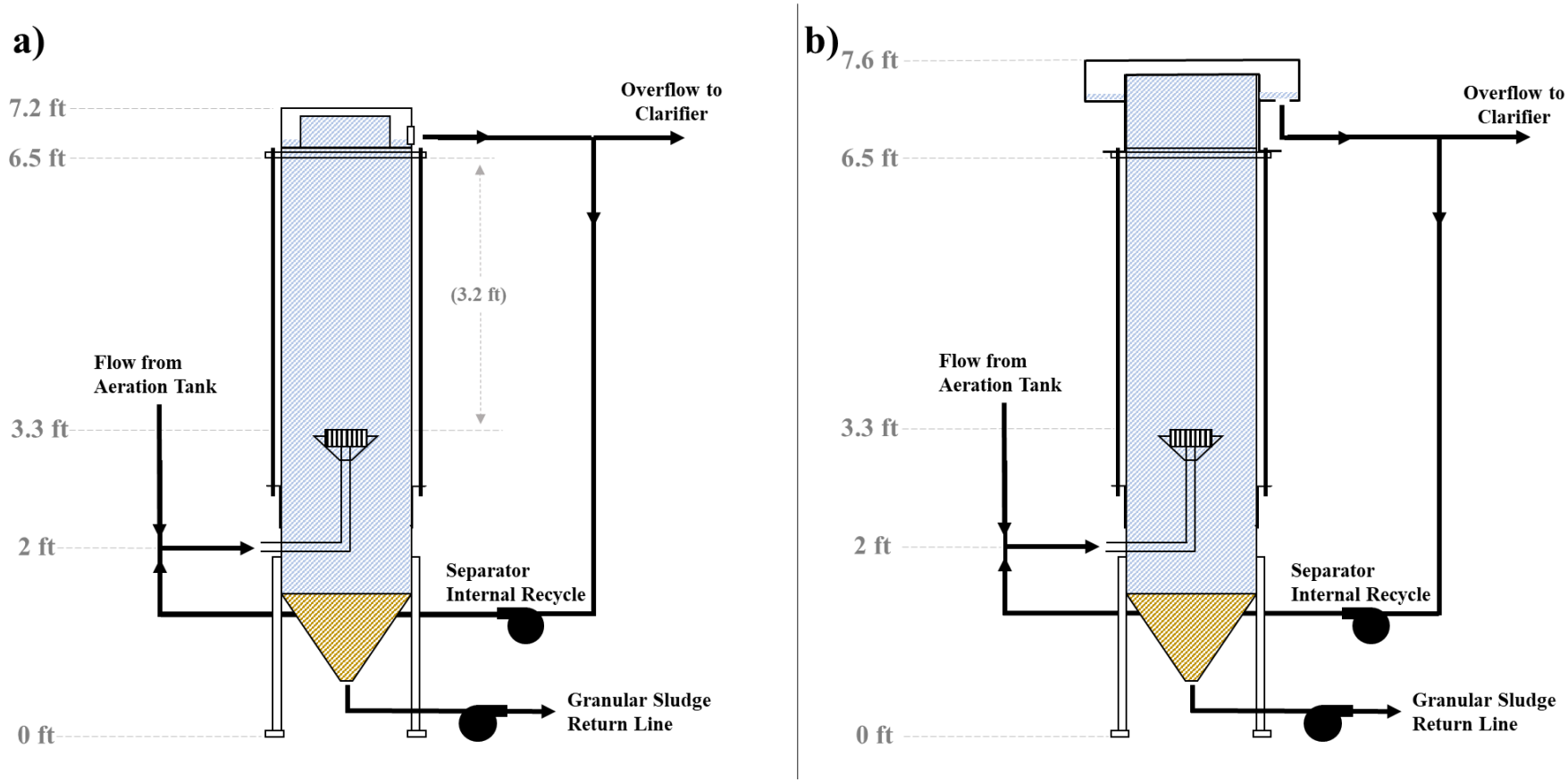

Figure 3-7. The granular upflow separator, a) during the first operational period, with the original acrylic effluent launder, and b) during the second operational period, with the modified stainless-steel effluent launder.

The launders in the two separator designs had separate effluent lines for the overflow to the clarifier and for flow to the internal recycle pump. As depicted above, the initial launder design (Figure 3-7a) had its effluent come from the side of the launder, while the second launder design (Figure 3-7b) had its effluent flow from the bottom to prevent sludge from settling out in the bottom of the launder.

Influent flow to the granular separator is combined aerobic reactor effluent and recycle of separator overflow effluent. The separator internal recycle could be varied to allow for higher upflow superficial velocity than from only the aeration tank effluent flow. The approximate range of superficial upflow velocities used was from 3 to 11 $m \cdot hr^{-1}$. The internal recycle was done using a Verder Inc. Verderflex peristaltic pump (Macon, Georgia, USA). The flow recycle could be varied from 0 to 4 gpm. The separator return underflow was pumped by a Rotho peristaltic pump made by Keco Pumps (San Diego, California, USA). This pump was operated primarily at 0.75 gpm, aside from a short stint at 0.5 gpm, and it was rated for 0.1 gpm to 1.7 gpm.

There were no sampling taps on the granular separator column, however, the sampling taps were located on the separator overflow and underflow lines. The overflow sampling was located slightly upstream of the secondary clarifier and the underflow tap was upstream of the return flow peristaltic pump.

3.2.4 Secondary Clarifier Description

The secondary clarifier was designed and manufactured by KC employees using a 250-gal McMaster-Carr® polyethylene plastic easy drain tank and steel base as a foundation. The tank had an internal diameter of 43 in, a height of 54.75 in, and a bottom slope of 19°. The scraper, scraper motor, and feed well were supported by a Unistrut™ frame. The relative orientations of the effluent weirs, the overflow, and the support structure is illustrated below in Figure 3-8.

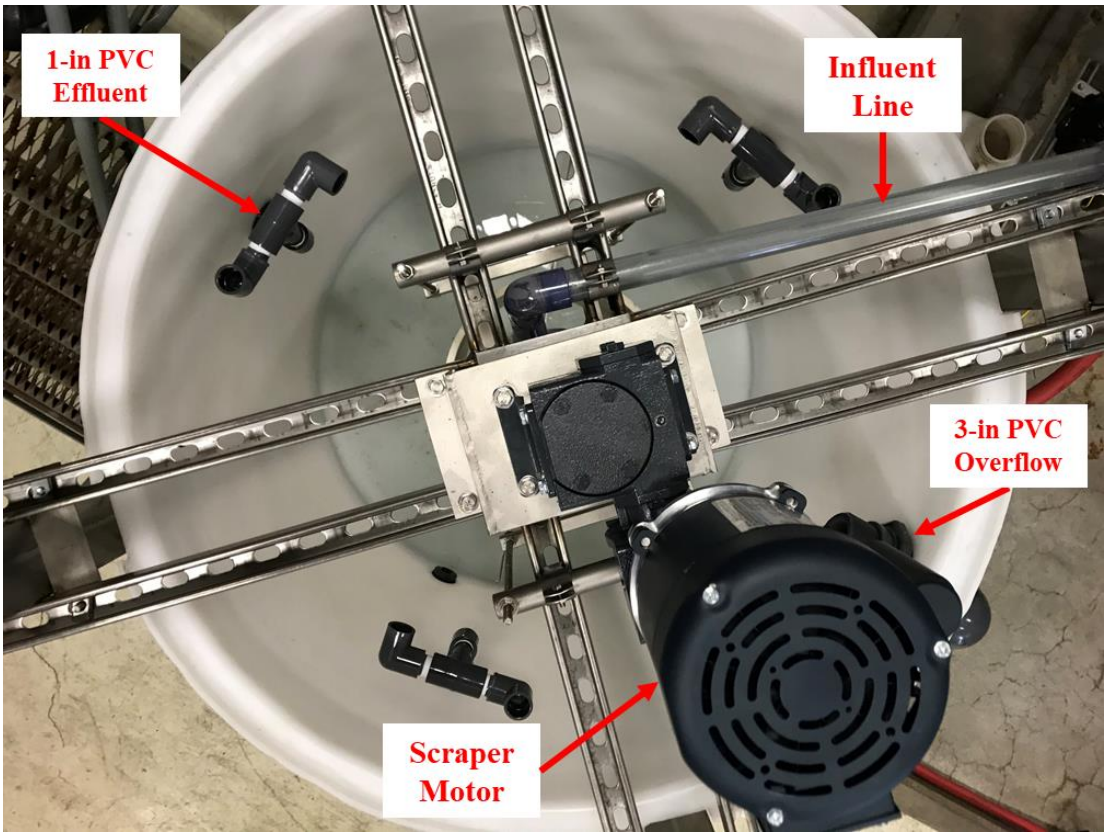

Figure 3-8. A top view of the secondary clarifier.

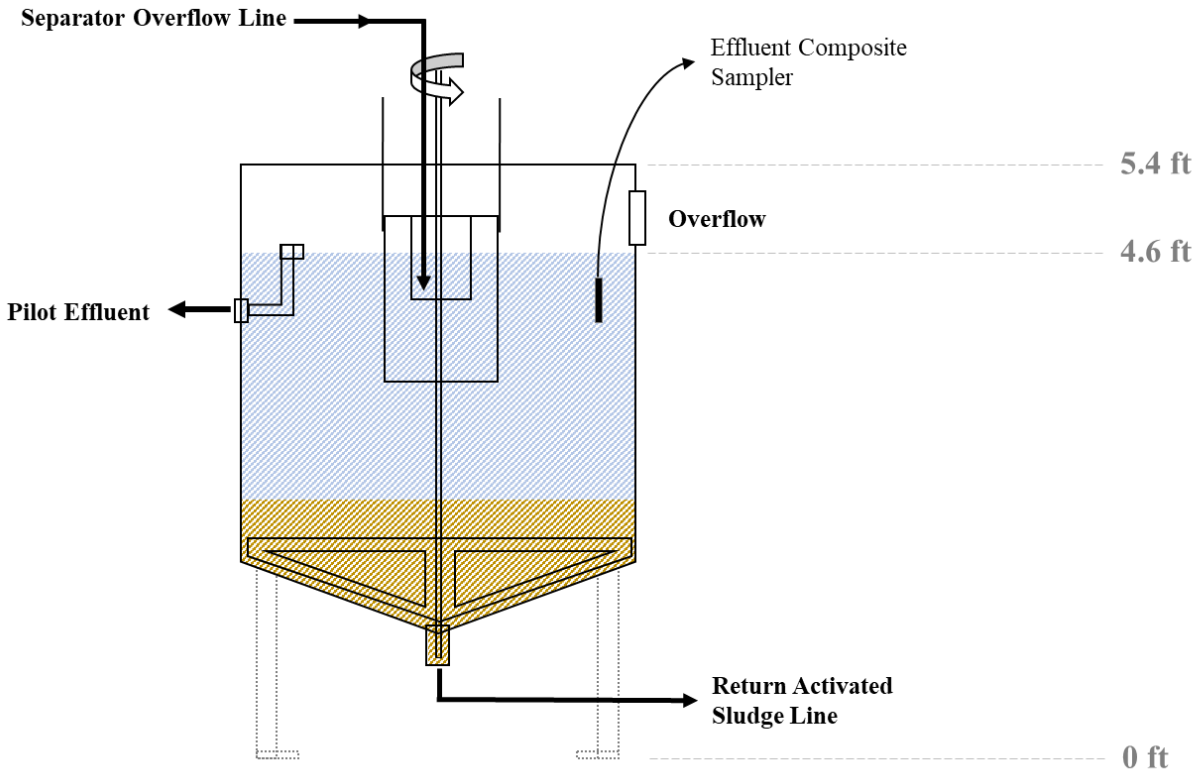

Figure 3-9. A profile view of the secondary clarifier.

The clarifier influent line was gravity fed through 1-inch PVC pipe into a 6-inch PVC pipe within a 12-inch PVC pipe, which together composed the feed well (Figure 3-9). Effluent overflows at the surface into three 1-in diameter PVC pipes, evenly distributed around the circumference. A 3-in diameter PVC overflow bulkhead fitting to a drain is located a few inches above the water line to prevent the clarifier from overflowing and flooding the pilot area. During the second operational period the scraper rotational speed was 1 rpm using a ½-Hp motor with an 1800:1 gearbox from Hub City (Beloit, Wisconsin, USA). During the first operational period (October 17, 2019 – November 25, 2019), a similar ¼-Hp motor was used but failed, requiring the pilot plant shut down.

RAS from the bottom of the clarifier was pumped at 1-2 gpm in a 1-inch PVC pipe to either the aeration tank or the first anaerobic tank using a Grace SoloTech ST23 peristaltic pump (Minneapolis, Minnesota, USA). Sludge wasting for SRT control was done from the RAS line. During the first operational period wasting was done 5-days per week by manually turning ball valves to direct RAS flow to a plastic 50-gal tank used to measure and sample the waste activated sludge (WAS). During the second operational period, a Masterflex peristaltic pump was used to waste with a ChronTrol tabletop controller to run the pump for 15 min every 3 hr, 7-days per week (San Diego, California, USA). The same batch tank was also used for measuring and sampling the waste sludge 5-days per week.

3.3 Sampling Program

The sampling program involved a sample schedule followed by KC and UW, sample handling and storage procedures, and sampling methods for the sidestream and mainstream systems.

3.3.1 Sample Handling

A sampling program was established with KC staff assisting at the plant and the sampling by UW was done 2-3 times per week. Consistent sampling and standard storage techniques were used. Samples for TBOD, TCOD, alkalinity, and mixed liquor samples for TSS, VSS, and granule size distributions were stored at 4°C until analyzed. Samples for soluble COD, inorganic nitrogen, orthophosphate, and acetate, were taken and immediately filtered using a 0.45-µm syringe filter and then stored at 4°C until analyzed. A storage cooler and reusable frozen gel packs were used to keep samples cold during transportation from WPTP to UW. Once samples arrived at UW, they were immediately stored at 4°C until they were removed for analysis.

Samples which were collected by KC employees for analysis at UW were stored on site at 4°C until they were picked within 24-72 hrs by a UW researcher. According to Armenta (2019), difference in holding times of influent and effluent liquid samples from 1 to 3 days, did not influence analytical measurements.

3.3.2 Sidestream Reactor Sampling Methods

All the samples from the sidestream SBR were taken at the 2-ft tap after opening and ejecting 300-500 mL of the reactor liquid, the ejected volume was returned to the reactor after the sampling period. The centrate, WPTP final effluent dilution water, and decant effluent were sampled using a plastic dipper. Both the centrate and WPTP final effluent dilution water were sampled from their feed containers, close to the outlet pipes. The decant effluent sample was taken after the decant effluent collection tank was manually well mixed. Furthermore, because granules tended to accumulate in the decant tank during draining after each cycle, the tank was flushed prior to the next decant sampling event. For granular size distribution analysis, approximately 500 mL of mixed liquor was sampled into a 1-L beaker during aeration, the 2-ft tap was flushed prior to sampling. Then, the 1-L beaker was well mixed by a magnetic stir plate and bar while removing two samples of 20-30 mL a broken-tip plastic pipette. For MLSS and MLVSS analysis, 400 mL was taken from the 2-ft tap during the aeration phase, after the tap was flushed. The granules were then lightly blended to get a more uniform TSS concentration distribution in the 400-mL sample. Then, two samples of 8-12 mL were taken from the mixed blended sludge using a plastic pipette.

3.3.3 Mainstream Sampling Methods

The mainstream pilot plant required sampling locations at the preanoxic tank, both anaerobic reactors, the aeration tank, the separator underflow and overflow, and at the RAS line, to ensure that operations and performance could be properly tracked. Furthermore, as with the sidestream, any sampling done through a tap was first flushed by 300-500 mL of the liquid in the reactor. After the sampling periods, the flushed volume was returned to the reactor. Samples from the anoxic reactor were sampled using the 4-ft sampling tap, immediately after the Pulsair unit mixed the reactor. Both the first and second anaerobic reactors were sampled from their 4-ft sampling taps. Because those reactors had continuous mechanically mixing, there was no sample timing constraint. The aerobic reactor was sampled from the lower sampling tap, at 4.5 ft. The separator overflow was sampled from a ball valve from the effluent pipe to the secondary clarifier. This line was also flushed before sampling, and the flushed volume was poured into the clarifier feed well. The separator underflow was sampled, just upstream of the granular sludge return pump, using a similar ball valve as the overflow. Again, the line was flushed before sampling and the flushed volume was poured back into the aeration tank.

The waste activated sludge (WAS) sampling method was different for operating phase 1 and 2. For both periods a plastic dipper was used to sample the WAS tank. During the phase 1, RAS wasting was done in 2 to 3 10-to-30-gal batches, spaced throughout the workday. A 100-mL sample was collected in a sample container from the WAS tank for each batch. After wasting had been concluded, the samples were mixed to create a daily WAS sample. During phase 2, because wasting was done automatically, one of the eight daily wasting events was sampled. Samples were taken from the WAS batch waste tank by closing the drain valve before a wasting event.

Then, after the wasting event, the WAS was mixed, sampled into a sample container, and the drain valve was opened. The mainstream influent and effluent were sampled using two separate refrigerated 24-hr composite samplers. The influent was sampled from a PVC wet well which was fed primary influent from same line feeding the first anaerobic tank. The sump was fed primary effluent at the bottom and had an effluent weir at the top, allowing for composite samples, taken once per hour, to measure the influent to the pilot. The pilot plant effluent was sampled between two of the effluent collection pipes, close to the secondary clarifier wall, from 1 ft below the liquid level, once per hour. The composite samplers were sampled and reset every 24 hours during the week and every 72 hours for the weekend.

3.4 Analytical Methods

Nutrient concentrations were determined using a Thermo Scientific™ Gallery™ Automated Photometric Analyzer. This device was used to spectrophotometrically measure NH_3-N, NO_2^--N, NO_3^--N, and orthophosphate for the entire study period. The respective wavelength and method used for each parameter is shown in Table 3-3.

Table 3-3. Summary of the spectrophotometric methods used to measure soluble nutrient concentrations.

Parameter	Wavelength (nm)	Method Used	Reference
NH_3	660	ISO 7150	(ISO, 2017)
NO_2^-	540	SM 4500-NO_2^-	(APHA, 2005)
NO_3^-	540	SM 4500-NO_3^-	(APHA, 2005)
PO_4^{3-}	880	SM 4500-P.E.	(APHA, 2005)

SM – Standard Methods for the Examination of Water and Wastewater, 2005

ISO – International Organization for Standardization

The NH_3-N, NO_2^--N, and PO_4^{3-}-P concentrations were measured directly using the methods described above. However, NO_3^--N was measured indirectly by reducing NO_3^- to NO_2^-, then measuring total oxidized nitrogen species and subtracting the NO_2^- concentration from the result. Acetate COD concentrations were measured using a Thermo Scientific™ Dionex™ ion chromatography system (ICS) (Pfaff, 1993). Standards for the above tests were batched at least every three months by dissolving the appropriate salts (NH_3Cl, $NaNO_2$, $NaNO_3$, KH_2PO_4, NaAc) into Milli-Q® ultrapure water (Resistivity = 18.2 MΩ-cm at 25°C).

Total suspended solids (TSS), volatile suspended solids (VSS), and sludge volume index (SVI) tests were performed according to Standard Methods 2540 D, 2540 E, and 2710 D, respectively (APHA, 2005). Furthermore, the SVI tests were conducted using a 1.4-L cylindrical Settleometer (Raven Environmental Products, St. Louis, Missouri, USA).

Additional tests were conducted by WPTP on-site process lab. The tests conducted and the methods used are detailed in Table 3-4.

Table 3-4. Summary of tests performed by WPTP process lab, and the Standard Methods procedures followed (APHA, 2005).

Test	Method Used
TSS	SM 2540 D
VSS	SM 2540 E
tCOD	SM 5220 B
sCOD	SM 5220 B
BOD_5	SM 5210 B
Alk	SM 2320 B

SM – Standard Methods for the Examination of Water and Wastewater, 2005.

Hach Intellical™ LDO101 and PHC101 probes were used with HQD portable meters to measure DO and pH respectively, during the mainstream batch kinetic tests (Loveland, Colorado, USA). The LDO101 probe was a plastic-body laboratory model, whereas the PHC101 probes was a stainless-steel-body model. The DO probe was calibrated using a 1-pt automatic air calibration method, according to the manufacturer's guidelines. Additionally, based on the Hach's guidelines, the pH probe was calibrated using a 2-pt (7.0 and 10.01) standard curve.

Granule and floc morphologies were observed and photographed with a ZEISS Stemi 508 stereomicroscope (Oberkochen, Germany) and an Olympus BH-2 polarizing trinocular light microscope (Shinjuku, Tokyo Japan). The stereomicroscope images were captured and scaled by an Axiocam ERc 5s microscope camera and ZEN lite software. Light microscope images were

captured by either an Olympus digital camera mounted to the microscope or a Motorola MOTO G5 smartphone camera through the viewfinder.

3.4.1 Sieve Analysis and Size Distribution

The relative proportion of different sized granules in the mainstream and sidestream were determined by using a series of small stainless-steel sieves, at descending mesh sizes. The sieves were 1.25-in tall with a 3-in diameter. The various sieves used in the sidestream and the mainstream are detailed below in Table 3-5.

Table 3-5. Summary of the sieves for the mainstream and sidestream mixed liquor samples to determine the granular size distribution.

Sieve Mesh	**Mesh Opening**	**Sieve Mesh**	**Mesh Opening**	**Sieve Mesh**	**Mesh Opening**
No.	**mm**	**No.**	**mm**	**No.**	**mm**
Sidestream Size Distribution Analysis Sieves					
70	0.212	18	1.00	10	2.00
40	0.425	16	1.18	8	2.36
30	0.600	14	1.40	7	2.80
20	0.850	12	1.70		
Mainstream Size Distribution Analysis Sieves					
70	0.212				
40	0.425				
20	0.850				
12	1.70				

The sieves used in the sidestream size distribution analysis were determined by Armenta (2019) and were carried through for this phase of the project to maintain data consistency. A reduced number of sieves were used in characterizing the mainstream granule size distribution to allow for the management of multiple samples per week. Four sieve sizes were chosen, 0.212 µm,

0.425 µm, 0.850 µm, and 1700 µm, to cover the range of granule sizes typically present in the study.

The size distribution sieve method used for both the sidestream and the mainstream mixed liquor involved stacking the sieves from the smallest mesh size at the bottom to the largest mesh size at the top. Then, a plastic beaker was placed underneath the sieve stack to catch any particles or water which fell through the bottom mesh. Next, a 20-30 mL sample was poured over the top sieve and DI water was rinsed over the top mesh until all particles smaller than the mesh size had passed through the mesh. Once all the particles smaller than the mesh size had been washed through, the size was backwashed into a container labeled with the mesh size of that sieve. This process, of wash, remove, backwash, was then repeated for each sieve in the stack. Once all sieves had been processed, TSS and VSS were measured for each size range using Standard Methods 2540 D and E (APHA, 2005).

The particle size distribution, assuming the granules were spherical, was then calculated by Equation 3-1 (Armenta, 2019).

$$Fraction\ of\ Mass\ for\ particle\ size\ range\ (FM_n) = \frac{TSS_n}{\sum_1^n TSS_n} \tag{3-1}$$

where TSS_n = mass retained on sieve n divided by total sample volume

Equation 3-2 was used determine the average granule size.

$$Weighted\ average\ diameter\ of\ mized\ liquor\ granules, mm = \sum_1^n FM_n(D_n) \tag{3-2}$$

where n = sieve size sequence number

D_n = average size of opening of sieve n and sieve n-1, mm

3.4.2 Quantitative Polymerase Chain Reaction

All quantitative polymerase chain reaction (qPCR) analyses and preparations were performed by Bao Nguyen Quoc, a UW PhD Candidate under the GOALI project. Mixed liquor sludge samples were regularly collected from the mainstream and sidestream reactors to track the relative abundances of AOBs, NOBs, GAOs, and PAOs. Granules were sieved using 212, 425, 600, 850, 1180, and 1400 µm sieves to determine the relative abundance within each size fraction.

Granules of each size fraction, or flocculent sludge, was transferred into 2-mL microtubes and centrifuged at 16,000 xg for 2 min in a Centrifuge 415D (Eppendorf, Germany). The supernatant was discarded, and the pellet was stored at -80 °C until analyzed. DNA was extracted, mostly following the manufacturer's guidelines, from 70 – 80 mg of AGS or floc, using DNeasy PowerBiofilm Kit (Qiagen, Germany). There were three deviations from the guidelines, 1) PowerBiofilm bead tubes were incubated at 65 °C for 10 min, 2) a Bead Beater FastPrep®-24 Instrument (MP, USA) was used for the mechanical cell lysing step at 4 m/s for 20 s, and 3) DNA samples were incubated with 200 µL of inhibitor removal solution for 30 min. DNA concentration and quality were first examined spectrophotometrically using a NanoDrop 2000, then DNA concentration was diluted with Ultrapure™ DNase/RNase-Free distilled water to 2 ng/µL. The DNA concentration was determined using the Qubit™ dsDNA HS Assay kit (ThermoFisher Scientific, USA).

qPCR was performed using a Roche LightCycler 96 (Roche, Germany), with a total volume of 10 µL composed of 5 µL SensiFast™ SYBR® No-ROX Kit 2X (BioLine, USA), 0.5 µm of each primer, and a 4 ng DNA template. The primers used for qPCR are shown in Table 3-6.

Table 3-6. Primers used for qPCR (provided by Bao Nguyen Quoc).

Target	**Primer**	**Sequence**	**Amplicon length**	**Reference**
16S rRNA PAO	PAO-651f PAO-846r	CTGGAGTTTGGCAGAGGG GTTAGCTACGGCACTAAAAGG	195	Fukushima et al. (2007)
Competibacter (GAO)	GAO-Gbf GAO-Gbr	GAGTGGGCTAGAGGATCGTG TTCCCCRGATGTCAAGGCC		Fukushima et al. (2010)
Bacterial *amoA* gene (AOB)	amoA-1F amoA-2R	GGGGTTTCTACTGGTGGT CCCCTCKGSAAAGCCTTCTTC	491	Rotthauwe et al. (1997)

3.4.3 Fluorescence in situ Hybridization

Fluorescence in situ hybridization (FISH) analyses and sample preparations were performed by Bao Nguyen Quoc, a UW PhD Candidate, under the GOALI project. Mainstream and sidestream reactor mixed liquor sludge samples were collected periodically to visualize the granule microbial distribution. Granular sludge samples were transferred into 2-mL microtubes and centrifuged at 16,000 *g* for 2 min and the supernatant was discarded. The granular sludge was then immediately resuspended with 4% paraformaldehyde and set on ice for 120 mins. This step is referred to as fixation and prevents cell lysis while making the cell walls permeable for hybridization. After the granules were fixed, the sample was centrifuged at 16,000 *g* for 2 mins

and the paraformaldehyde supernatant was discarded. Subsequently, the granular sludge was resuspended with 1x phosphate buffer saline (PBS), centrifuged at 16,000 *g* for 2 min, and the supernatant was then discarded. The PBS wash was repeated once. Samples were then stored in Ethanol/PBS 1.25:1 solution at -20°C until analyzed. The ethanol solution keeps the granules from being frozen.

Fixed granules were removed from the Ethanol/PBS solution and rinsed with Milli-Q water before being frozen at -10°C in a tissue freezing medium (Richard-Allan Scientific™ Neg-50™, ThermoFisher Scientific, USA) and cut into 10-14 µm slices using a microtome-cryostat (CryoStar NX50, Thermofisher Scientific, USA). The slices accounted for between 0.3 and 7% of the granule biofilm depth, depending on the granule diameter. Then, granule slices were adhered to gelatin-coated glass microscope slides and incubated at 46°C until dried. Each slide had 6 wells separated with a Teflon coating to prevent mixing of probes between wells. The granule cells were then dehydrated by dipping the slides in three consecutive ethanol solutions (50%, 80%, and 90% (v/v) concentrations) for 3 mins each. Next, 10 µL of hybridization buffer solution (0.9 M NaCl, 0.02 M Tris-HCl, 35% (v/v) formamide, 0.02% (w/v) sodium dodecyl sulfate (SDS)) was added to each well. Afterwards, 1 µL of fluorescently labelled oligonucleotide probe mix (0.5 pmol for Cy3/Cy5 and 0.83 pmol for fluorescein-labelled probes) was added to each well. Hybridization then took place in a humid chamber for 6 hrs at 46°C.

Immediately after hybridization, unbound probes were washed off by placing the slide above a 60°C water bath and adding 20 µL of washing buffer (20mM Tris-HCl (pH 8), 0.01% (w/v) SDS, 0.08 mM NaCl, and 0.005 mM EDTA), preheated to 60°C, to each well, and set for 3 min.

The washing buffer was then replaced with new washing buffer, and this was repeated for 20 min. Afterwards, the slides were rinsed with Milli-Q water twice and set to air dry in a dark room and room temperature.

Prior to observation under the microscope, 2 µL of antifade fluorescent mounting medium (20mM Tris (pH 8.0), 0.5% N-propyl gallate, and 90% glycerol) was added to each well and the slide was covered with a cover slip. Then, slices were observed using a Zeiss Axioskop 2 MOT microscope (LSM 5 pascal, Carl Zeiss, USA), which was equipped with a mercury lamp, an argon laser (453-514 nm), a green helium/neon laser (543 nm), and a red helium/neon laser (633 nm). The FISH probes used are shown in Table 3-7.

Table 3-7. FISH probes used in this thesis (provided by Bao Nguyen Quoc).

Probe	**Sequence**	**Target**	**Fluorescent dyes**	**Position**
PAO 462	CCGTCATCTACWCAGGGTATTAAC	PAO	Cyanine 5	5’
PAO 651	CCC TCTGCCAAACTCCAG		Cyanine 5	5’
PAO 846	GTTAGCTACGGACTAAAAGG		Cyanine 5	5’
GAO Q989	TTCCCCGGATGTCAAGGC	GAO	Fluorescein	5’
GAO Q431	TCCCCGCCTAAAGGGCTT		Fluorescein	5’
NSO190	CGATCCCCTGCTTTTCTCC	AOB	Cyanine 3	5’
NSO1225	CGCCATTGTATTACGTGTGA		Cyanine 3	5’

3.5 Biological Kinetics Tests

3.5.1 Mainstream Specific Nitrification Rates

During the second mainstream operational period, weekly batch tests were performed to determine the aeration tank mixed liquor specific nitrification rates (SNRs). The NH_3-N removal, NO_2-N production, and NO_3-N production rates were determined for aeration tank granular sludge, flocculent sludge, and overall mixed liquor. The batch tests were performed at 2 $mg \cdot L^{-1}$ DO concentration to observe nitrification rates at a similar DO concentration to the mainstream.

The test procedure consisted of first obtaining 3 liters aeration tank mixed liquor in a 1-L beaker and a 2-L plastic container. The 1-L beaker was used to test the overall mixed liquor SNR directly, while the 2-L plastic container was sieved to obtain the flocculent and granule mixed liquor samples. After a 10-min settling period in the 2-L container the supernatant was poured off. The remaining mixed liquor was then sieved on a 212-µm sieve to capture the granular sludge. To ensure that no particles stuck to the granules and that all material was provided with ample opportunity to pass through the sieve, mainstream pilot effluent was used to thoroughly rinse the material retained on the sieve. The flocculent (passing) and granular (retained) sludges were collected in separate containers. Once the 2 L of mixed liquor had been sieved, the granular sludge and flocculent sludge were diluted individually with mainstream pilot effluent to a total volume of 1 L, each.

Each of the three sludge samples (mixed liquor, mixed liquor granules, and mixed liquor flocculent sludge) were then tested with the procedure described below. One liter of the sample to be tested was placed in a 1-L beaker and spiked with 30 mL of 1000-$mg \cdot L^{-1}$ NH3-N stock

solution. A porous stone was used to distribute air/N_2 flows to maintain an average DO of 2 $mg \cdot L^{-1}$. The DO generally ranged from 1.5 to 2.5 $mg \cdot L^{-1}$. Additionally, CO_2 could be delivered through the porous stone to maintain a pH of 7-8. Because the gas flow through the stone was often insufficient to keep the beaker fully mixed, supplemental mechanical mixing was supplied using a magnetic stir plate and bar. The stir plate speed was minimized while ensuring the particles were sufficiently suspended. The batch test reactor was sampled at the beginning of the experiment and every 10 min for between 50 min and 60 min for NH_3-N, NO_2-N, and NO_3-N concentrations. At each sampling interval, the DO, pH, and temperature was recorded. At the end of the sampling period, at least two 10-mL samples of the test beaker liquid were taken for TSS analysis.

The NH_3-N removal, NO_2^--N production, and NO_3^--N production rates were determined by fitting a linear trend line to Excel® data plots. The rates were then corrected to 20°C using a temperature activity coefficient of 1.072 (Melcer et al, 2003). Furthermore, the rates were divided by the VSS concentration to obtain the specific rates (mgN/gVSS-hr). The NO_2^--N production rate was determined by the sum of the NO_3^--N and NO_2^--N accumulation rates, to account for NO_2^--N that was converted to NO_3^--N. The test NH_3-N removal rate was then checked with the NO_2^--N production rate to validate the test. In cases where the NO_2^--N production rate was greater than that NH_3-N removal rate, the NO_2^--N production rate was used to determine the SNR. The lower observed NH_3-N rate could have been affected by NH_3-N production from biomass endogenous decay.

3.5.2 Sidestream Anaerobic Acetate Utilization Kinetics

To better understand the acetate utilization kinetics in the sidestream SBR, two tests were conducted on August 26 and September 30, 2019. The tests were conducted by sampling during the anaerobic phase of the sidestream SBR. The anaerobic phase was fully mixed with nitrogen gas and consisted of a 5-min idle phase, a 10-min acetate feeding period, and a 45-min uptake period.

Samples were collected and handled according to Sections 3.3.1 and 3.3.2. However, ejected reactor liquid, used to clear the sampling line before each sample, was returned to the SBR every 5 mins. The total volume taken from the reactor was about 10%, so with the regular return sampling and ejecting did not cause a significant change in reactor volume. Sampling was started at the beginning of anaerobic feeding and occurred every 1 to 1.5 minutes for the first 25 minutes, then every 5 mins for the remainder of the anaerobic phase. A total of 23 and 22 samples were collected on August 26 and September 30, respectively. The samples were then analyzed for acetate-COD using an ICS (Section 3.4).

3.6 Biological Kinetics Computations

Specific nitrification rates (SNRs) for the sidestream granular sludge is an important parameter for assessing the nitrification capacity of the bioaugmented biomass and the potential impact for nitrogen removal in the mainstream system. The SNRs of the mainstream mixed liquor was also an important parameter for assessing the impact of bioaugmentation and the fate of the sidestream fed granules. Determining the SNR value of the mixed liquor in the sidestream reactor and mainstream aeration tank relied on mass balance computations that included the

reactor influent and effluent NH_3-N concentrations and considerations of contributions by influent organic nitrogen and consumption for growth of heterotrophic bacteria. The following subsections describe the computational procedure to determine the SNR of the sidestream granules and the SNR of the mainstream aeration tank mixed liquor. In addition, the procedure to determine the acetate uptake biokinetics during feeding in the anaerobic phase of the sidestream SBR is presented.

3.6.1 Sidestream Specific Nitrification Rate

The sidestream SNR was calculated by determining the amount of feed NH_3-N that was nitrified, the rate that it was oxidized, and dividing by the reactor VSS concentration. All mass calculations were normalized to the feed flow. The amount of NH_3-N nitrified accounts for the influent, effluent and cell synthesis.

$$NO = N_o - N_e - N_{syn} \quad (3\text{-}3)$$

where NO = NH_3-N nitrified, mg/L

N_o = Influent NH_3-N, mg/L

N_e = Effluent NH_3-N, mg/L

N_{syn} = Nitrogen used for biomass growth, mg/L

The NH_3-N used in cell synthesis was calculated based on the net biomass production, or net yield, from heterotrophic biomass growth on the acetate COD fed, cell debris from endogenous decay, and reactor SRT using Equation 3-4, which was adapted from Tchobanoglous et al. (2014).

$$Y_{net} = \frac{Y}{1 + (b_{20} \cdot b_{,\theta}{}^{T-20}) \cdot SRT} + \frac{f_d \cdot (b_{20} \cdot b_{,\theta}{}^{T-20}) \cdot Y \cdot SRT}{1 + (b_{20} \cdot b_{,\theta}{}^{T-20}) \cdot SRT} \quad (3\text{-}4)$$

where Y_{net} = net mass of biomass produced for mass of COD removed, gVSS/gCOD

Y = synthesis growth MLVSS of biomass produced from COD consumption, gVSS/gCOD

b_{20} = biomass specific endogenous decay coefficient at 20°C, gVSS/gVSS-d

T = temperature, °C

$b_{,\Theta}$ = endogenous decay coefficient correction for temperature, unitless

f_d = debris production from endogenous decay, gVSS/gVSS

SRT = biomass SRT in SBR reactor, days

The coefficient values used for Equation 3-4 are shown in Table 3-8.

Table 3-8. Parameters and coefficient values from Tchobanoglous et al. (2014), used in calculating the NH_3-N used for net biomass production.

Parameter	Value	Units
Y	0.45	gVSS/gCOD
b_{20}	0.12	gVSS/gVSS-d
$b_{,\Theta}$	1.04	Unitless
f_d	0.12	gVSS/gVSS

The amount of nitrogen used for synthesis was then determined from the net biomass yield, the amount of acetate COD used, and a biomass nitrogen content of 12% (Tchobanoglous et al., 2014), as shown by Equation 3-5.

$$N_{syn} = (0.12)(COD)(Y_{net}) \quad (3\text{-}5)$$

where N_{syn} = NH_3-N used for biomass production, mg/L

COD = acetate COD used, mg/L

The sidestream reactor nitrification rate equals the amount of NH_3-N oxidized per hour during the SBR 4.5-hr aeration phase.

$$R_{nit} = \frac{NO}{t_{aer}} \quad (3\text{-}6)$$

where R_{nit} = NH_3-N oxidation rate, mg/L-hr

t_{aer} = SBR cycle aeration time, hr

The SNR equals the nitrification rate divided by the MLVSS concentration.

$$SNR = \frac{R_{nit}}{X} \quad (3\text{-}7)$$

where SNR = specific nitrification rate, mg/g-hr

X = reactor MLVSS concentration, g/L

3.6.2 Mainstream Aeration Tank Nitrification Rate and Specific Nitrification Rate

The nitrification in the mainstream aeration tank and SNR of the mixed liquor was determined in the same manner as that for the sidestream reactor with the exception that it included the biodegradable organic nitrogen in the influent primary effluent (PE) wastewater in addition to the NH_3-N. Organic nitrogen plus inorganic NH_3-N is represented by total Kjeldhal nitrogen (TKN). The PE influent TKN value was determined from the influent NH_3-N concentration data

by using a ratio of TKN:NH_3-N based on weekly analysis of TKN and NH_3-N composite PE samples by the KC laboratory from July 29, 2019 to March 2, 2020. The data is tabulated in Appendix B and the average NH_3-N/TKN ratio was 0.686 (TKN/NH_3-N = 1.46) with a standard deviation of 0.046.

Not all of the organic nitrogen is biodegradable and based on typical wastewater characteristic parameter values from Melcer et al (2003) and mainstream influent wastewater characteristics measured in Phase 2, 95% of the influent TKN concentration was assumed to be bioavailable for conversion to NH_3-N for nitrification. The assumptions and parameters used in the calculation of biodegradable influent TKN concentration from the influent NH_3-N concentration measured are summarized in Table 3-9.

Table 3-9. Parameters and assumptions used to calculate the influent biodegradable TKN concentration.

Parameter	Relationship	Units	Reference
TKN	1.46 gTKN-N/gNH_3-N	mg/L	KC NH_3-N Data
ubCOD	0.09•tCOD	mgCOD/L	BioWin
ubTKNp	0.05•ubCOD	mgN/L	Melcer et al, 2003
ubTKNs	0.02•TKN	mgN/L	BioWin
ubTKN	ubTKNs + ubTKNp	mgN/L	Melcer et al, 2003

tCOD = Total influent COD, ub = unbiodegradable, TKN_p = particulate organic N, TKN_s = soluble organic N, BioWin = Envirosim BioWin Biological Process Software Model wastewater characterization default value

Based on characteristics of the weekly average PE concentrations fed to the mainstream reactor, the fraction of total unbiodegradable TKN to influent TKN ranged from 0.050 to 0.057 g/g. A fraction of 0.05, or 5%, was selected to best estimate the bioavailable influent TKN. The mainstream bioavailable influent TKN was then calculated as follows:

$$bTKN_o = N_o(1.46)(0.95) \quad (3\text{-}8)$$

where $bTKN_o$ = bioavailable influent N, mg/L

1.46 = gTKN/gNH_3-N

0.95 = g$bTKN_o$/gTKN

N_o = influent NH_3-N concentration, mg/L

The amount of nitrification in the aeration tank is the difference between the influent bTKN and effluent NH_3-N concentration minus the amount of nitrogen used for cell synthesis.

$$NO = bTKN_o - N_e - N_{syn} \quad (3\text{-}9)$$

where $bTKN_o$ = bioavailable influent nitrogen, mg/L

The equations to determine the amount of nitrogen used for biomass synthesis (N_{syn}) is the same as that used in 3.6.1 to calculate the Y_{net} (Equation 3-4) and N_{syn} (Equation 3-5).

The mass of nitrogen oxidized in mg/d is:

$$mNO = Q(NO) \quad (3\text{-}10)$$

where mNO = mass of nitrogen oxidized, mg/d

Q = influent flow rate, L/d

The aeration tank nitrification rate is then:

$$R_{nit} = \frac{mNO}{(24)(V_{aer})} \quad (3\text{-}11)$$

where V_{aer} = aeration tank volume, L

R_{nit} = nitrification rate, mg/L-h

24 = h/d

The SNR is calculated as before by Equation 3-7:

$$SNR_{aer} = \frac{R_{nit}}{X_{aer}} \quad (3\text{-}12)$$

where SNR_{aer} = specific nitrification rate in the aeration tank, mg/gVSS-h

X_{aer} = MLVSS concentration, g/L

3.6.3 Sidestream Anaerobic Acetate Utilization Kinetics

Acetate utilization kinetics during feeding in the sidestream SBR anaerobic phase are described by Michaelis-Menten kinetics for substrate utilization.

$$R_s = \frac{KSX}{K_s + S} \quad (3\text{-}13)$$

where R_s = substrate utilization rate, mg/L-hr

S = substrate COD concentration, mg/L

X = solids concentration, mgVSS/L

K = maximum specific substrate utilization rate coefficient, mgCOD/mgVSS-min

K_s = half-velocity coefficient, mg/L

The acetate kinetics were evaluated with in situ tests (Section 3.5.2) and the maximum uptake rate (K) and the apparent half-saturation constant (K_s) were determined using Mathworks Matlab®. A mass balance describes the acetate COD uptake during the feeding period. The

change in volume during feeding is ignored because the fed volume was a small fraction of the mixed volume after decanting; only about 0.7%.

$$V\frac{dS_t}{dt} = QS_f - \frac{KS_tXV}{K_s + S_t} \quad (3\text{-}14)$$

This reduces to:

$$\frac{dS_t}{dt} = \frac{Q}{V}S_f - \frac{KS_tX}{K_s + S_t} \quad (3\text{-}15)$$

where V = reactor volume, 88 L

S_t = acetate COD concentration at time t, mgCOD/L

S_f = acetate feed COD concentration, mg/L

Q = acetate feed rate, L/min

After feeding stopped the acetate COD concentration was always greater than 100 mg/L. Thus, there was a period when S was much greater than K_s and the acetate uptake was linear. Therefore, the substrate utilization rate for the constant acetate utilization rate is described by:

$$\frac{dS}{dt} = -KX \quad (3\text{-}16)$$

Integration with respect to time yields:

$$S_t = S_{t-1} - KXt \quad (3\text{-}17)$$

where S_{t-1} = acetate COD concentration at time t-1, mg/L

The polyfit® function in Matlab was used to apply a linear fit to the linear portion of the acetate uptake curve. The K was then determined from the slope of the fit. Coefficients of determination (R^2) of > 0.99 were achieved using this method for both data sets. After the constant substrate

uptake period, Equation 3-13 was used to solve for K_s. Without feeding, the substrate utilization rate was equal to the change in the substrate concentration over time.

$$\frac{dS_t}{dt} = -\frac{KS_tX}{K_s + S_t} \tag{3-18}$$

Equation 3-18 was then solved in Matlab® using the ode23® function, which solves differential equations using an explicit Runge-Kutta method. To determine K_s, the value was varied from 0 in 0.1-unit increments until an R^2 of >0.999 was achieved. Once K_s and K had been determined, Equation 3-15 was solved using ode23® to model the acetate kinetics during anaerobic feeding.

4 Results and Discussion

The following sections cover the pilot plant field investigation from September 1, 2019 to March 16, 2020. The sidestream pilot SBR was operated continuously for the 6.5-period while the mainstream CFAS pilot had two operating phases. In Phase 1 the mainstream was started up on October 17, 2019 with KC South Plant EBPR sludge and operated until November 26, 2019, when it was shut down due to a failure of the secondary clarifier scrapper motor. There was no granule bioaugmentation during Phase 1 because the flocculent seed sludge began nitrifying during the first week of operation. Phase 2 began on January 21, 2020. After two weeks (more than 5 SRTs) of operation with low nitrification, the mainstream was charged with stored granules and monitored for about 3 weeks before continual bioaugmentation began. Bioaugmentation lasted for about 3 weeks until the pilot facility was shut down on March 16, 2020 due to restrictions from COVID-19. The operation and results of the sidestream SBR and mainstream CFAS Phases 1 and 2 are discussed in Sections 4.1, 4.2, and 4.3, respectively.

4.1 Sidestream Operation and Treatment Performance

4.1.1 Sidestream Operating Conditions

The sidestream reactor was operated continuously for over 2 years from its start-up on February 8, 2018 until the shutdown on March 16, 2020. The operational period for this report is from September 1, 2019 to March 16, 2020. Operating conditions prior to this have been described by Armenta (2019).

4.1.1.1 Sequencing Batch Reactor Operating Phases

The sidestream SBR was fed 4 times per day for a 6-hr operating cycle. The reactor operation had 4 6-hr cycles per day, which included a 55-min anaerobic phase, 4.5-hr aerobic phase, 8-min of settling, a 3.5-min decant, and a 23.5-min idle phase (Figure 4-1). The 55-min anaerobic phase had 5-min of N_2 sparge mixing before a 10-min acetate feed period. Within 5 min after the start of the aeration phase, the feed centrate (13.5 L) and final effluent dilution water (74.5 L) were added over a 15-min period. These same operating conditions were used the month prior to this study.

On January 10, 2019, the acetate feeding period was increased to 15 minutes, but the same volume was fed by decreasing the feed pumping rate. The change was made to lower the bulk liquid acetate COD concentration during the feeding period, based on the rationale that a lower bulk liquid concentration results in lower biofilm penetration depth by diffusion and would thus favor smaller size granules. A smaller average granule size for the same amount of biomass produced would increase specific surface area, which is expected to then increase the specific nitrification rate because most of the nitrifiers grow on the oxygen rich outer portion of the granules.

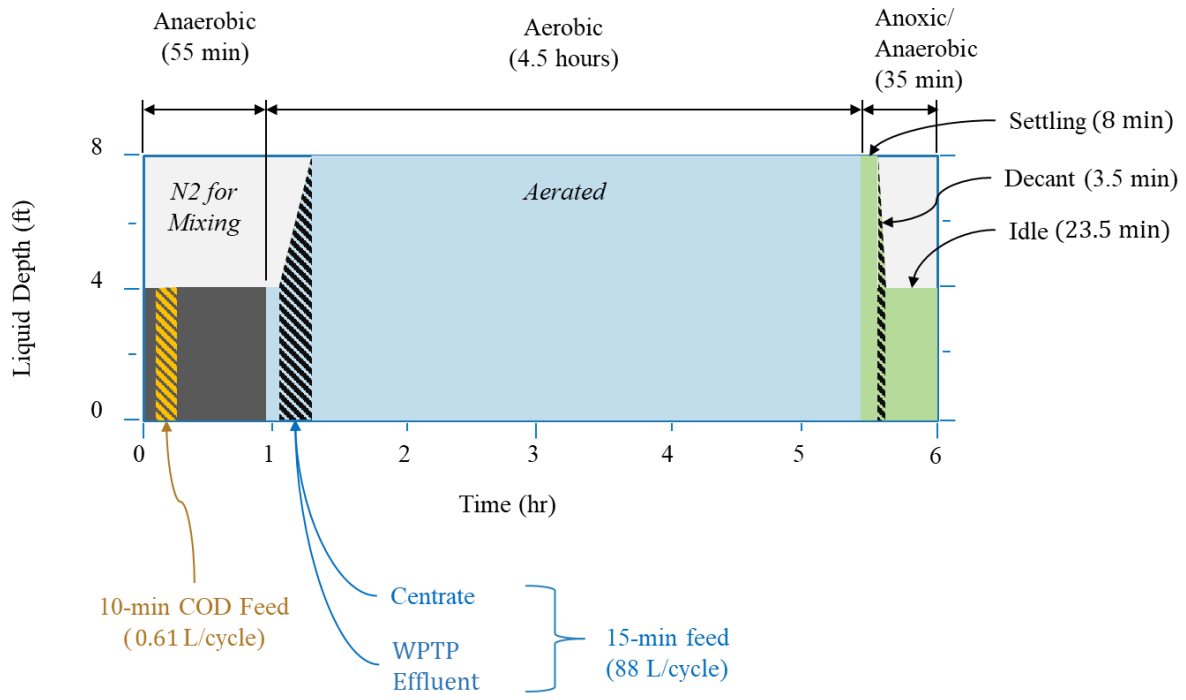

Figure 4-1. Sidestream SBR 6-hr cycle consisting of anaerobic, aerobic, settling, decanting, and idle phases and respective times, and reactor depth. (Adapted from Armenta, 2019)

4.1.1.2 Sidestream Reactor Target NH_3-N Loading and Operating Conditions for Study Period

The sidestream reactor NH_3-N loading was based on having the sidestream treat 10 to 20% of the ammonia load normally fed to the secondary process, to represent typical conditions of full-scale wastewater treatment plants with anaerobic digestion and centrate return. This resulted in selecting a target NH_3-N volumetric loading of 0.30 to 0.35 g NH_3-N/L-d. In addition, the target SRT was set at 25 days, and the reactor DO concentration and feed COD:N were based on conditions in the previous study that sustained shortcut nitrogen removal and minimized the required COD feed amount. Minimal changes in operating parameters were made to maintain a consistent and stable operation. The key operation conditions are summarized in Table 4-1. With shortcut nitrogen removal, a feed COD:N ratio of 3.5 g/g was adequate in the previous study to maintain high denitrification efficiency. An effluent NH_3-N concentration of 20 mg/L or more

with a control DO of 2.0 mg/L suppressed NOB growth to produce a high proportion of NO_2-N from nitrification. The DO concentration was increased from 2.0 to 2.2 in mid-September to increase the nitrification rate of the granular sludge in response to observing lower SNRs than for previous months of operation.

Table 4-1. Summary of the target operating conditions for the sidestream reactor from September 1, 2019 to March 16, 2020.

Date of Change	Ammonia Loading g NH_3-N/L-d	COD:NH_3-N Feed Ratio gCOD/gN	Target SRT days	DO Set Point mg/L
9/1/2019	0.30	3.5	25	2.0
9/19/2019				2.2
12/1/2019	0.35			

4.1.2 Sidestream Treatment Performance

The results in Figure 4-2 show variations in the NH_3-N loading to the sidestream SBR and the influent and effluent NH_3-N concentrations. The influent concentration is based on the combined flows to the SBR. The NH_3-N loading varied from 0.25 to 0.45 g/L-d due to the variations in the centrate used for each feed batch. However, the monthly average NH_3-N loading ranged from 0.25 to 0.35 g/L-d, as shown in Tables 4-2 and 4-3. Variations in the effluent NH_3-N concentration generally followed the influent NH_3-N loading variations. However, in March 2020 the effluent NH_3-N concentration was higher than for operations at similar NH_3-N loading, and a gradual increase to 100 mg/L was observed. Additionally, in late November 2019 and early December 2020, a decrease in effluent NH_3-N from about 100 to 0 mg/L was caused by an increase in daily average DO, which gradually increased from 2.3 to 4.6 mg/L. The increase in DO occurred when the mainstream system was shut down after Phase 1, which resulted in too

much air flow to the sidestream from the common air feed line until the line pressure regulator was adjusted.

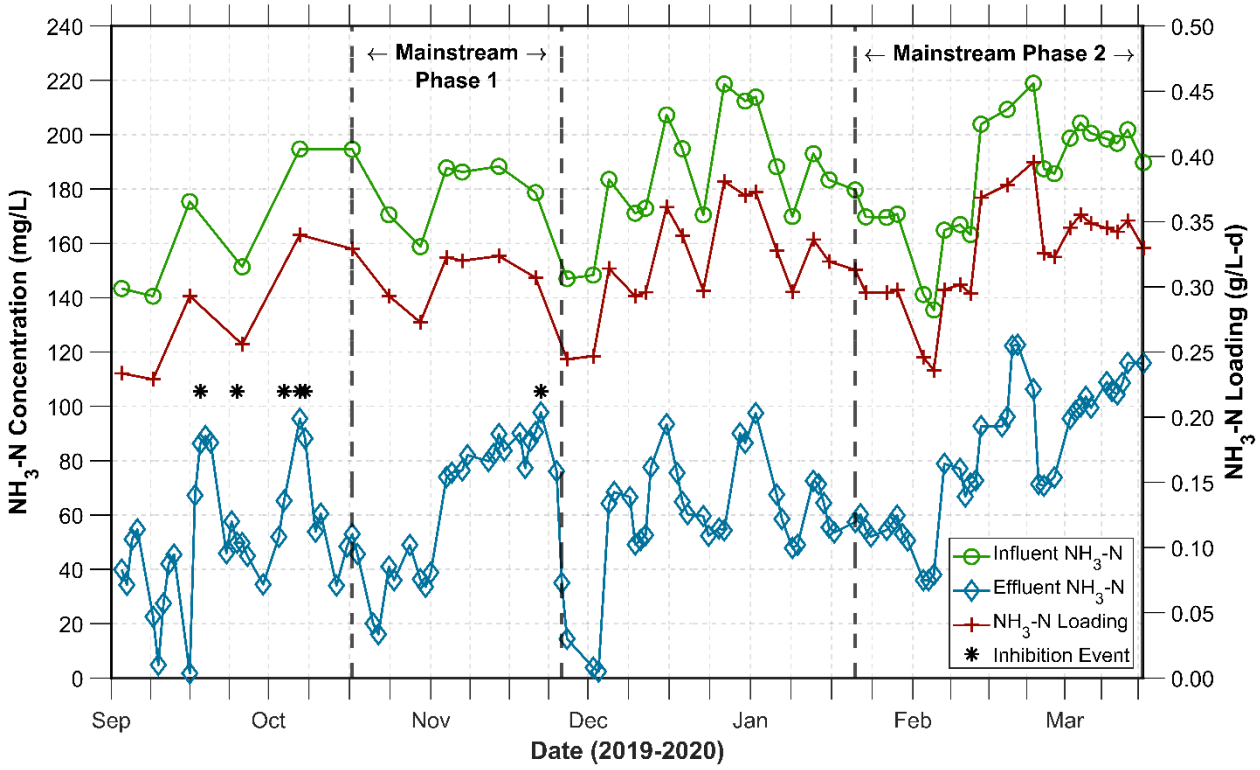

Figure 4-2. Sidestream reactor NH_3-N influent and effluent concentrations, NH_3-N loading, and inhibition events from September 1, 2019 to March 16, 2020.

As shown in Figure 4-3, the percentage of the bioavailable influent nitrogen in the effluent increased from September 2019 to March 2020 and the nitrification efficiency decreased. The lower nitrification efficiency in March was affected by a lower reactor MLSS concentration from increased wasting of granules for bioaugmentation from December to March. Over the September to March operating period the average nitrification efficiency was 61 ± 10%, the ammonia used in cell synthesis averaged 4 ± 1% of the NH_3-N fed, and the remaining NH_3-N was in the effluent, which averaged 35 ± 10% of the NH_3-N fed. However, the average

nitrification efficiency was above 80% during August and July 2019. After inhibition events during August and September the average monthly SNR decreased from about 2.5 to 1.25 mgN/gVSS-h (Figure 4-3). Inhibition events were defined as when the acetate COD leakage into the aerobic phase was ≥ 2% of the acetate COD fed and when the nitrification efficiency dramatically decreased. The average acetate leakage was 1% between September 2019 and March 2020. In response to the inhibition events the NH_3-N loading was decreased, which resulted in a monthly average NH_3-N loading of 0.25 g/L-d during September. After September, NH_3-N loading averaged between 0.30 and 0.35 g/L-d (Table 4-2, Table 4-3).

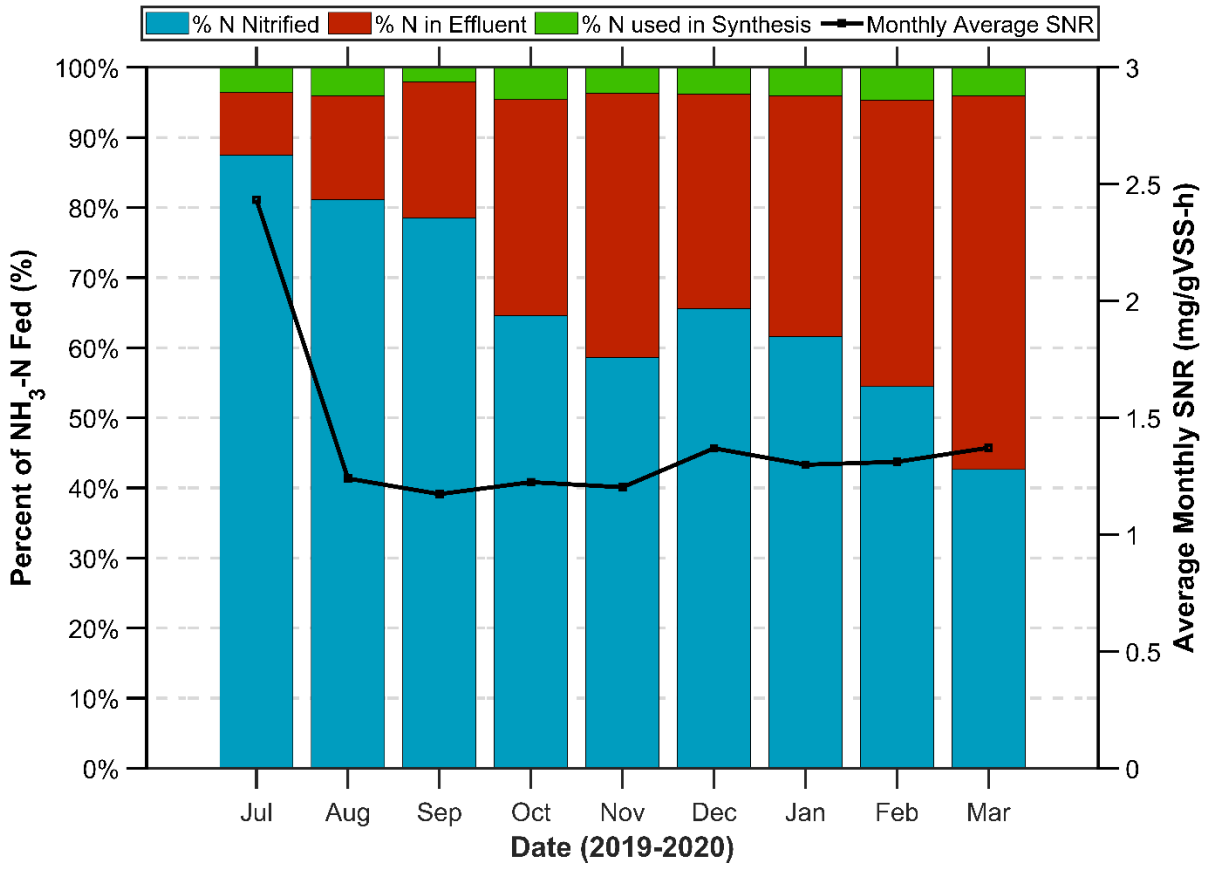

Figure 4-3. Sidestream SBR monthly average values for the fate of bioavailable influent nitrogen between % nitrified, % in the effluent, and % used for biomass synthesis, and monthly average SNR from July 2019 to March 2020.

The average monthly operating conditions and performance are summarized in Tables 4-2 for September 2019 through December 2019 and Table 4-3 for January 2020 through March 16, 2020.

Table 4-2. Monthly average treatment performance for the sidestream reactor between Sep 1, 2019 and Dec 31, 2019 (standard deviation in parenthesis).

		Month			
Parameter	**Units**	**September**	**October**	**November**	**December**
7-day Moving Average SRT	d	65 (12)	32 (8)	35 (9)	33 (4)
Aeration Phase DO	mg/L	2.3 (0.3)	2.4 (0.1)	2.6 (0.6)	2.5 (0.6)
Aeration Phase pH		7.8 (0.1)	7.8 (0.1)	8.0 (0.2)	8.1 (0.1)
Anaerobic Phase pH		7.4 (0.1)	7.4 (0.1)	7.8 (0.2)	8.0 (0.1)
Temperature	°C	20.6 (1.7)	18.3 (1.7)	17.1 (0.9)	16.3 (0.4)
MLSS	g/L	12.8 (2.0)	14.4 (1.1)	12.1 (0.8)	12.6 (0.9)
MLVSS/MLSS		0.80 (0.02)	0.74 (0.01)	0.73 (0.03)	0.70 (0.02)
Loading					
NH_3-N loading	g/L-d	0.25 (0.03)	0.31 (0.03)	0.30 (0.03)	0.32 (0.04)
Feed COD:N Ratio	g/g	3.6 (0.3)	3.8 (0.5)	3.7 (0.1)	3.6 (0.4)
Granular Sludge Characteristics					
Diameter	mm	1.9 (0.1)	N/A	1.57	1.65
SVI_{30}	mL/g	24 (2)	24 (1)	26 (2)	28 (3)
SVI_5/SVI_{30}		1.00 (0.00)	1.01 (0.00)	1.01 (0.01)	1.02 (0.01)
Removal Efficiency					
NH_3-N	%	81 (12)	69 (11)	62 (15)	69 (11)
TIN	%	74 (6)	67 (10)	54 (4)	61 (9)
SND	%	92 (8)	96 (1)	89 (15)	91 (19)
PO_4-P	%	91 (5)	78 (20)	49 (41)	70 (36)
$COD_{fed}/N_{removal}$	g/g	4.7 (1.1)	6.1 (1.2)	6.6 (1.3)	5.6 (0.8)
Effluent					
NH_3-N	mg/L	46.8 (23.1)	48.7 (20.2)	73.6 (21.8)	59.3 (23.3)
NO_2-N	mg/L	1.9 (2.8)	1.8 (0.6)	3.1 (5.1)	4.4 (9.3)
NO_3-N	mg/L	0.7 (1.1)	0.5 (0.2)	0.7 (0.8)	1.0 (1.8)
PO_4-P	mg/L	4.0 (7.3)	2.8 (5.8)	4.8 (6.1)	3.0 (5.5)

Table 4-3. Monthly average treatment performance for the sidestream reactor between January 1, 2020 and March 16, 2020 (standard deviation in parenthesis).

		Month		
Parameter	**Units**	**January**	**February**	**March**
7-day Moving Average SRT	d	30 (2)	26 (1)	25 (1)
Aeration Phase DO	mg/L	2.3 (0.1)	2.3 (0.1)	2.2 (0.3)
Aeration Phase pH		8.1 (0.1)	8.0 (0.1)	7.8 (0.1)
Anaerobic Phase pH		7.9 (0.2)	7.9 (0.1)	7.6 (0.2)
Temperature	°C	17.6 (1.0)	17.1 (0.7)	17.0 (0.4)
MLSS	g/L	12.8 (0.8)	11.3 (0.5)	8.6 (0.6)
MLVSS/MLSS		0.70 (0.01)	0.69 (0.01)	0.72 (0.02)
Loading				
NH_3-N loading	g/L-d	0.32 (0.02)	0.32 (0.05)	0.35 (0.01)
Feed COD:N Ratio	g/g	3.7 (0.3)	3.7 (0.7)	3.2 (0.1)
Granular Sludge Characteristics				
Diameter	mm	1.4	1.54	1.25
SVI_{30}	mL/g	28 (1)	31 (1)	37 (3)
SVI_5/SVI_{30}		1.01 (0.01)	1.01 (0.01)	1.00 (0.00)
Removal Efficiency				
NH_3-N	%	66 (5)	59 (8)	47 (4)
TIN	%	62 (4)	53 (9)	43 (3)
SND	%	94 (2)	89 (5)	92 (5)
PO_4-P	%	90 (5)	66 (25)	28 (37)
$COD_{fed}/N_{removal}$	g/g	6.0 (0.3)	6.7 (1.0)	7.5 (1.0)
Effluent				
NH_3-N	mg/L	59.9 (11.2)	78.0 (25.4)	105.1 (6.5)
NO_2-N	mg/L	2.6 (1.1)	4.3 (2.2)	2.8 (1.7)
NO_3-N	mg/L	0.6 (0.2)	1.0 (0.4)	0.6 (0.4)
PO_4-P	mg/L	3.1 (5.4)	4.7 (5.0)	13.5 (10.1)

The phosphorus removal efficiency averaged 28 to 91% (Tables 4.2 and 4.3). The average PO_4-P removal efficiency during November 2019 was 49% which was lower than the preceding and following months due to two events where the removal efficiency dramatically decreased from about 90% to about 30% and quickly recovered. Similar events during October and December caused slightly lower removal efficiencies of 78 and 70%, respectively. The PO_4-P removal efficiency averaged 66 and 25% in February and March, respectively, correlating with a decrease in MLVSS because of higher wasting for bioaugmentation during those months. Mixed liquor wasting was curtailed during inhibition events in August and September 2019 (Figure 4-2) which resulted in an average monthly SRT of 65 days. The average monthly SRT varied between 25 and 35 days after September. The mixed liquor and AGS SRTs of the sidestream reactor versus time are shown in Figure 4-4. The AGS SRT is longer than the MLSS SRT because flocculent sludge is disproportionally wasted in the effluent. The effluent percent granules averaged 24% from September 2019 to March 2020, while the average percent of granules in the reactor MLSS was 98%. The average granule diameter also increased during September to 1.9 mm, which is 35% larger than the average diameter of 1.4 mm (Armenta, 2019) in the months before September. The SND efficiency ranged from 89 to 96%, indicating that there always was sufficient anoxic/anaerobic volume and stored carbon by the PAOs in the inner core of the granules to result in a high denitrification efficiency at average bulk liquid DO concentrations between 2.2 to 2.6 mg/L.

Throughout the operational period, the monthly average SVI_5/SVI_{30} ranged from 1.00 to 1.02, indicating a system dominated by granular sludge system (Table 4-2, Table 4-3). The average SVI_{30} ranged from 20 to 31 mL/g for the months prior to March, which averaged 37 mL/g. The

higher SVI_{30} may be related to the much lower MLSS concentration of 8.6 g/L during that month (Table 4-3). The effluent TSS concentrations were between 50 and 120 mg/L, for the entire operational period, which is typical for the sidestream SBR. However, the manual wasting rate was increased by about 20% on January 16th and by about 17% on February 27th to increase bioaugmentation, which caused the MLSS reduction.

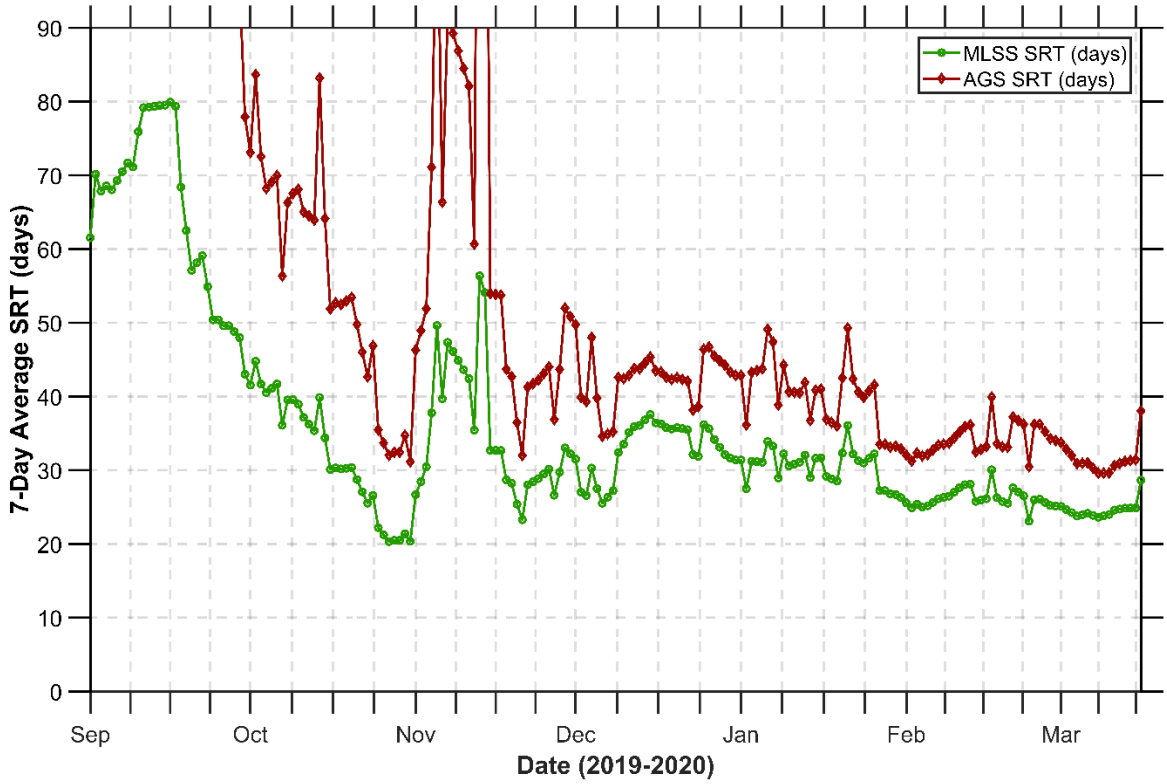

Figure 4-4. Sidestream SBR 7-day average MLSS SRT and AGS SRTs from September 2019 to March 2020. Because of the reduced wasting in August and September the AGS SRT ranged from 100 to 600 days (data points not shown).

The monthly average pH during the aeration phase was 7.8 to 8.1 and 7.4 to 8.0 during the anaerobic phase. Aeration and anaerobic phase pH were about 0.4 units higher than previous reported pH averages within the reactor (Armenta, 2019). The higher pH was likely a result of

higher alkalinity within the reactor, resulting from less nitrification of the centrate feed containing NH_4HCO_3.

4.1.3 Sidestream Granular Sludge Characteristics

During the 6.5-month operational period the sidestream SBR had a monthly average MLSS of 8.6 to 14.4 g/L, an average granule diameter of 1.25 to 1.90 mm, and an average SVI_5/SVI_{30} ratio of 1.00 – 1.02 (Tables 4-4). To track the granule size distribution in the sidestream, sieve analyses were performed monthly during the full operation period (Section 3.4.1). Based on monthly sieve analysis, the MLSS percent granules in the reactor varied between 95 and 99%. The lowest MLSS percent granules of 95% was measured in March 2020, which was the same month for the lowest MLSS concentration and SRT. The SVI_5/SVI_{30} ratios of 1.00 to 1.02 also show that the mixed liquor was predominantly granular sludge.

Table 4-4. Average monthly granule sludge characteristics for the sidestream reactor (standard deviation in parenthesis).

		Month						
Parameter	Units	September	October	November	December	January	February	March
7-day Moving Average SRT	d	65 (12)	32 (8)	35 (9)	33 (4)	30 (2)	26 (1)	25 (1)
MLSS	g/L	12.8 (2.0)	14.4 (1.1)	12.1 (0.8)	12.6 (0.9)	12.8 (0.8)	11.3 (0.5)	8.6 (0.6)
MLSS Percent Granules	%	98 (1)	N/A	98	99	99	98	95
Average Diameter	mm	1.9 (0.1)	N/A	1.57	1.65	1.4	1.54	1.25
50th Percentile Diameter	mm	2.0 (0.1)	N/A	1.4	1.4	1.0	1.2	1.1
SVI_{30}	mL/g	24 (2)	24 (1)	26 (2)	28 (3)	28 (1)	31 (1)	37 (3)
SVI_5/SVI_{30}		1.00 (0.00)	1.01 (0.00)	1.01 (0.01)	1.02 (0.01)	1.01 (0.01)	1.01 (0.01)	1.00 (0.00)

As shown in Figure 4-5, there was a spike in the abundance of larger granules in early September 2019; the fraction of granules greater than 2900 µm increased 25% between August 8th and September 9th. This followed the nitrification upsets in August and increase in the reactor SRT to a high monthly average SRT of 65 ± 12 days (Table 4-4). Furthermore, the average granular size decreased after September, corresponding to a decrease in SRT, and approached the August 2019 size distribution during December 2019 (Figure 4-5). After December, the average granule diameter and 50th percentile diameter decreased further, corresponding to a further decrease in the SRT. The acetate feed time was increased on January 10, 2020, which did not seem to influence the average granule diameter. The results suggest that the SRT is an important factor affecting the granular size.

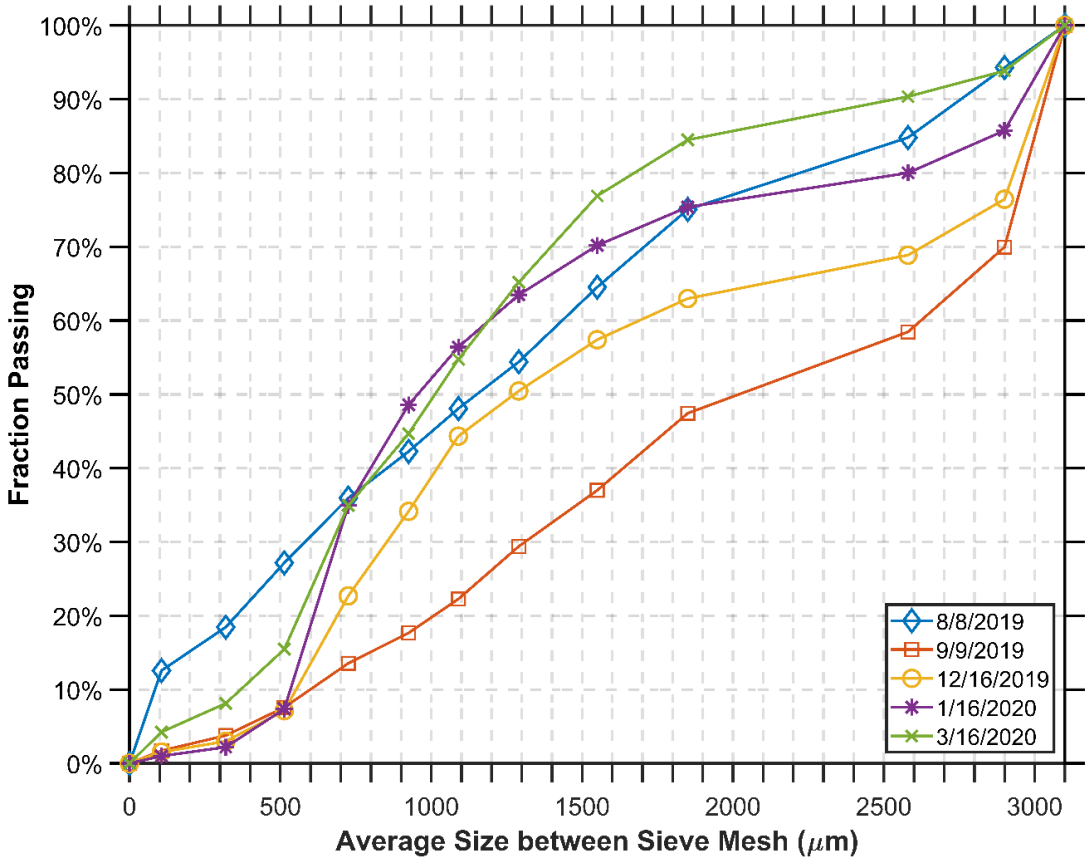

Figure 4-5. Sidestream granule size distribution between August 8, 2019 and March 16, 2020.

The photos in Figure 4-6 show that the sidestream mixed liquor maintained a relatively spherical morphology, with nodules growing throughout the granule surfaces. Filaments can be seen growing off the granules in the photos taken on February 26th and March 16th, which corresponds to an increased SVI_{30} during those months. The monthly average SVI_{30} was from 24 to 28 mL/g before February 2020 and 31 to 37 mL/g after February (Table 4-4).

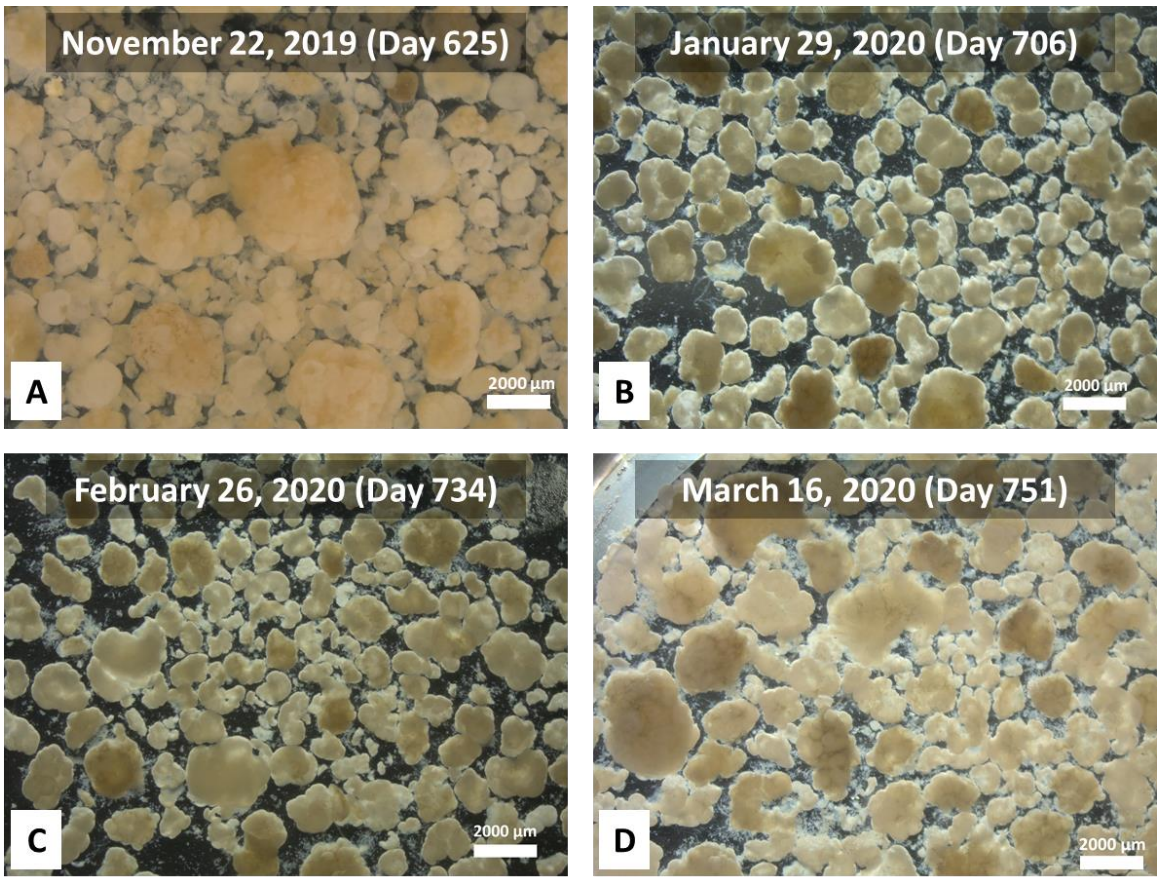

Figure 4-6. Images of sidestream aerobic granules taken with a camera mounted to a stereo microscope.

4.1.4 Sidestream Shortcut N Removal

One of the primary goals of the sidestream reactor operation was to maintain shortcut nitrogen removal, which requires less oxygen for nitrification and less COD for nitrogen removal, by

supporting AOB growth and suppressing NOB growth. Four criteria used to evaluate the occurrence of shortcut nitrogen removal are; 1) a frequent effluent NO_2^--N:NO_3^--N concentration ratio of ≥ 1.0, 2) an AOB:NOB qPCR ratio of > 2.5, 3) a much higher NH_3 oxidation rate than NO_2 oxidation rate in batch tests, and 4) a COD_{used}:NO_x-$N_{removed}$ ratio of significantly less than 4.8 g/g. The basis of these ratio values is explained in the following.

The ratio of AOB:NOB biomass for complete nitrification to NO_3^- is proportional to the synthesis yield coefficients per unit of N oxidized, assuming equal specific endogenous decay rates. Fang et al. (2009) reported AOB:NOB yield ratios of 2.1 to 2.5. Thus, assuming that qPCR abundance is equally representative of AOB and NOB biomass concentration, a qPCR AOB:NOB ratio of greater than 2.5 implies NOB suppression. Figure 4-7 shows that the qPCR AOB:NOB ratio was consistently between 3 and 4 indicating NOB suppression. Additionally, Figure 4-8 shows that the effluent NO_2^--N:NO_3^--N concentration ratio was generally in the range of 3.0 and 4.0, which indicates NOB suppression because NOB have a higher growth rate than AOB and thus convert NO_2 to NO_3 almost as fast as NO_2 is produced. . Three different sidestream mixed liquor batch kinetic tests on November 27, 2019, December 5, 2019, and March 16, 2020, confirmed specific NO_2 production rates between 3 and 10 times greater than the specific NO_2-N oxidation rates.

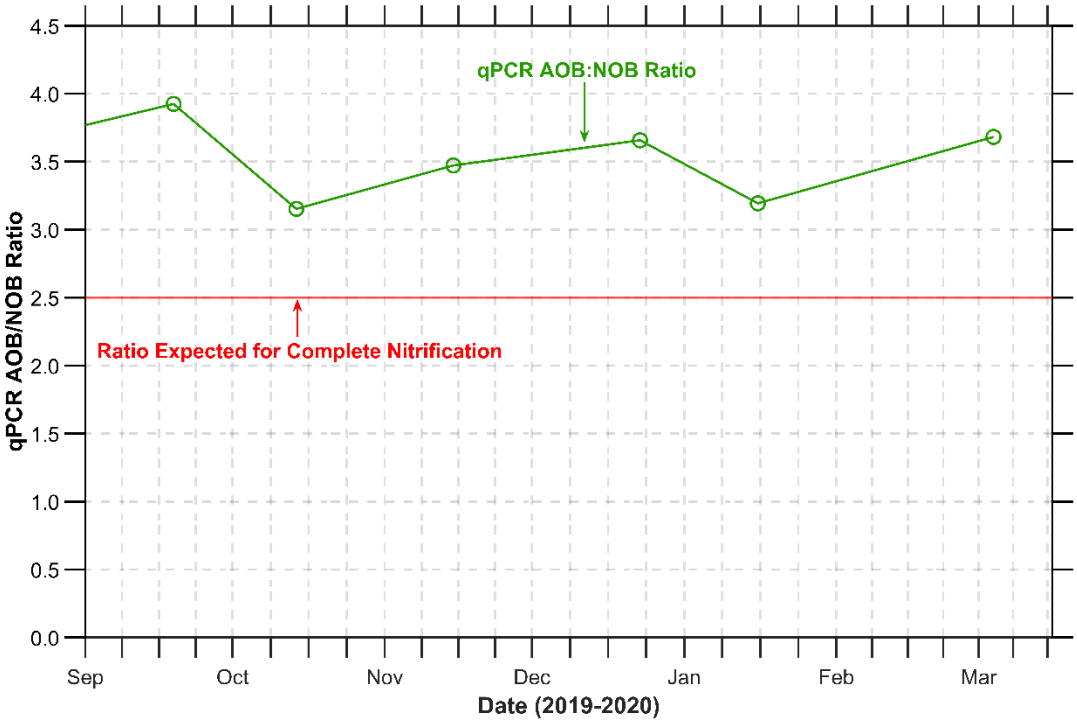

Figure 4-7. The sidestream SBR qPCR AOB:NOB ratio and the ratio expected for complete nitrification. qPCR data was provided by Bao Ngyuen Quoc, UW PhD candidate.

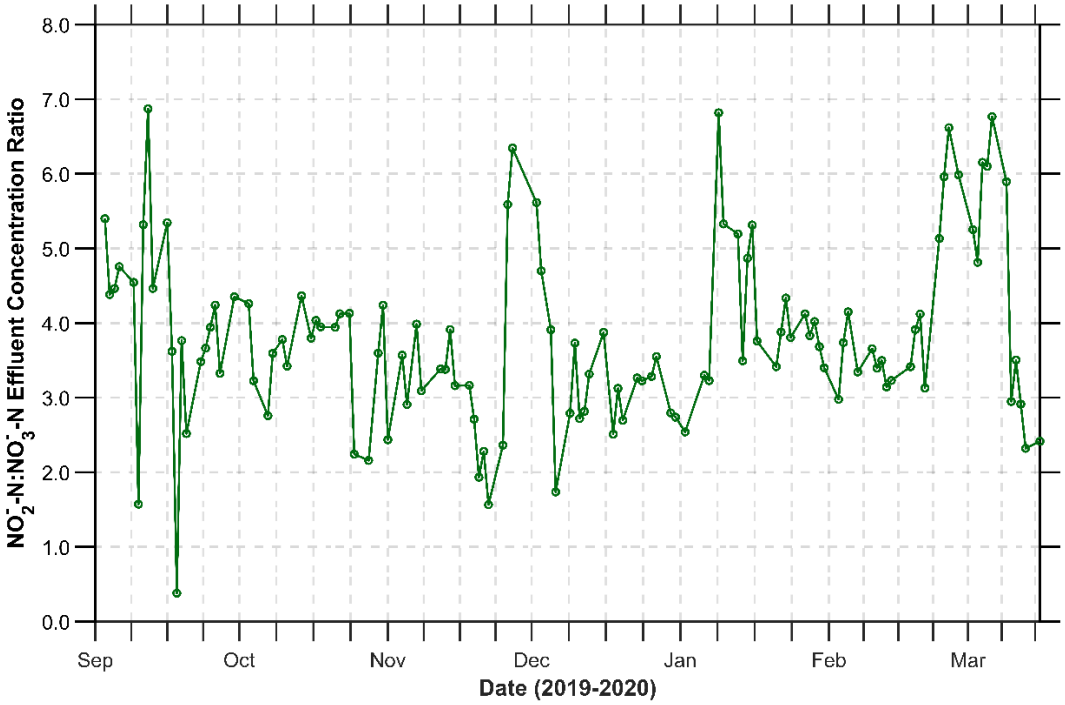

Figure 4-8. The sidestream effluent NO_2^--N:NO_3^--N concentration ratio from September 1, 2019 to March 16, 2020.

The DO:NH_3-N ratio has proven to be indicative of NOB suppression in granular sludge, at ratios less than 0.41 mgO_2/mgN providing 80 to 100% inhibition (Table 2-1). The mechanism for NOB inhibition based on DO:NH_3-N ratio is a result of the diffusion limitations of granules and the need for AOB to produce NO_2 first before NOBs can grow, which should favor their growth. At higher bulk liquid NH_3-N concentration, increased AOB growth rate may allow them to dominate the granule outer layer. AOBs also have a higher biomass yield than NOBs, which favors their dominance on the granule outer layer. DO consumption by AOB and diffusion limitation can result in lower NOB activity in the inner granule layers. At the same bulk liquid NH_3-N concentration, a higher DO concentration would increase both AOB and NOB activity, but at a lower DO concentration the NOB activity would be decreased more than the AOB activity due to less oxygen in the inner layers and a higher half velocity coefficient values for NOB than for AOB. Thus lower DO:NH_3-N ratios favor AOB growth more than NOB growth and higher DO:NH_3-N ratios are expected to decrease the AOB/NOB growth ratio. In this study the critical DO:NH_3-N ratio was calculated as the DO concentration at the end of aeration divided by the effluent NH_3-N concentration, because any DO:NH_3-N ratio during aeration before that is lower due to the higher NH_3-N concentration.

Monthly average DO:NH_3-N ratios of between 0.02 and 0.58 mg/mg were measured in the sidestream SBR between September 1, 2019 and March 16, 2020. The months of September and December both had high DO:NH_3-N averages with high standard deviations, 0.34 ± 1.01 and 0.58 ± 1.20 mg/mg, respectively. This is likely a result of the large variation in effluent NH_3-N during those months (Figure 4-2). During every other month, the average DO:NH_3-N ratio was between 0.02 and 0.06 mg/mg, indicative of NOB inhibition.

4.1.5 Sidestream Nitrification Kinetics

Table 4-5 summarizes the average monthly SNRs and relevant sidestream reactor operating characteristics including the ammonia loading rate, MLSS concentration, and granular sludge characteristics. The nitrification rates are based on ammonia removal rates during the SBR aeration phase. The average monthly specific nitrification rate (SNR) ranged between 1.2 and 1.4 mgN/gVSS-hr. During this operating period, the NH_3-N loading used was lower than that normally used during previous periods and the effluent NH_3-N concentration was higher than expected. Monthly average values ranged from 46 to 105 mg/L and the average monthly NH_3-N oxidation efficiency ranged from 43 to 66% except for a value of 78% in September (Table 4-5). The NH_3-N oxidation efficiency was much higher for the sidestream reactor operation by Armenta (2019) during stable operating periods with similar NH_3-N loading, of 0.36 g/L-d. The two operating periods had average NH_3-N oxidation efficiencies of 90 and 89%, respectively, with much lower effluent NH_3-N concentrations. The average SNR values reported for those periods were 1.6 and 1.8 mg/gVSS-hr. This suggests that the SNR during the operating period was hindered or inhibited compared to the previous operating periods by Armenta (2019).

Table 4-5. Average monthly ammonia loading rate, aeration phase DO, granular sludge characteristics, and nitrification rate (standard deviation in parenthesis).

		Month						
Parameter	Units	September	October	November	December	January	February	March
NH_3-N loading Rate	g/L-d	0.25 (0.03)	0.31 (0.03)	0.30 (0.03)	0.32 (0.04)	0.32 (0.02)	0.32 (0.05)	0.35 (0.01)
Aeration Phase DO	mg/L	2.3 (0.3)	2.4 (0.1)	2.6 (0.6)	2.5 (0.6)	2.3 (0.1)	2.3 (0.1)	2.2 (0.3)
Feed COD:N Ratio	g/g	3.6 (0.3)	3.8 (0.5)	3.7 (0.1)	3.6 (0.4)	3.7 (0.3)	3.7 (0.7)	3.2 (0.1)
MLSS	g/L	12.8 (2.0)	14.4 (1.1)	12.1 (0.8)	12.6 (0.9)	12.8 (0.8)	11.3 (0.5)	8.6 (0.6)
Granular Sludge Characteristics								
Diameter	mm	1.9 (0.1)	N/A	1.57	1.65	1.4	1.54	1.25
Specific Surface Area	cm^2/gVSS	67 (4)	N/A	86	81	87	89	108
Nitrification								
NH_3-N Oxidation Efficiency	%	78 (13)	65 (10)	59 (14)	66 (11)	62 (5)	54 (7)	43 (4)
NH_3-N Oxidation Rate	mg/L-hr	12.2 (3.0)	11.8 (1.5)	10.4 (1.5)	12.4 (1.6)	11.5 (0.5)	10.0 (1.1)	8.8 (1.0)
Specific nitrification rate (SNR)	mg/gVSS-hr	1.2 (0.2)	1.2 (0.3)*	1.2 (0.2)	1.4 (0.2)	1.3 (0.1)	1.3 (0.2)	1.4 (0.2)

*SNRs in October were calculated with the monthly average MLVSS due to sample coordination difficulties.

Ammonia oxidation rate depends on reactor NH_3-N, DO, and AOB concentrations and growth kinetics (Tchobanoglous et al., 2014). The relationship between nitrification kinetics and NH_3-N and DO concentrations is described by Michaelis-Menten substrate utilization kinetics. The reactor effluent NH_3-N concentration was typically greater than 40 mg/L (Figure 4-2), which is high enough to not limit the nitrification rate. Thus, the rate was related to the DO concentration and AOB concentration available on the outer aerobic layers of the granules. The SNR, which is related to the granular mass, would also be affected by the granular size. Assuming spherical granules and AOB activity in the outer layer, as the granule diameter increases the surface area to volume ratio decreases and thus the SNR would decrease. Therefore, a smaller average granule diameter should correlate to a higher SNR. The effect of granular size is evaluated in Figure 4-9 by comparing the SNR values to the average specific surface area of the granular sludge for this study and for Armenta (2019) results from stable performance periods. Though a trend of a lower SNR with a lower specific surface area is indicated by Armenta's results, there is no such trend for the data in this study. Lower and similar SNRs are shown for specific surface areas ranging from 60 to 110 cm^2/gMLVSS.

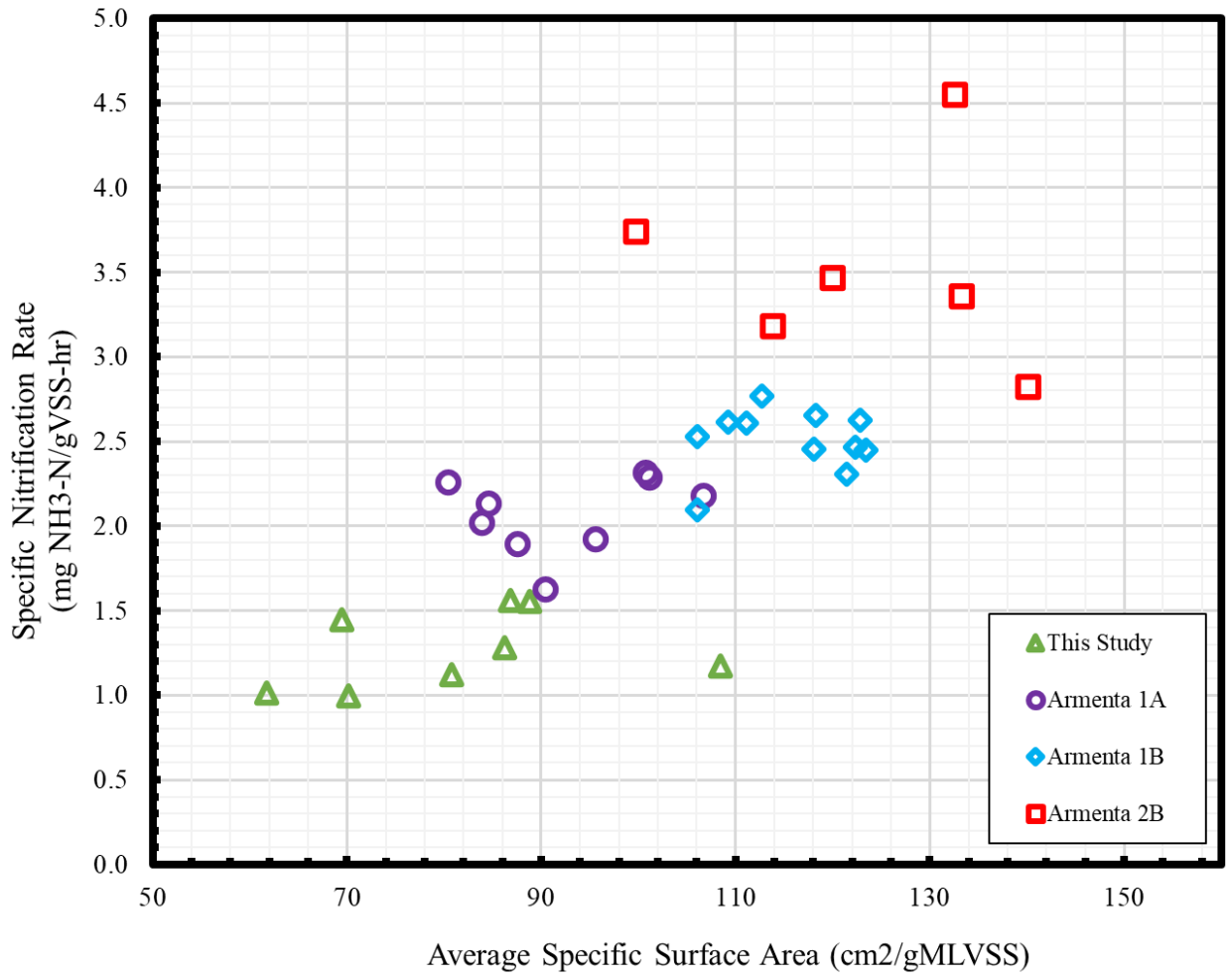

Figure 4-9. Specific Nitrification Rate (SNR) versus average granular sludge specific surface area for stable operating periods during previous operation periods (1A, 1B, 2B) by Armenta (2019) and this study.

Molecular analyses of the sidestream granules were applied to understand the cause of the lower SNR and NH_3-N oxidation efficiency.

In August and September 2019, a significant nitrification inhibition event decreased the nitrification efficiency, which was sustained for the entire study period. During this period, the amount of acetate fed was maintained and over 99% of it was consumed in the anaerobic phase

to suggest that the PAO/GAO population was maintained. Because of the relative carbon and NH_3 feed amounts and the much lower yield of autotrophic bacteria, the AOB and NOB population was expected to be a much lower fraction of the total bacteria population. In addition, the decrease in nitrification efficiency with less NH_3-N oxidized suggests a lower fraction of AOB in the total biomass DNA. The measurement of the *amoA* gene copy number per ng DNA confirms the expected decrease in AOB relative to the heterotrophic bacteria growth, as shown in Figure 4-10. A significant decrease in the SNR is correlated with the decrease of the AOB population. The decrease in the SNR correlates well the with the decreased fraction of the AOB in the biomass. There was a slight increase in AOB population in December, which correlates to a slight increase, from 1.2 to 1.3-1.4 mgN/gVSS-g, in monthly average SNR (Table 4-5). There was a further increase in the AOB population fraction observed on March 4, 2020, which correlated to an SNR increase to about 1.5 mgN/gVSS-h. However, the nitrification efficiency declined in March, from about 50% to 35% (Figure 4-3), most likely caused by a decreased MLSS concentration. The pilot was shut down on March 16, 2020, so it is unknown whether the AOB population fraction declined, causing the decline in SNR after March 4, 2020 (Figure 4-10).

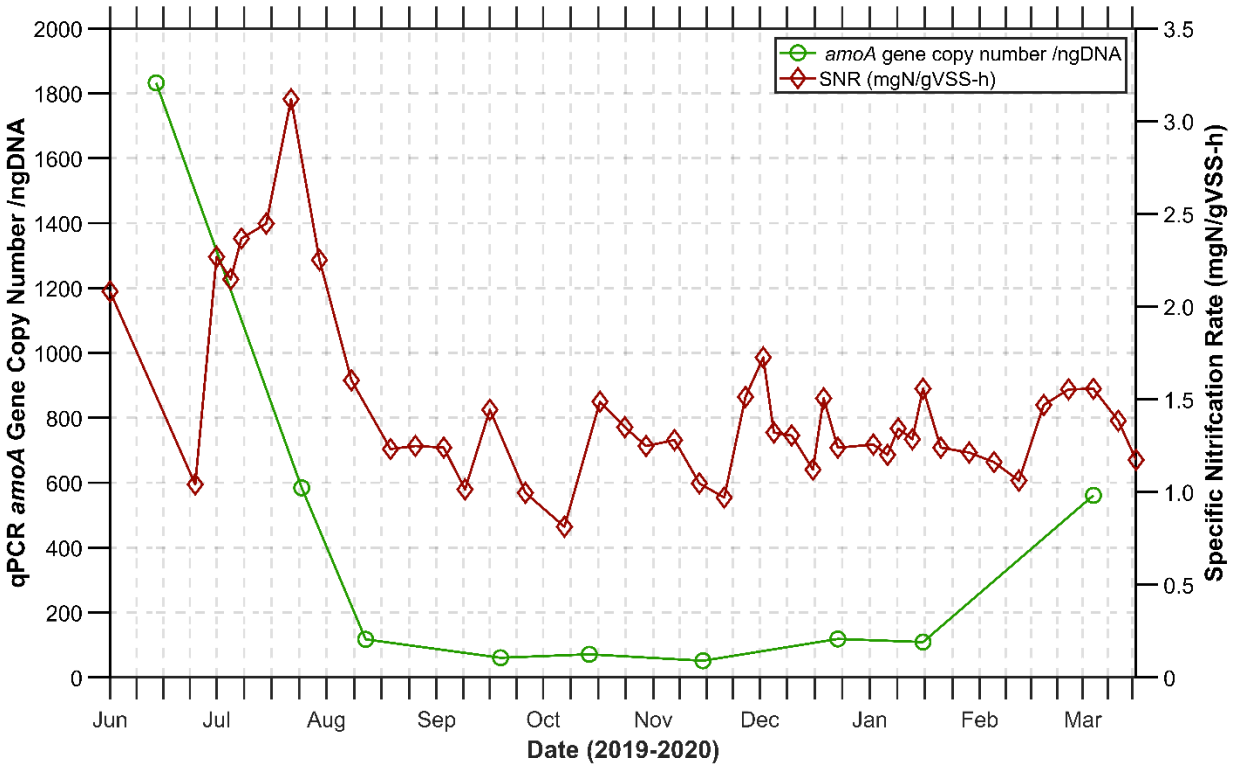

Figure 4-10. Fraction of AOB in biomass based on ratio of *amoA* gene copy number per 1 ngDNA and mixed liquor specific nitrification rate (mgN/gVSS-h) from June 2019 to March 2020. (qPCR data was provided by Bao Ngyuen Quoc, UW PhD candidate)

A hypothesis to explore the lower SNR considers the COD:N feed ratio and the COD_{fed}:NO_x-$N_{removed}$ ratio. The operating goal for this study was to maintain a COD:N feed in the range of 3.5 because that was shown to be an acceptable ratio during the previous work by Armenta (2019) with shortcut nitrogen removal. However, the net amount of COD used per NO_x removed in this study was much higher because of the lower nitrification efficiency. An expected COD_{used}:NO_2^--$N_{removed}$ ratio is in the range of 2.9 to 3.7 gCOD/gN (Bowden et al., 2016). The monthly average COD:N fed ratio varied between 3.2 and 3.8 g/g (Tables 4-2 and 4-3), which is in the range for shortcut nitrogen removal but the COD_{used}/NO_x-$N_{removed}$ ratio was from 6 to 7 g/g, showing that more acetate COD was added than needed for shortcut nitrogen removal.

About 99% of the acetate fed during the anaerobic phase to the SBR was taken up by the biomass before aeration. If the $COD_{fed}/NO_x\text{-}N_{removed}$ equals the $COD_{used}/NO_x\text{-}N_{removed}$ ratio close to the theoretical value needed for mainly NO_2 reduction it can be assumed that COD fed is used for PAO growth using NO_2 as the electron acceptor. The PAOs would use NO_2 diffusing to the interior of the granule during nitrification in the aerobic phase for oxidation of their stored products from acetate uptake during anaerobic feeding. At the higher COD_{used}:$NO_x\text{-}N_{removed}$ ratios dissolved oxygen must be used to oxidize some of the acetate COD taken up during anaerobic conditions. This suggests that PAOs and/or GAOs are growing in aerobic zones of the granules and competing for oxygen with the nitrifiers. Growth of PAOs and/or GAOs near the surface would also complete with nitrifiers for space. The competition by these heterotrophs for space and oxygen would affect the SNR at a given reactor DO concentration due to oxygen diffusion limitations. Understanding the population density and granular distribution of AOBs, PAOs, and GAOs, may help to understand changes in SNR values during the sidestream pilot plant operation.

The results of the fluorescence in situ hybridization (FISH) analysis for February 2020 and June 2019 samples of the sidestream granules shown that there was a greater quantity of PAOs in the outer granule layers during this study period with lower SNRs than in the previous operation. The FISH images in Figure 4-11 show a distinct AOB layer on the outside of the granule in June 2019, while in February 2020 AOBs and PAOs sharing the same space. Because GAOs appear to be relatively insignificant in both qPCR and FISH data, the FISH analysis helps to reinforce that PAOs were growing on the outside of the granules and competing with AOBs for oxygen and growth sites.

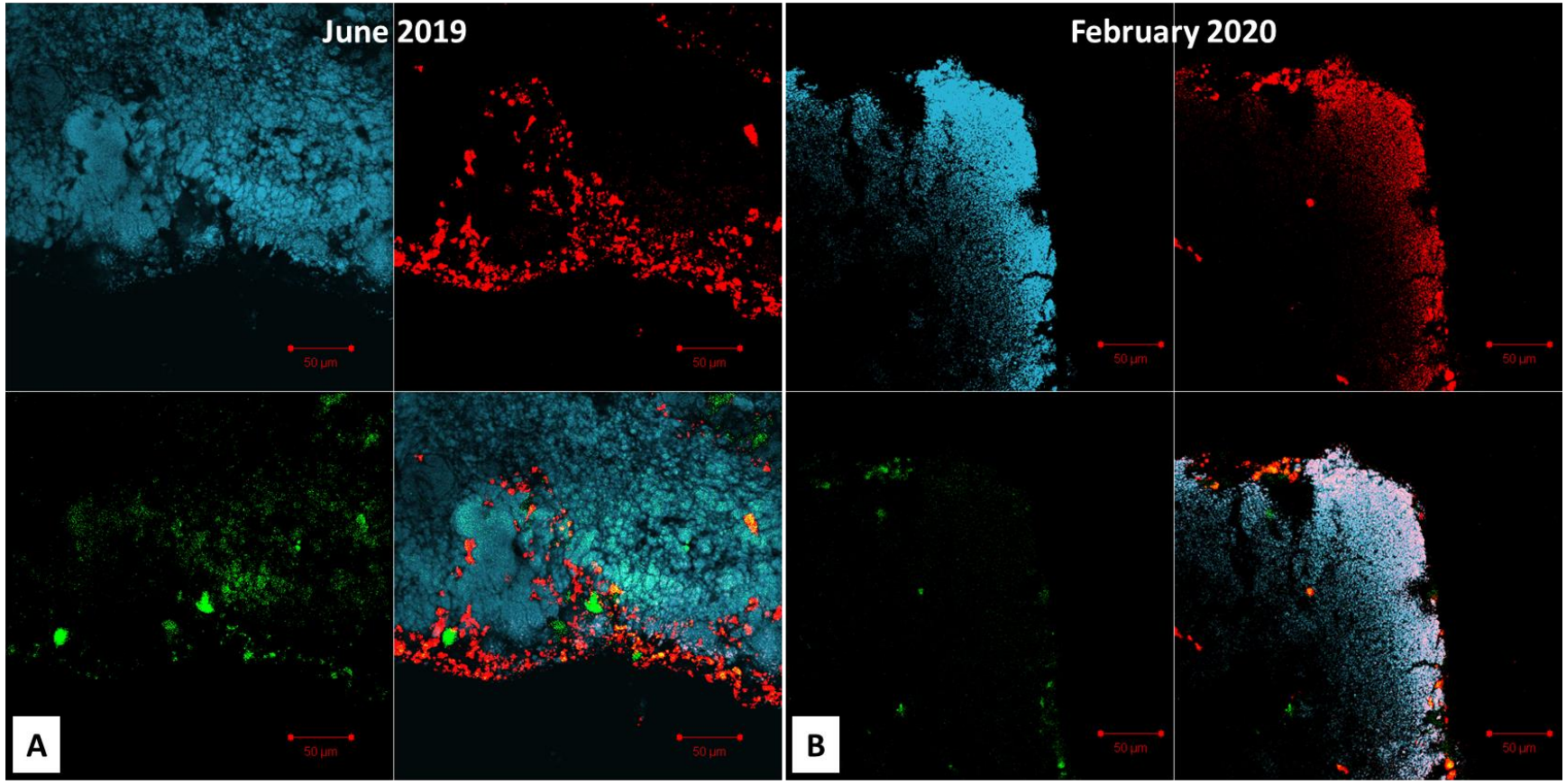

Figure 4-11. Fluorescence in situ hybridization (FISH) images of sidestream SBR granules from June 2019 and February 2020. PAOs are represented in blue, while AOBs are in red, GAOs are in green. FISH analysis was performed by Bao Ngyuen Quoc, UW PhD candidate.

The qPCR results in Figure 4-12 show that the GAO abundance was about 5% throughout the operating period but the PAO abundance varied with time. From early September to January it increased from about 5% to 30% and then declined to about 15% in March. In a similar sidestream laboratory SBR treating WPTP centrate, Figdore et al. (2018a) found, through mixed liquor sample sequencing, that PAOs and GAOs accounted for 13 and 11% of the bacteria abundance, respectively. The other bacteria (~75% of the total) had to grow on endogenous decay byproducts from the primary substrate consumers, PAOs and GAOs. When the PAO abundance was increased from September to January the only significant operating change was the reduction in SRT. The amount of endogenous decay is less at lower SRTs which may explain the decrease in the other bacteria and the relative increase in the PAO abundance. However, the cause of the decrease in PAO abundance from January to March is not known and the SRT decreased further during the period. An increase in PAO abundance suggests a decrease in the amount of other bacteria grown on byproducts of endogenous decay. One explanation for the decrease is that a different PAO or GAO was present that was not detected by the qPCR probes used.

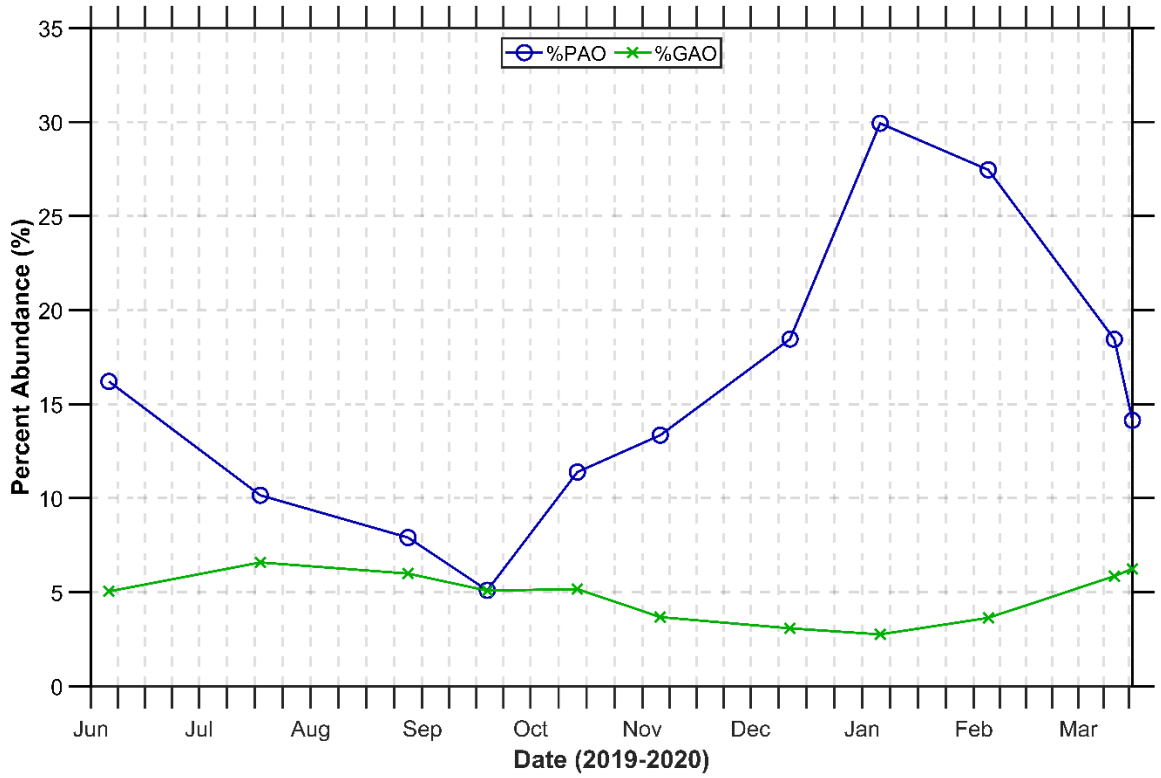

Figure 4-12. Relative abundance of PAOs and GAOs in the sidestream SBR based on gene copy number per ng DNA for qPCR (qPCR data was provided by Bao Ngyuen Quoc, UW PhD candidate).

4.1.6 Sidestream Acetate Utilization Kinetics

Acetate utilization kinetics were assessed with in situ tests for the sidestream reactor to determine the maximum uptake rate (K) and the apparent half-saturation constant (K_s) for the Michaelis-Menten substrate utilization kinetic model. Tests were performed on August 26 and September 30, 2019 to follow the acetate COD concentration during the anaerobic phase during and after feeding. But an inhibition event prevented obtaining useful acetate utilization data for kinetic analysis. However, the test of September 30th yielded useful results. The computation method used was given in Section 3.6.3. The maximum specific substrate utilization rate, K, was 2.7 mgCOD/gVSS-d and the half-velocity coefficient, K_s, was 9.7 mgCOD/L (Figure 4-13). Diffusion limitation likely elevated the observed K_s to0 be higher than a K_s value for suspended or dispersed biomass.

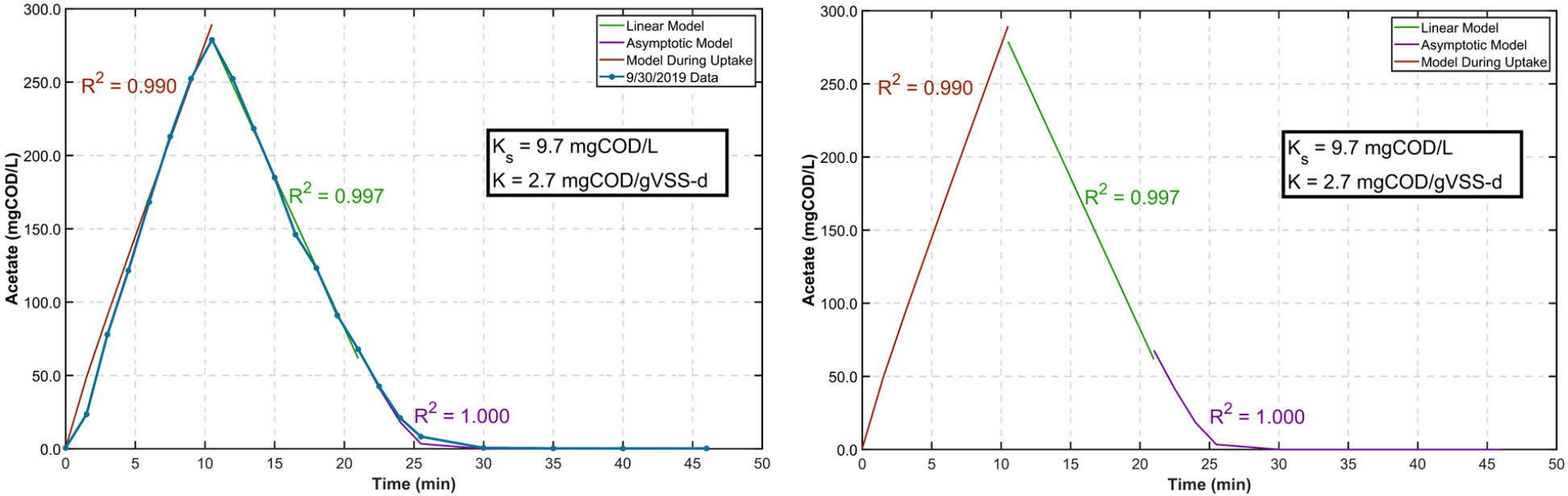

Figure 4-13. Sidestream SBR acetate utilization kinetics batch test on September 30, 2019. The linear model is Equation 3-17, while the asymptotic model is Equation 3-18, and the model during uptake is Equation 3-15. The measured acetate-COD data is displayed on the left graph in blue.

4.2 Mainstream Phase 1 Operation and Treatment Performance

4.2.1 Mainstream Phase 1 Operating Conditions

The plan for Phase 1 was to establish a stable operation and collect process performance at low SRT without nitrification before starting granular sludge bioaugmentation from the sidestream. EBPR was expected to continue as was occurring at the South Plant. After seeding the mixed liquor suspended solids (MLSS) concentration was about 3500 mg/L, and the system was operated at its target condition; an expected temperature of 16°C, a primary influent flow rate of 1.5 gpm, and an initial SRT of 4.0 days. The SRT was selected to simulate the King County South Plant winter operation in which EBPR occurred but not nitrification. The SRT was based on the aeration tank mass and was controlled by manual RAS volume wasting 1-3 times per day, Monday through Friday.

Table 4-6 summarizes the operational changes made on respective dates during Phase 1 in response to the mainstream performance in effort to operate without nitrification. The primary effluent feed rate was 1.0 gpm for the first 4 days and then increased to the target flow of 1.5 gpm. At the primary effluent feed flow rate of 1.5 gpm, the 3.6 ft diameter clarifier surface overflow rate was 214 gpd/ft^2. The granular return sludge rate was always maintained at 0.75 gpm during Phase 1 and the RAS rate was at 1.0 gpm for the first month of operation. This resulted in a separator superficial upflow velocity of 9.8 m/h, which based on prior pilot plant testing would theoretically allow granules of size 0.425 µm or greater to settle to the separator underflow. A high DO of 5.0 mg/L was initially set upon start up to ensure that there would be sufficient air for mixing because a lower oxygen demand than design was expected due to the lack of nitrification in the seed sludge. A low DO concentration set point and a low oxygen demand could result in insufficient aeration for mixing due to air flow control by a modulating

valve that is opened in response to difference between the set point and the online DO concentration. The pulse aeration unit was also operating at a frequency of 1 min aeration every 10 min. On November 18th, the pulse aeration unit was shut off because it was observed to cause a surge in flow to the secondary clarifier when it was turned on, by increasing the liquid level in the aeration tank.

Table 4-6. Changes in mainstream operating conditions for Phase 1 (October 17, 2019 to November 26, 2019)

Date of change	PE Feed Rate, gpm	SRT Goal, days	DO Set Point, mg/L	Return Activated Sludge Rate, gpm	Acetate COD Feed, mg/L	Pulse Aeration Frequency, min/10 min
10/17/2020 Startup	1.0	4.0	5.0*	1.0	0	1
10/21/2020	1.5				26	
10/25/2020		3.0			50	
10/28/2020			3.0			
10/29/2020		2.5				
11/1/2020			2.5		26	
11/18/2020			1.5	2.0		0
11/26/2020 Shut down	1.5	2.5	1.5	2.0	26	0

The initial seed was not nitrifying but after 2 weeks of operation there was a significant increase in nitrification due to the unexpected aeration tank temperatures of 18.6-19.6°C, resulting from high primary effluent temperatures. The target SRT was reduced to 3.0 days on October 25th and then to 2.5 days on October 29th. Because of the weak wastewater characteristics due to wet

weather sodium acetate was added to the feed on October 21st at 26 mg/L, based on the feed flow rate and was increased to 50 mg/L on October 25th to ensure that there would be sufficient readily available biodegradable COD (rbCOD) for PAO growth. The aeration target DO was set at 3.0 mg/L on October 28th, reduced to 2.5 mg/L on November 1st, and finally reduced to 1.5 mg/L on November 18th. As nitrification increased there was rising sludge in the final clarifier and on November 18th the RAS rate was increase to 2.0 gpm to reduce the sludge blanket time in an attempt to reduce denitrification in the clarifier. The resultant flow to the separator increased the superficial upflow velocity to 11.3 m/hr.

4.2.2 Mainstream Phase 1 Treatment Performance

The goal of Phase 1 was to document a stable operation and treatment performance with flocculent sludge at a low SRT, without nitrification, prior to granular bioaugmentation. However, due to issues with the flocculent sludge beginning to nitrify and the secondary clarifier scraper motor failure which ended Phase 1, no granules were added to the system. Instead, data collected during Phase 1 detailed the effective BOD and nutrient treatment of the mainstream pilot, the growth of small granules, and the maintenance of a good SVI_{30} within the system. Additionally, Phase 1 informed necessary pilot plant modifications such as the clarifier motor replacement, the hydraulic upflow separator effluent launder replacement, the surge issue with the Pulsair unit in the aeration tank, and the necessity of having semi-continuous wasting.

Nitrification and PO_4-P removal quickly developed at the beginning of Phase 1, after the first week, and average weekly nitrification efficiencies were between 50 and 60%, and the PO_4-P removal efficiencies were above 80%, aside from inhibitions on October 24th, November 4th, 13th, and 24th (Figure 4-14). No nitrification was observed with the EBPR inhibition, and the

system operation in terms of aeration DO, SRT control, and pH was not changed. This suggests that the EBPR inhibition may have been caused by something in the primary effluent feed. Denitrification was observed at between 30 and 40% for most of Phase 1. The recycle to the preanoxic tank was 50% of the feed flow and on average accounted for 58% of the total N removal, indicating some SND in the aeration tank (Figure 4-14). Nitrification, denitrification, and phosphorus removal decreased after the temperature dropped to below 18°C and the 7-day average SRT dropped below 1.5 days on November 18th.

A small growth of granules was observed during Phase 1. The seed sludge contained about 6% granules, which increased to 25% within the first week of operation (Table 4-7). The increase in small granules was likely due to retention in the secondary clarifier. The SVI_{30} ranged from 59 to 109 mg/L, was not affected by the slight changes in mixed liquor percent granules, and there was no clear trend of change in the SVI_5/SVI_{30}, which ranged from 2.0 to 2.3.

The effluent TSS was high for the duration of Phases 1 and 2, the weekly average effluent TSS ranged from 60 to 147 mg/L and 51 to 75 mg/L, respectively (Table 4-7, Table 4-12). During Phase 2, batch quiescent 45-min settling tests were performed with clarifier influent. These batch tests produced supernatant TSS concentrations between 15 and 25 mg/L, illustrating that the high effluent TSS was likely a result of some hydraulic inefficiencies within the small secondary clarifier. However, during the fourth week of Phase 1, floating sludge was observed on the clarifier surface. This was caused by denitrification in the clarifier, resulting from higher NO_x-N concentrations in the clarifier influent. To mitigate this effect, the RAS ratio was

increased from 0.67 to 1.33, which successfully reduced the effluent TSS, but it remained relatively high, likely caused by other hydraulic inefficiencies.

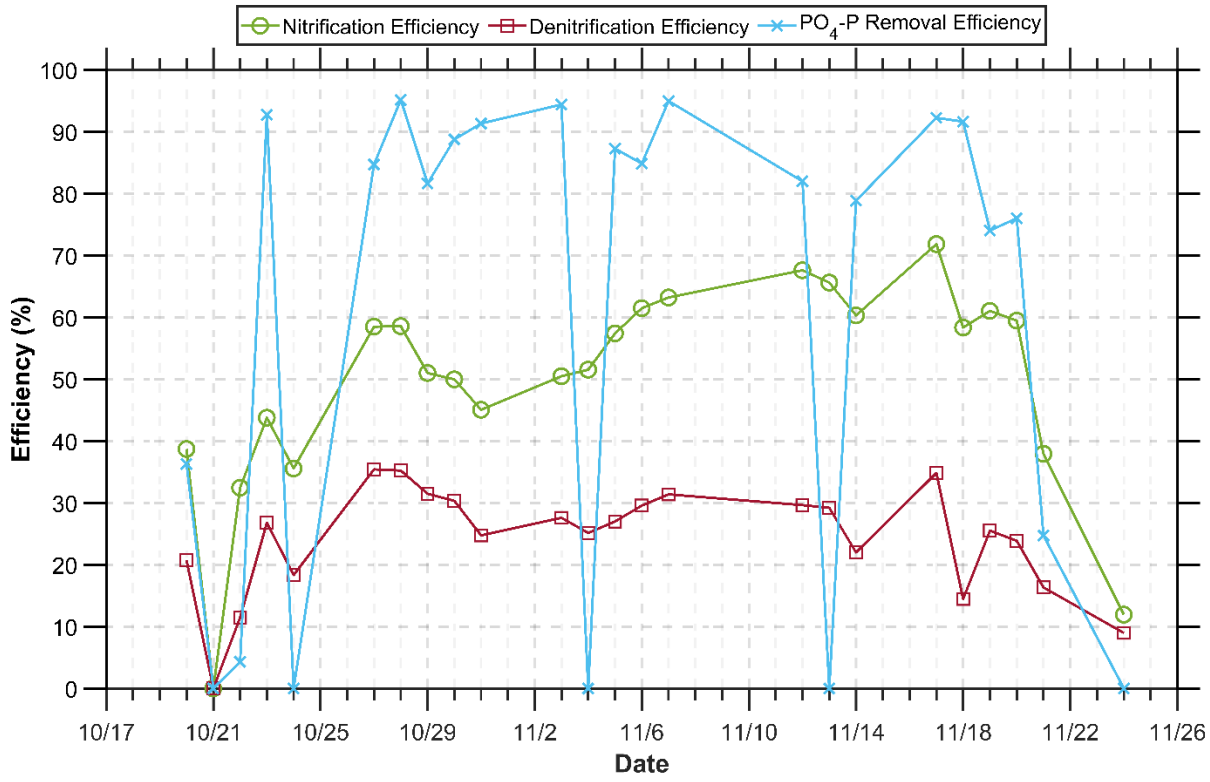

Figure 4-14. Nitrification, denitrification, and PO_4-P removal efficiencies during mainstream Phase 1.

Table 4-7. Phase 1 mainstream average weekly performance (standard deviation in parenthesis)

		Week Ending				
Parameter	Units	25-Oct	1-Nov	8-Nov	15-Nov	22-Nov
Aeration Tank						
7-day Moving Average SRT	d	4.2 (0.4)	3.1 (0.6)	2.1 (0.1)	2.1 (0.1)	1.42 (0.2)
Average DO	mg/L	5.0 (0.2)	4.1 (0.8)	2.1 (0.2)	1.8 (0.5)	1.1 (0.4)
pH		6.9 (0.1)	6.9 (0.0)	6.8 (0.0)	6.7 (0.1)	6.6 (0.1)
Temperature	°C	18.7 (0.9)	18.8 (0.3)	18.6 (0.1)	18.1 (0.2)	17.5 (0.7)
Primary effluent feed						
BOD	mg/L	116 (49)	153 (15)	172 (12)	162 (7)	133 (17)
Total COD	mg/L	218 (81)	305 (23)	303 (11)	288 (17)	245 (38)
soluble COD	mg/L	83 (50)	124 (8)	127 (10)	109 (10)	88 (21)
NH3-N	mg/L	22.2 (6.8)	29.7 (2.0)	32.3 (1.2)	27.7 (2.4)	24.5 (4.5)
Estimated TKN	mg/L	30.9 (9.4)	41.2 (2.8)	44.8 (1.7)	38.5 (3.3)	33.9 (6.2)
PO4-P	mg/L	2.9 (1.4)	5.1 (2.7)	4.6 (2.6)	2.8 (0.5)	2.6 (0.5)
TSS	mg/L	56.8 (18.8)	44.8 (10.0)	51.6 (4.6)	53.5 (5.0)	55.4 (5.6)
VSS	mg/L	50.6 (14.5)	36.0 (5.8)	44.4 (3.9)	46.8 (4.3)	44.8 (4.0)
Effluent						
soluble COD	mg/L	27	26	37	112	33
TSS	mg/L	61.2 (19.1)	75.4 (8.2)	81.4 (11.5)	146.7 (44.9)	97.6 (24.3)
VSS	mg/L	52.8 (15.4)	64.2 (7.3)	67.8 (9.9)	122.0 (34.0)	82.6 (21.9)
NH_3-N	mg/L	14.4 (3.9)	11.2 (2.1)	8.3 (1.5)	3.6 (1.7)	5.4 (4.5)
NO_2-N	mg/L	0.5 (0.2)	0.5 (0.0)	0.9 (0.2)	1.2 (0.2)	1.1 (0.2)
NO_3-N	mg/L	4.6 (2.4)	8.2 (0.5)	12.0 (1.7)	13.0 (1.0)	10.4 (1.9)
PO_4-P	mg/L	4.1 (4.7)	0.5 (0.2)	1.1 (1.4)	1.3 (1.2)	0.8 (0.7)
Sludge Characteristics						
MLSS	mg/L	3985 (168)	4233 (425)	3692 (475)	3251 (939)	2650 (902)
MLVSS/MLSS	%	81 (1)	82 (1)	85 (2)	85 (2)	84 (1)
Granule MLSS	%	24.5	19.2	22.9	25.4	28
SVI_{30}	mL/g	109	76	81	59	84
SVI_5/SVI_{30}		2.0	2.1	2.3	2.0	2.1

4.2.3 Mainstream Phase 1 Nitrification and Nitrogen Removal

Phase 1 was characterized by nitrification by the seed flocculent sludge, without any granule addition. This was primarily a result of high temperatures, around 19 °C, and a 7-day average SRT more than 4 days for the first two weeks (Table 4-7). On average during phase one, 50% of the influent biodegradable TKN was nitrified, while 25% was used for cell synthesis, and 28% escaped in the effluent. The total of the averages is greater than 100% because on days with no nitrification, the effluent NH_3-N composite sample had a great concentration than the estimated influent TKN. Furthermore, the estimated total inorganic nitrogen (TIN) removed averaged 35% during the first week, and between 52 and 53% for the remaining four weeks (Table 4-8). After the first week, the average estimated NH_3-N nitrified increased from 10.6 to 21.6 mg/L, the average SNR increased from 1.4 to 2.6 mg/gVSS-h, and the average estimated nitrification rate increased from 4.4 to 9.1 mg/L-h (Table 4-8). During the third and fourth weeks of the operational period the average estimated NH_3-N nitrified was above 24 mg/L and the average SNR was between 3.6 and 3.7 mg/gVSS-hr. The total fate of bioavailable NH_3-N is summarized in Figure 4-15, showing an increase in nitrification efficiency the first week and variations in the amount of NH_3-N used for synthesis which was a function of the influent BOD concentration.

qPCR results confirm the presence of nitrifiers in the mixed liquor, granular, and flocculent sludge (Figure 4-16). Based on the *amoA* gene copy number, the granules appear to be more abundant in AOB than the floc on October 24th, 30th, and November 15th. On November 22nd, the opposite is seen but the results are questionable because both the granules and flocculent sludge measured higher *amoA* abundance than the mixed liquor.

Table 4-8. Mainstream Phase 1 nitrogen removal analysis (standard deviation in parenthesis).

		Week Ending				
Parameter	Units	25-Oct	1-Nov	8-Nov	15-Nov	22-Nov
Influent flowrate	gpm	1.5	1.5	1.5	1.5	1.5
7-day moving average SRT	d	4.2 (0.4)	3.1 (0.6)	2.1 (0.1)	2.1 (0.1)	1.42 (0.2)
Nitrogen Concentrations						
Influent NH_3-N	mg/L	22.2 (6.8)	29.7 (2.0)	32.3 (1.2)	27.7 (2.4)	24.5 (4.5)
Bioavailable influent TKN	mg/L	30.9 (9.4)	41.2 (2.8)	44.8 (1.7)	38.5 (3.3)	33.9 (6.2)
Effluent NH_3-N	mg/L	14.4 (3.9)	11.2 (2.1)	8.3 (1.5)	3.6 (1.7)	5.4 (4.5)
Effluent NO_2-N	mg/L	0.5 (0.2)	0.5 (0.0)	0.9 (0.2)	1.2 (0.2)	1.1 (0.2)
Effluent NO_3-N	mg/L	4.6 (2.4)	8.2 (0.5)	12.0 (1.7)	13.0 (1.0)	10.4 (1.9)
TIN removal efficiency	%	35 (18)	52 (2)	53 (1)	53 (4)	50 (5)
Estimated Nitrification						
NH_3-N used in synthesis	mg/L	7.6 (2.3)	8.7 (1.3)	10.8 (0.7)	10.1 (0.4)	9.7 (1.4)
NH_3-N nitrified	mg/L	10.6 (5.9)	21.6 (1.5)	25.5 (3.1)	24.4 (2.1)	19.4 (4.7)
Nitrification rate	mg/L-h	4.4 (2.5)	9.1 (0.6)	10.7 (1.3)	10.3 (0.9)	8.2 (2.0)
Aeration tank average MLVSS	mg/L	3234 (129)	3463 (339)	3123 (441)	2737 (760)	2224 (765)
Specific nitrification rate	mg/gVSS-h	1.4 (0.9)	2.6 (0.1)	3.6 (0.8)	3.7 (0.4)	3.0 (0.7)
Estimated Denitrification						
N removal by denitrification	mg/L	6.9 (2.6)	12.9 (1.2)	12.6 (1.4)	10.2 (1.4)	9.1 (2.3)
Preanoxic denitrification	mg/L	3.3 (1.4)	4.3 (0.2)	6.5 (1.0)	7.4 (0.8)	6.4 (0.6)
Simultaneous nitrification denitrification	mg/L	3.6 (2.5)	8.6 (1.2)	6.1 (0.9)	2.8 (1.8)	2.7 (2.1)
Percent denitrification by SND	%	45 (22)	66 (4)	49 (5)	26 (15)	26 (16)

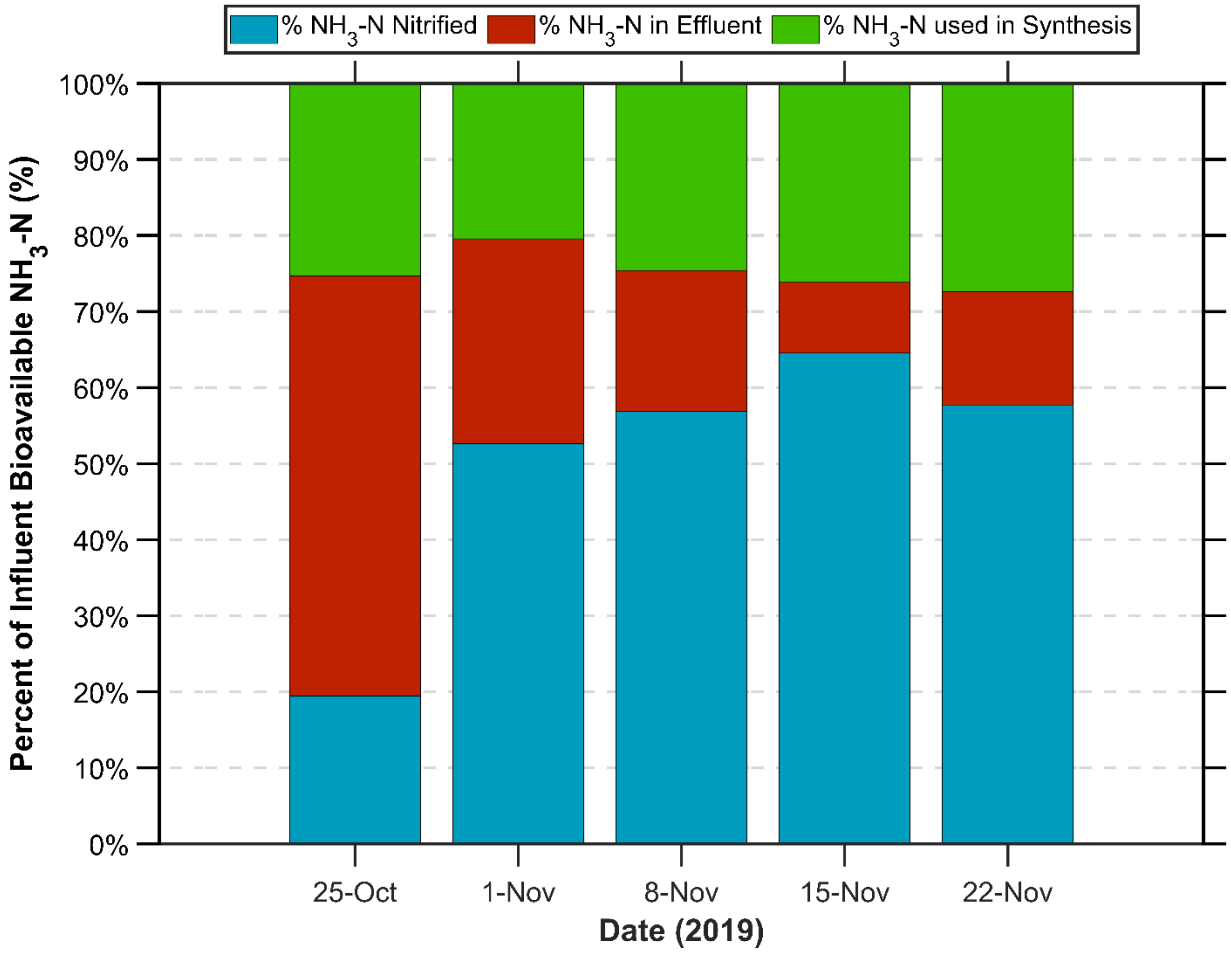

Figure 4-15. Mainstream Phase 1 weekly average fate of influent bioavailable NH_3-N.

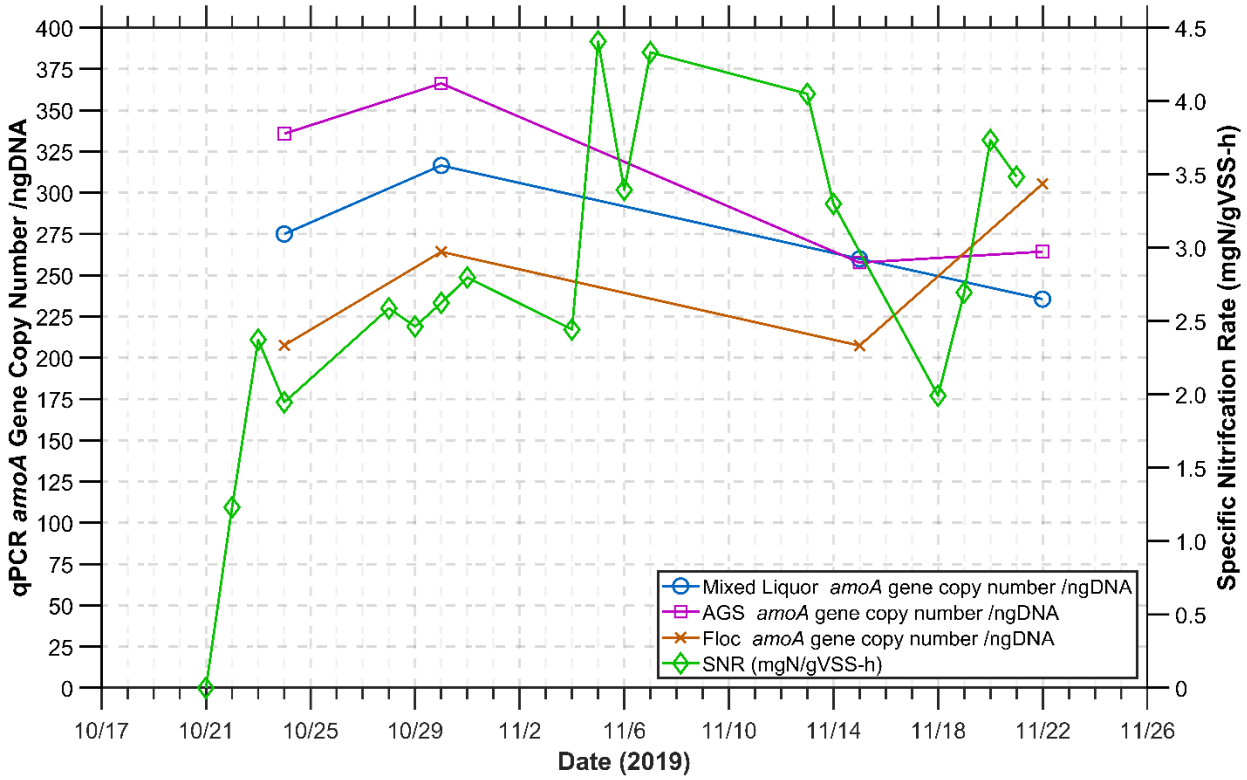

Figure 4-16. Mainstream Phase 1 *amoA* gene copy number for the aeration mixed liquor, granules, and flocculent sludge with SNR (mgN/gVSS-h). qPCR data provided by Bao Ngyuen Quoc.

4.2.4 Mainstream Phase 1 Separator Performance

The main purpose of the mainstream separator was to decouple the SRTs of the flocculent sludge and the granular sludge to accumulate and sustain the granule sludge nitrification capability. However, the mainstream operation had to be terminated for repair before sidestream granule bioaugmentation was initiated. Thus, for Phase 1 the separator performance was monitored to determine if the granule portion in the activated sludge, from seeding or from growth, could be selectively retained over floc. The upflow superficial velocity was maintained at 9.8 m/h for the first four weeks of operation and was then increased to 11.3 m/h on November 18, 2019 for the remainder of the phase (Table 4-9). The average weekly TSS concentration in the separator overflow ranged from 1020 to 2470 mg/L, which was less than the aeration tank feed MLSS concentration. Based on the mass rate of solids to the separator and the mass rate of solids in the separator underflow, the separator solids removal efficiency was 56 to 65%. On occasions when there was TSS data for the separator overflow, but not the underflow, the underflow solids removed rate was assumed to be equal to difference between the separator influent and overflow solids rates. However, the granular solids removal efficiency performance was less at about 29% during the first week, and from 38 to 52% for the remainder of the phase. Thus, decoupling of the granule and floc SRTs for the Phase 1 mixed liquor was not demonstrated.

Table 4-9. Weekly average performance of the mainstream hydraulic separator for Phase 1 (standard deviation in parenthesis).

		Week Ending				
Parameter	Units	25-Oct	1-Nov	8-Nov	15-Nov	22-Nov
Upflow superficial velocity	m/h	9.8	9.8	9.8	9.8	10.9 (0.7)
Aeration Effluent						
MLSS	mg/L	3985 (168)	4233 (425)	3692 (475)	3251 (939)	2650 (902)
Granular TSS	mg/L	989	901	1076	894	939
Percent granules	%	24	19	25	25	28
TSS feed rate to separator	kg/d	70.6 (3.0)	75.0 (7.5)	65.4 (8.4)	57.6 (16.6)	61.4 (20.9)
Granule feed rate to separator	kg/d	17.5	16.0	19.1	15.8	21.8
Separator Overflow						
TSS	mg/L	1802 (453)	1984 (275)	2473 (1092)	1379 (517)	1018 (573)
Granular TSS	mg/L	390	386 (88)	399	279	591
Percent granules	%	16	17 (4)	25	31	29
TSS effluent rate in overflow	kg/d	24.6 (6.2)	27.0 (3.7)	33.7 (14.9)	18.8 (7.1)	19.4 (10.9)
Granule effluent rate in overflow	kg/d	5.3	5.3 (1.2)	5.4	3.8	11.3
Separator Underflow						
TSS	mg/L	9068 (134)	9353 (534)	9084 (481)	8804	7838 (56.5)
Granular TSS	mg/L	1254	1253 (311)	2090	1996	2034
Percent granules	%	14	13 (2)	22	23	26
TSS effluent rate in underflow	kg/d	39.1 (0.6)	38.2 (2.2)	37.1 (2.0)	36.0	32.0 (0.2)
Granule effluent rate in underflow	kg/d	5.1	5.1 (1.3)	8.5	8.2	8.3
Separator Performance						
Removal efficiency of solids	%	64 (10)	58 (10)	56 (3)	61 (2)	65 (15)
Removal efficiency of feed granules	%	29	40	45	52	38

4.2.5 Mainstream Aeration Tank Granules and Granule Fate during Phase 1

Because there was no bioaugmentation during Phase 1, only two sieves were used to analyze granule sizes in the mainstream, 212µm and 425µm. Biomass which was retained on the 212 µm sieve, or any larger sieve, was defined as granular sludge. Only two sieves were necessary because about 6% of the South Plant seed sludge was retained on the 212 µm sieve, while 0.5% was retained on the 425 µm sieve.

The MLSS, granule MLSS, percent granules, and sieve analysis results are shown in Table 4-9. After the first week of the mainstream operation, the percent granules in the aeration tank MLSS had increased to 24.5%, with 22.9% being retained on the 212 µm sieve and 1.6 being retained on the 425 µm sieve (Table 4-10). The last three weeks of Phase 1 were characterized by between 1.6 and 2.4% of TSS being retained on the 425 µm sieve, while 23 to 28% of TSS was retained on the 212 µm sieve. There was no significant granular growth or decay, aside from the initial growth. Because the separator did not show any significant granule retention it is likely that the percent granule increase was due to retention in the secondary clarifier.

Table 4-10. Weekly mainstream aeration tank granular sludge characteristics in Phase 1 (standard deviation in parenthesis).

		Sample Date				
Parameter	Units	21-Oct	28-Oct	4-Nov	14-Nov	18-Nov
Daily Bioaugmentation	Yes/No	N	N	N	N	N
MLSS	mg/L	4044	4704	4225	3522	3350
Granule MLSS	mg/L	989	901	1076	894	939
	%	24.5	19.2	22.9	25.4	28
MLSS >212 <425 um	mg/L	925	850	964	822	886
	%	22.9	18.1	20.5	23.3	26.4
MLSS >425 <850 um	mg/L	64	51	112	72	53
	%	1.6	1.1	2.4	2	1.6

4.3 Mainstream Phase 2 Operation and Treatment Performance

4.3.1 Mainstream Phase 2 Operating Conditions

Phase 2 began on January 21, 2020 after completing repair and modifications to the mainstream system. The system was seeded with non-nitrifying EBPR activated sludge from the King County South Plant to an initial MLSS concentration of 3600 mg/L. Table 4-11 summarizes the key mainstream operating conditions and changes made from January 21st to its final operation on March 16th. At the start, the primary effluent feed flow was 1.5 gpm, the clarifier RAS rate was 1.5 gpm (1.0 recycle ratio), and the separator recycle flow rate was 0.75 gpm (0.50 recycle ratio). The RAS flow rate was not changed during Phase 2 but a higher recycle ratio occurred because of a decrease in the influent flow rate. The target aerobic SRT was 2.5 days but increased to 4.0 days on March 4th to provide more nitrification. Sodium acetate addition at startup was 26 mg/L, based on the primary effluent feed rate, and was increased to 47 mg/L on February 4th. In view of weaker wastewater strength due to wet weather flow, potassium dibasic phosphate was added at 16 mg/L on February 1st and increased to 31 mg/L on February 4th.

Table 4-11. Changes in mainstream operating conditions for Phase 2 (January 21, 2020 to March 16, 2020).

Date of change	PE Feed Rate, gpm	SRT Goal, days	DO Set Point, mg/L	Separator Internal Recycle Rate, gpm	Granular Sludge Recycle Rate, gpm	Separator Upflow Velocity, m/hr	Acetate COD Feed, mg/L	K_2HPO-P Feed, mg/L
1/21/2020 Startup	1.5	2.5	1.5	0	0.75	4.5	26	0
1/25/2020				4		10.5		
2/1/2020								16
2/4/2020	1.3	Added 40 gallons of stored granular sludge from past sidestream wasting					47	31
2/10/2020			1.8					
2/13/2020				2.5		8		
2/25/2020		Started daily transfer of sidestream waste granule sludge volume						
2/27/2020			2.2		0.5			
3/4/2020		4	2.2					
3/6/2020	0.9		2.2	0	0.75	3.6		
3/16/2020 Shutdown	0.9	4	2.2	0	0.75	3.61	47	31

At start up the separator internal recycle pump was turned off and the superficial upflow velocity was 4.5 m/hr, based on the influent flow and clarifier RAS feed rates. Solids appeared to be collecting in the separator from visual observations, so on January 25th the separator internal recycle flow was used to increase the superficial upflow velocity to 10.5 m/hr. However, this did not result in changes in appearance of solids on the walls of the plexiglass column and it was determined that the solids had a sticky characteristic and thus collected on the wall.

After operating for 15 days (5.2 SRTs), the MLSS concentration averaged around 3400 mg/L, which was higher than anticipated suggesting a higher sludge yield than expected for the primary effluent treatment. The influent flow was decreased to 1.3 gpm on February 4th to reduce the

aeration tank MLSS concentration. On February 4th, 40 gallons of granular sludge wasted from the sidestream system and stored at 4°C during the prior 6 months, were added to the mainstream system to jumpstart the granular/flocculent sludge system operation.

On February 10th, the aeration DO set point was increased from 1.5 to 1.8 mg/L to improve nitrification by the bioaugmented granules. On February 13th, the separator internal recycle flow was decreased to reduce the superficial upflow velocity from 10.2 to 8.0 m/hr, to observe the effect on the separator granular sludge recovery efficiency. Prior to that time the separator granular sludge recovery efficiency was in the range of 45 to 50%.

On February 25th, daily bioaugmentation of granules from the sidestream reactor began. Each day, Monday to Friday, the waste sludge from the sidestream reactor was manually added to the mainstream aeration tank. The sidestream reactor granule mixed liquor contained about 95% granules with an average granule size in the range of 1.5 mm.

Due to the lower than expected nitrification efficiency the aeration DO set point was increased from 1.8 to 2.2 mg/L on February 27th. The separator underflow recycle ratio was also decreased from 0.58 to 0.38 to determine if that would improve the separator granular sludge recovery efficiency. On March 4th, the aerobic SRT was increased to 4.0 days to improve nitrification efficiency. Part of the logic for this SRT increase was that the potentially improved SVI by operating a granular/flocculent sludge system would allow a higher solids loading on the secondary clarifier and thus allow a higher MLSS and SRT concentration. The influent feed rate was decreased from 1.3 to 0.9 gpm on March 6th to provide more aeration time and lower the effluent NH_3-N concentration. Also on March 6th, the separator internal recycle was stopped to

observe the effect of a lower superficial upflow velocity on the separator performance. Operation ceased on March 16, 2020 due to COVID-19 outbreak concerns.

4.3.2 Mainstream Phase 2 Treatment Performance

The average aeration tank MLSS during Phase 2 varied between 3100 and 3800 mg/L, with an SVI_{30} of between 81 and 106 mL/g, and an SVI_5/SVI_{30} ratio of 1.8 to 2 (Table 4-12). During the last week, the SVI_{30} spiked to 161 mL/g, but examination under the light microscope found that the sludge was not dominated by filamentous organisms, but that there was bridging of large floc (Figure 4-17).

Table 4-12. Average weekly performance for the mainstream system in Phase 2 (standard deviation in parenthesis).

		Week Ending						
Parameter	Units	31-Jan	7-Feb	14-Feb	21-Feb	28-Feb	6-Mar	13-Mar
Aeration Tank								
7-day Moving Average SRT	d	2.4 (0.3)	2.3 (0.3)	2.9 (0.2)	2.5 (0.1)	2.6 (0.1)	2.3 (0.2)	3.5 (0.7)
Average DO	mg/L	1.5 (0.0)	1.5 (0.0)	1.6 (0.1)	1.8 (0.0)	2.0 (0.2)	2.2 (0.0)	2.2 (0.0)
pH		6.8 (0.0)	6.6 (0.1)	6.7 (0.0)	6.7 (0.0)	6.7 (0.0)	6.8 (0.1)	N/A
Temperature	°C	14.0 (0.5)	14.2 (0.8)	15.1 (0.4)	15.3 (0.4)	15.8 (0.4)	15.8 (0.6)	15.0 (0.4)
Primary effluent feed								
BOD	mg/L	56 (13)	54 (17)	83 (14)	128 (3)	125 (5)	136 (10)	118 (8)
Total COD	mg/L	130 (24)	129 (44)	164 (21)	234 (13)	258 (15)	247 (22)	231 (34)
soluble COD	mg/L	46 (6)	46 (15)	67 (11)	105 (8)	113 (9)	105 (14)	93 (14)
NH3-N	mg/L	11.1 (2.0)	11.4 (4.7)	16.6 (3.4)	23.0 (1.3)	25.1 (2.0)	23.8 (1.1)	24.0 (0.8)
Estimated TKN	mg/L	15.4 (2.8)	15.9 (6.6)	23.0 (4.7)	31.9 (1.8)	34.8 (2.8)	33.1 (1.6)	33.3 (1.1)
PO4-P	mg/L	1.5 (1.2)	6.1 (5.0)	3.7 (4.3)	2.6 (0.5)	2.1 (0.1)	2.4 (1.3)	2.4 (0.5)
TSS	mg/L	36.6 (5.2)	38.6 (4.5)	34.6 (3.7)	48.0 (6.4)	44.4 (4.8)	50.0 (9.0)	51.2 (6.6)
VSS	mg/L	27.0 (6.2)	30.8 (7.0)	28.8 (5.9)	41.7 (3.3)	36.6 (3.1)	38.2 (6.0)	42.2 (4.8)
Effluent								
soluble COD	mg/L	16	81	24	25	25	22	31
TSS	mg/L	62.2 (7.3)	66.6 (5.2)	56.4 (2.8)	55.5 (7.5)	51.0 (7.8)	71.0 (1.4)	75.4 (8.0)
VSS	mg/L	49.6 (5.0)	52.6 (7.4)	41.6 (2.4)	41.3 (4.1)	38.8 (5.8)	54.2 (5.4)	56.0 (7.8)
NH_3-N	mg/L	11.6 (3.0)	11.3 (8.8)	11.7 (2.9)	14.8 (1.0)	16.5 (1.9)	17.7 (2.8)	20.1 (4.7)
NO_2-N	mg/L	0.2 (0.0)	0.5 (0.1)	0.7 (0.2)	0.26 (0.1)	0.1 (0.0)	0.3 (0.2)	0.1 (0.0)
NO_3-N	mg/L	0.2 (0.1)	0.4 (0.1)	1.2 (0.2)	1.1 (0.1)	1.1 (0.1)	1.3 (0.7)	1.2 (0.1)
PO_4-P	mg/L	5.3 (5.6)	8.3 (15.3)	4.1 (2.6)	1.1 (0.3)	1.7 (1.3)	6.2 (5.1)	18.2 (19.7)
Sludge Characteristics								
MLSS	mg/L	3317 (527)	3609 (784)	3596 (287)	3167 (203)	3613 (211)	3146 (117)	3764 (364)
MLVSS/MLSS	%	80 (2)	81 (2)	75 (1)	75 (1)	76 (2)	82 (2)	82 (4)
SVI_{30}	mL/g	85	99	81	106	92	101	161
SVI_5/SVI_{30}		1.9	1.9	1.8	1.9	1.9	2	1.8

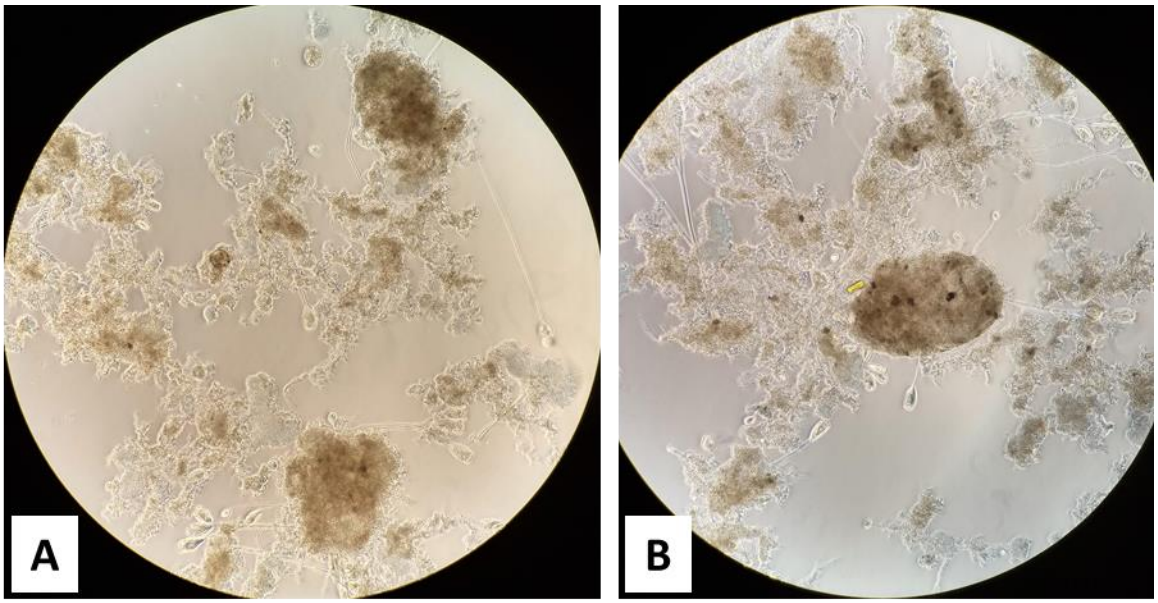

Figure 4-17. Images taken on March 16, 2020 of Phase 2 mainstream mixed liquor using a smartphone through a light microscope viewfinder. Stalked ciliates can be seen growing in the bridged flocculent sludge (original magnification 100x).

Because Phase 2 took place during the winter months, the average weekly temperature in the aeration tank varied from 14.0 to 15.8 °C. Similarly, to the Phase 1, the pH of the aeration tank during Phase 2 was relatively low, varying between 6.6 and 6.8. As mentioned above, low alkalinity is characteristic of Western Washington wastewater. This is further exacerbated by the winter wet weather conditions. Because the King County collection system has some areas with combined wastewater and stormwater sewers, the influent wastewater tends to be very dilute after wet weather events. The large variation in influent BOD during Phase 2, from 54 mg/L to 136 mg/L, was also characteristic of wet weather conditions.

Due to wet weather flows, the influent wastewater was relatively weak. For instance, the average weekly influent PO_4-P concentration varied between 1.5 and 6.1 mg/L (Table 4-12). The weekly average effluent PO_4-P varied between 1.1 and 18.2 mg/L. The standard deviation in the effluent

PO_4-P is notably large, varying from ± 0.3 to ± 19.7 mg/L. This is largely due to brief inhibition events on February 4th and March 1st, 5th, and 10th, where the effluent PO_4-P would spike for 24 hours, before returning to pre-inhibition levels (Figure 4-18). These inhibition events also appeared to affect the nitrifiers in the system, during all the events the nitrification efficiency would decrease a similar magnitude to the phosphorus removal efficiency and return to pre-inhibition levels within 24 to 48 hrs (Figure 4-18). Due to the brevity of the events, it is likely that inhibition was caused by a constituent in the primary effluent feed.

The weekly average effluent NH_3-N concentrations were relatively high throughout Phase 2, varying between 11.3 and 20.1 mg/L (Table 4-12). Based on the influent estimated TKN, there was no nitrification during operation with only the South Plant seed sludge. However, after the addition of waste sidestream granules on February 4, 2020, a limited degree of nitrification was observed. The weekly average effluent NO_2-N and NO_3-N concentrations stayed low during Phase 2, varying from 0.1 to 0.7 mg/L and from 0.2 to 1.3 mg/L, respectively.

4.3.3 Mainstream Phase 2 Nitrification and Nitrogen Removal

Nitrification and denitrification efficiency are shown in Figure 4-18, before and after granular sludge addition. After stored granular sludge was added to the mainstream, on February 4, 2020, the nitrification efficiency reached 60% and the denitrification efficiency was 50%. However, these efficiencies declined to about 30% and 25%, respectively, presumably due to a low of granules in sludge wasting. Continual bioaugmentation was started on February 25, 2020, but the subsequent operating time was too short to enable the assessment of the long-term performance with sidestream bioaugmentation.

The results in Figure 4-18 also show high phosphorus removal efficiency by the EBPR process but on February 4th and March 1st, 5th, and 11th, the EBPR appeared to be inhibited, likely by a substance in the primary effluent feed. The nitrification inhibition is also inhibited on the same days.

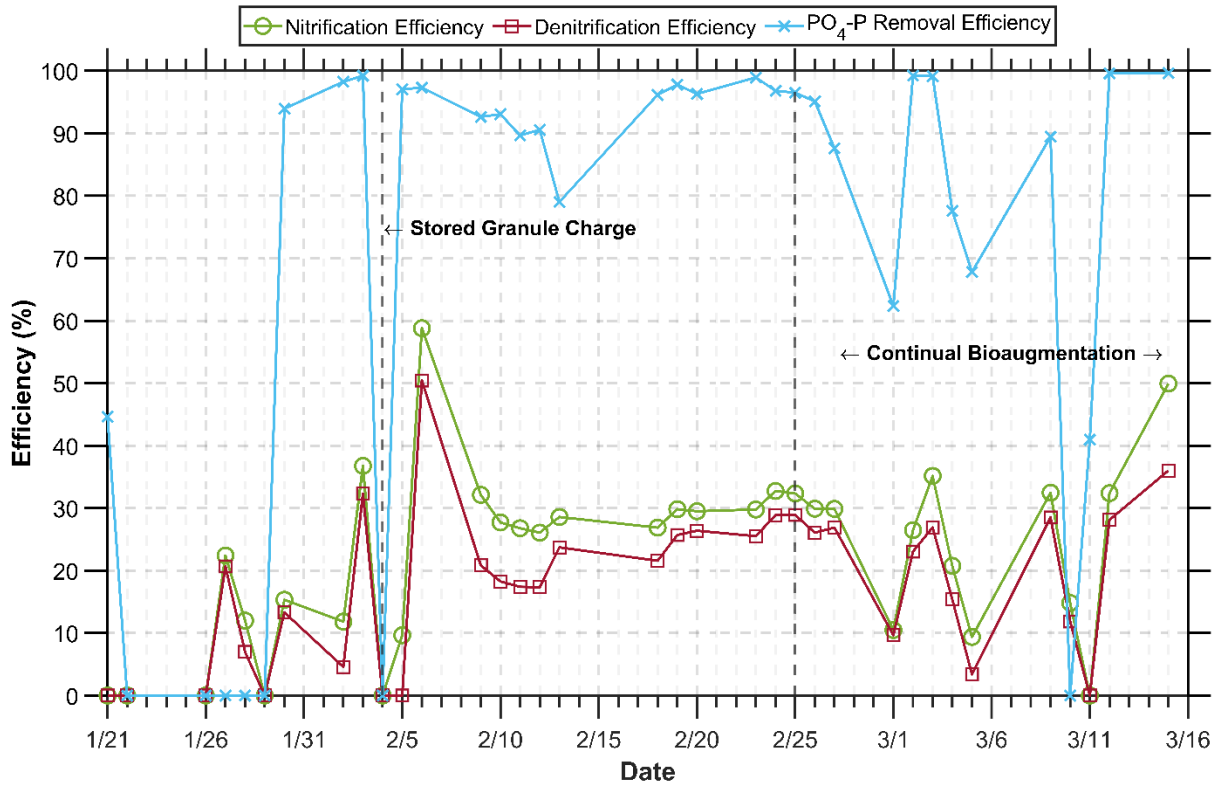

Figure 4-18. PO_4-P removal, nitrification, and denitrification efficiencies in mainstream system during Phase 2.

During Phase 2, the weekly average TIN removal efficiency was about 25% before bioaugmentation, and between 35 and 49% after sidestream bioaugmentation (Table 4-13). After bioaugmentation the average estimated amount of NH_3-N nitrified increased from 1.6 mg/L to between 6.4 and 10.8 mg/L. Additionally, the SNR increased from about 0.3 mg/gVSS-h to between 0.9 and 1.5 mg/gVSS-h. The increase in ammonia removal by nitrification occurred after the granule bioaugmentation spike on February 4, 2020, when 40 gal of sidestream granules were added to the mainstream system and continued during daily bioaugmentation. Weekly average values are shown in Figure 4-19 for the fate of the feed bioavailable nitrogen between NH_3-N for biomass synthesis, nitrification, and the effluent.

Tables 4-13. Mainstream phase 2 nitrogen removal analysis (standard deviation in parenthesis).

		Week Ending						
Parameter	Units	31-Jan	7-Feb	14-Feb	21-Feb	28-Feb	6-Mar	13-Mar
Daily bioaugmentation	Yes/No	N	Spike	N	N	Y	Y	Y
Influent flowrate	gpm	1.5	1.3	1.3	1.3	1.3	1.3	0.9
7-day moving average SRT	d	2.4 (0.3)	2.3 (0.3)	2.9 (0.2)	2.5 (0.1)	2.6 (0.1)	2.3 (0.2)	3.5 (0.7)
Nitrogen Concentrations								
Influent NH_3-N	mg/L	11.1 (2.0)	11.4 (4.7)	16.6 (3.4)	23.0 (1.3)	25.1 (2.0)	23.8 (1.1)	24.0 (0.8)
Bioavailable influent TKN	mg/L	15.4 (2.8)	15.9 (6.6)	23.0 (4.7)	31.9 (1.8)	34.8 (2.8)	33.1 (1.6)	33.3 (1.1)
Effluent NH_3-N	mg/L	11.6 (3.0)	11.3 (8.8)	11.7 (2.9)	14.8 (1.0)	16.5 (1.9)	17.7 (2.8)	20.1 (4.7)
Effluent NO_2-N	mg/L	0.2 (0.0)	0.5 (0.1)	0.7 (0.2)	0.26 (0.1)	0.1 (0.0)	0.3 (0.2)	0.1 (0.0)
Effluent NO_3-N	mg/L	0.2 (0.1)	0.4 (0.1)	1.2 (0.2)	1.1 (0.1)	1.1 (0.1)	1.3 (0.7)	1.2 (0.1)
TIN removal efficiency	%	25 (13)	35 (23)	41 (2)	49 (1)	49 (2)	41 (9)	36 (14)
Estimated Nitrification								
NH_3-N used in synthesis	mg/L	4.4 (1.6)	3.4 (1.1)	4.5 (1.2)	6.9 (1.1)	7.6 (0.2)	8.2 (0.7)	6.6 (0.4)
NH_3-N nitrified	mg/L	1.6 (1.5)	3.9 (4.0)	6.4 (1.1)	9.2 (0.9)	10.8 (0.9)	6.9 (3.5)	6.6 (4.4)
Nitrification rate	mg/L-h	0.7 (0.6)	1.6 (1.6)	2.3 (0.4)	3.4 (0.3)	3.9 (0.3)	2.5 (1.3)	1.7 (1.1)
Aeration tank average MLVSS	mg/L	2638 (468)	2900 (618)	2692 (243)	2390 (152)	2726 (115)	2578 (115)	3093 (325)
Specific nitrification rate	mg/gVSS-h	0.3 (0.2)	0.7 (0.9)	0.9 (0.2)	1.4 (0.1)	1.5 (0.1)	1.0 (0.5)	0.6 (0.4)
Estimated Denitrification								
N removal by denitrification	mg/L	2.2 (1.0)	5.2 (3.4)	4.5 (1.3)	7.9 (1.1)	9.5 (1.0)	5.3 (3.0)	7.6 (2.4)
Preanoxic denitrification	mg/L	0.2 (0.1)	0.6 (0.1)	1.0 (0.2)	0.9 (0.3)	0.7 (0.1)	0.6 (0.3)	1.0 (0.1)
Simultaneous nitrification denitrification	mg/L	2.0 (1.0)	4.6 (3.3)	3.5 (1.4)	7.0 (1.2)	8.8 (1.0)	4.7 (2.8)	6.5 (2.3)
Percent denitrification from SND	%	88 (14)	68 (34)	75 (8)	88 (4)	93 (2)	80 (24)	85 (4)

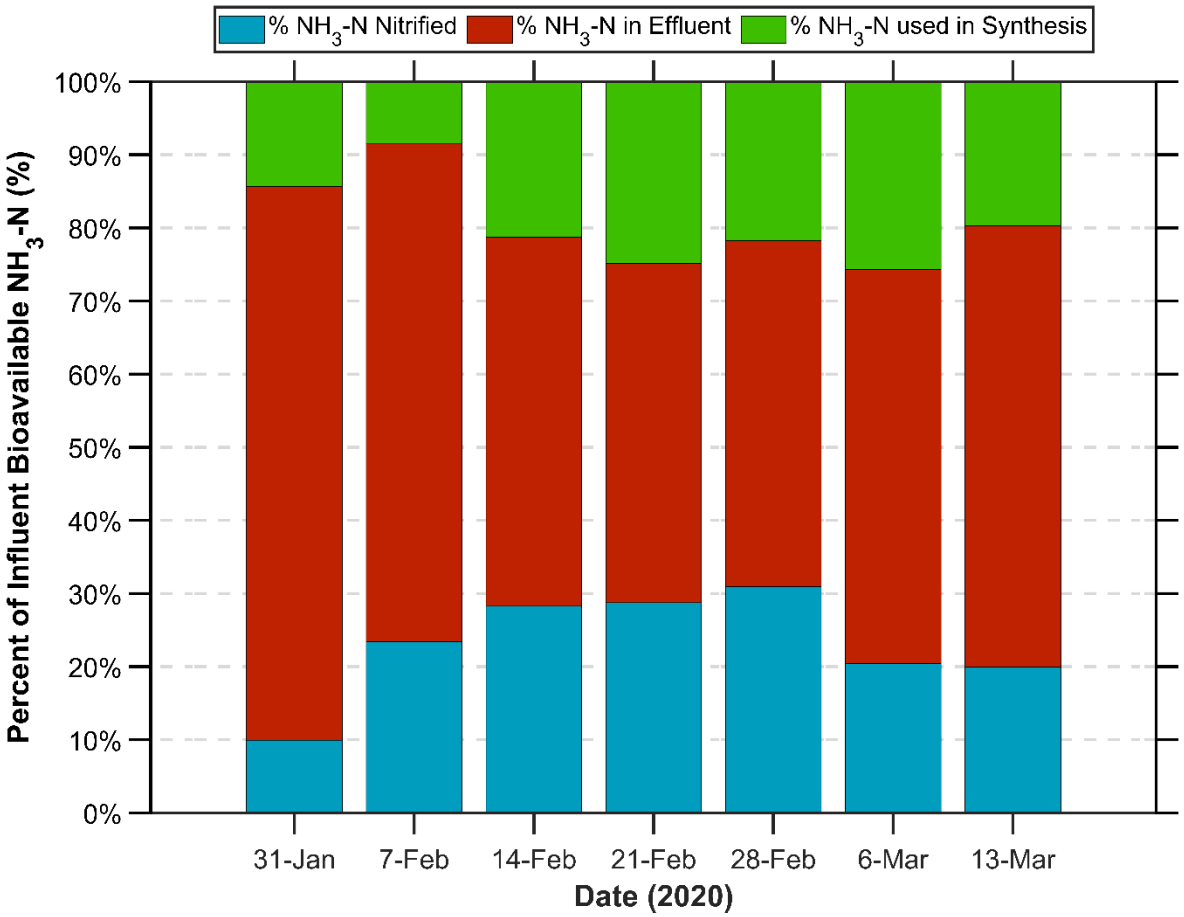

Figure 4-19. Weekly average fate of influent bioavailable NH_3-N during Phase 2.

The *amoA* gene copy number was investigated in the mixed liquor, granular, and flocculent sludges between February 5, 2020 and March 4, 2020. Comparison of the qPCR *amoA* gene copy number results in Figure 4-20 and 4-9 shows that the stored granule *amoA* gene copies/ngDNA was about 30% of the original granules before storage. As the SNR in the mainstream increased, it was expected that the *amoA* gene copy number in the granules would increase, as higher nitrification rates are correlated with increased AOB abundance. However, as SNR increased, *amoA* gene copy number decreased in both the floc and granule sludge (Figure 4-20). There are two explanations for this trend, 1) because qPCR assays are always normalized to the total DNA sample, it's possible that a great increase in heterotrophic bacteria would skew the results so that

AOB would have a lower relative abundance, and 2) qPCR detected the DNA of inactive AOB from the stored granules, which were washed out because they could not be revived. Assuming that the rate of washout of the inactive fraction was higher than the growth rate of new AOB, the apparent *amoA* gene copy number would be reduced, while the SNR increases. Continual bioaugmentation was started on February 25th, but the sample on the 27th did not show any increase in AOB abundance likely because too few granules had been added to the mainstream to affect the abundance. However, after a couple weeks of bioaugmentation, the fraction of added granules was significantly higher. On March 4th, the *amoA* gene copy number was about 225 per ngDNA, which is reflected by a spike in the SNR to 1.64 mgN/gVSS-h (Figure 4-20). The following two samples, on March 11th and 16th, both had *amoA* gene copy numbers of 128 and 115, respectively. Thus, the value on March 4th is likely an outlier because the *amoA* gene copy number is shown to drop, despite continual granule addition. The inhibition events on February 4th and March 1st, 5th, and 11th, are reflected in the SNR values, however, the *amoA* gene copy number was unaffected.

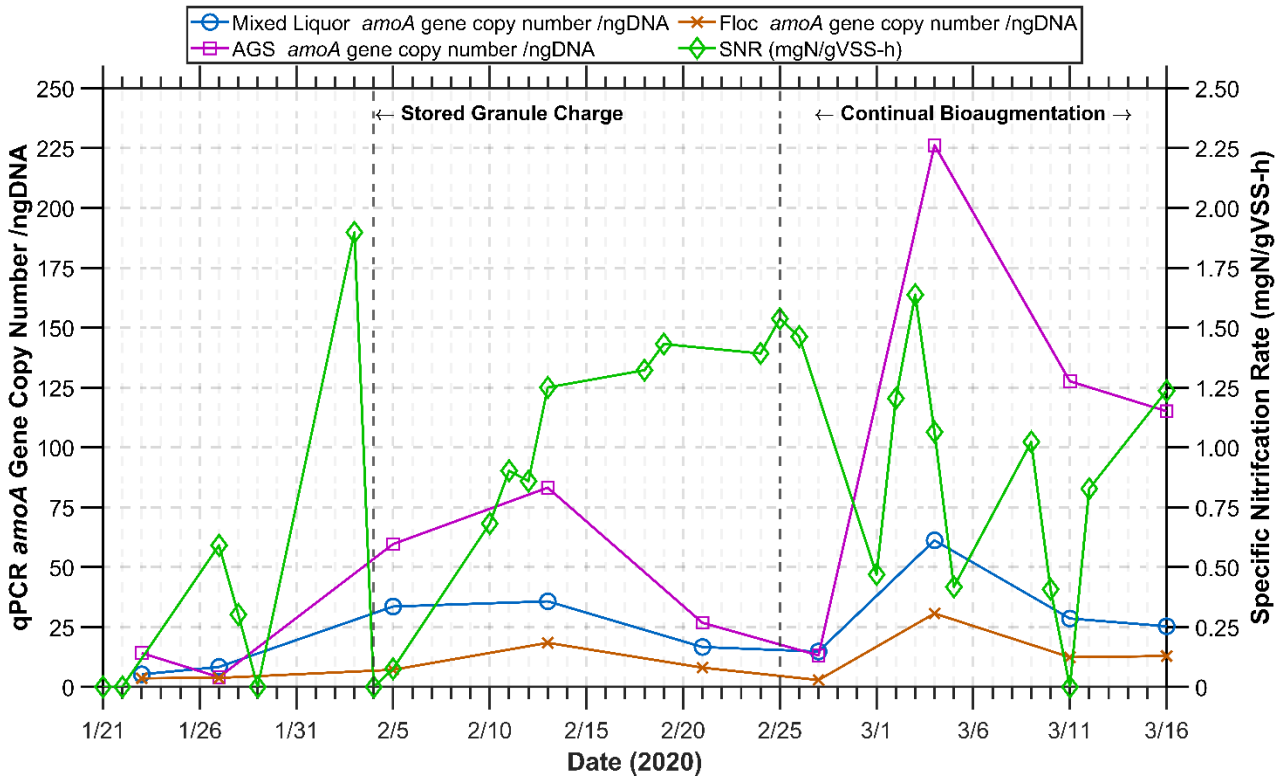

Figure 4-20. Mainstream Phase 2 *amoA* gene copy number for the aeration mixed liquor, granules, and flocculent sludge and SNR (mgN/gVSS-h) values. (qPCR data provided by Bao Ngyuen Quoc)

4.3.3.1 Mainstream Batch Nitrification Kinetics Testing

Batch nitrification kinetics tests were performed weekly after February 4, 2020, to track the relative nitrification rates of the granular sludge, flocculent sludge, and mixed liquor. The procedure for these tests is described in Section 3.5. Batch kinetic tests were performed at an average DO of 2 mg/L, to model the conditions in the aeration tank. These kinetics tests indicate that the flocculent sludge developed some nitrification ability, from nitrifier growth and/or nitrifiers falling off of the bioaugmented granules, and that the SNRs of the flocculent, granular, and mixed liquor sludge generally increased during Phase 2 (Figure 4-21).

The SNRs in Figure 4-21 were calculated as the sum of the NO_2^--N and NO_3^--N production rates. The NO_2^--N and NO_3^--N production rates fit linear trends with an average R^2 value of 0.85 and 0.99, respectively, compared to an average R^2 of 0.44 for the NH_3-N removal rate. The discrepancy in linear trends was likely a result of the greater accuracy of the nutrient tests used for NO_x-N, than those used for NH_3-N. Calculating SNR based on the NO_x-N production rates does not account for SND. Denitrification efficiency was about 25% for most of Phase 2 (Figure 4-19), while the percent of denitrification from SND varied from 68 to 93% (Table 4-13). This means that the SNR values in Figure 4-21 are likely underestimates by between 17 and 23%.

Based on the batch tests, the average SNR of the mixed liquor was 0.81 mgN/gVSS-h, while the flocculent and granular SNRs averaged 1.15 and 1.33 mgN/gVSS-h, respectively. However, it is impossible for the mixed liquor SNR to be less than the granular and flocculent SNRs because the mixed liquor contains both the flocculent and granular sludges. Thus, the predicted mixed liquor was calculated as the sum of the granule and flocculent sludge SNR contributions, based on their relative percentage of the mixed liquor. The predicted SNR shows that the mixed liquor SNR was likely dominated by flocculent sludge nitrification. On average, granule SNR accounted for 26% of the predicted mixed liquor SNR and 22% of the MLSS concentration. The highest granule contribution was achieved on February 10th, when the granule SNR accounted for 39% of the predicted mixed liquor SNR and 32% of the MLSS concentration.

The Phase 2 average SNR of the mixed liquor was 0.88 mgN/gVSS-h, while the batch test predicted mixed liquor SNR averaged 1.18 mgN/gVSS-h. The difference in SNRs is likely a

result of the batch test being an imperfect representation of the aeration tank in volume, temperature, mixing regime, and DO profile.

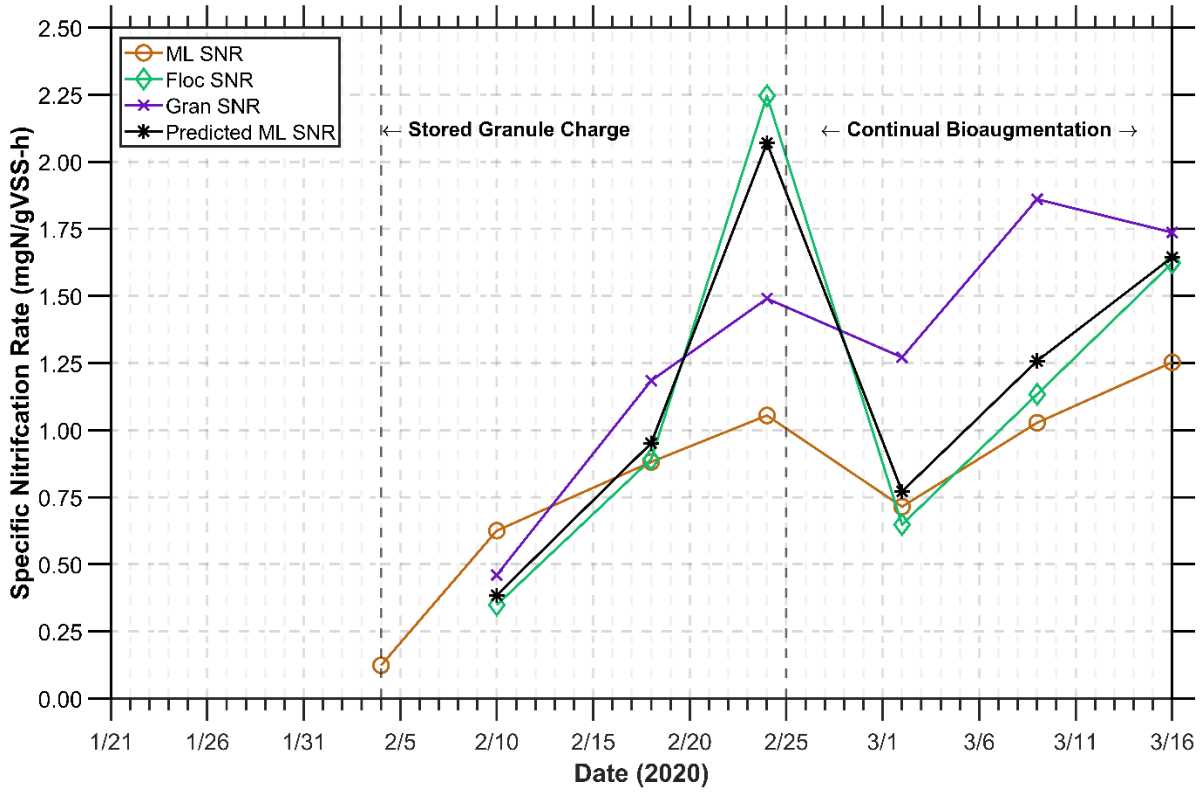

Figure 4-21. Phase 2 specific nitrification rate (SNR) calculated from NO_x-N production rates measured in batch kinetic tests of mainstream mixed liquor samples. The predicted mixed liquor SNR is based on the rates of the granular and flocculent sludges and their percent abundance in the mixed liquor.

4.3.4 Mainstream Phase 2 Separator Performance

The primary function of the separator was to achieve decoupled granule and flocculent SRTs. Throughout Phase 2, the granule SRT was about 1.5 times greater than that of the mixed liquor SRT (Figure 4-22). The largest SRT difference was between the mixed liquor and the large (>425µm in diameter) granules. After the stored granule charge, the large granule SRT was about 4 times greater than the mixed liquor SRT. During this time, granules >425 µm in diameter accounted for 25.9% of the MLSS concentration and about 64% of the total granule TSS.

Similarly, after about two weeks of continual bioaugmentation, when the granules >425 µm in diameter accounted for 5.6% of the MLSS concentration and 33% of the granule TSS, the >425 granule SRT was about 3 times greater than the mixed liquor SRT. However, this difference in large granule and mixed liquor SRT declined in early March. The increases in granule to mixed liquor SRT ratio appears to correspond to higher separator removal efficiencies (greater than 50%), however, high separator removal efficiencies were also observed with low granule to mixed liquor SRT ratio during the week ending with February 21st. Overall, the variation in separator efficiency had little effect on the granule to mixed liquor SRT ratio, as the ratio is fairly constant at about 1.5 while the separator efficiency varied from 38 to 53 (Table 4-14). The small difference in granule and mixed liquor SRTs is indicative that the separator failed to achieve significant granule and flocculent TSS separation.

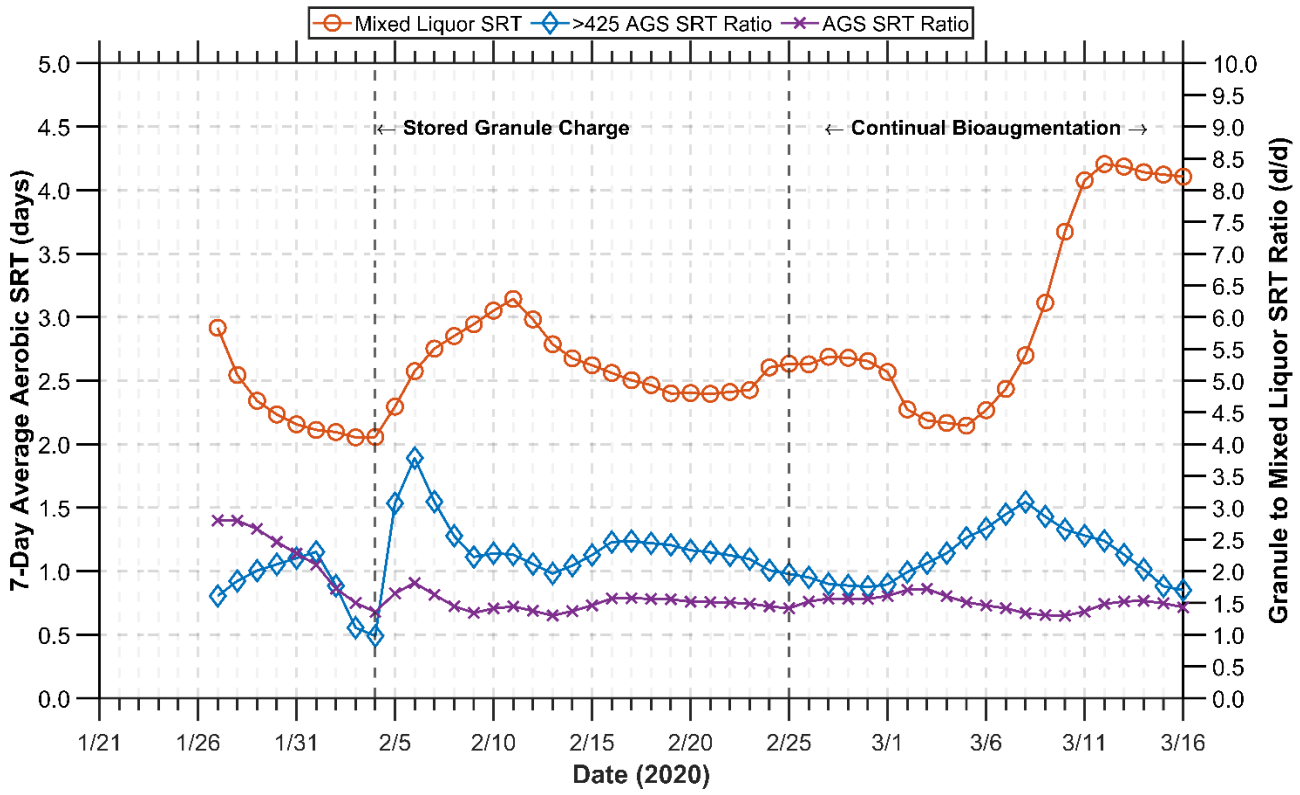

Figure 4-22. Mixed liquor 7-day average aerobic SRT, and granule to mixed liquor SRT ratio for granular sludge and granular sludge > 425 µm, during Phase 2.

Table 4-14. Phase 2 mainstream hydraulic upflow separator performance (standard deviation in parenthesis).

		Week Ending						
Parameter	Units	31-Jan	7-Feb	14-Feb	21-Feb	28-Feb	6-Mar	13-Mar
Superficial upflow velocity	m/h	10.5	10.4 (0.15)	9.6 (1.0)	8.0	8.0	7.4 (1.5)	3.6
Aeration Effluent								
MLSS	mg/L	3317 (527)	3609 (784)	3596 (287)	3167 (203)	3613 (211)	3146 (117)	3764 (364)
Granular TSS	mg/L	468	966 (648)	1290	591	850 (174)	634	558
Percent granules	%	16	25 (12)	32	20	24 (4)	20	17
TSS feed rate to separator	kg/d	67.8 (10.8)	70.5 (14.3)	69.6 (5.6)	61.3 (3.9)	68.8 (5.9)	55.9 (2.1)	64.6 (6.3)
Granule feed rate to separator	kg/d	9.6	18.8 (12.4)	25.0	11.4	16.2 (3.8)	11.4	9.6
Separator Overflow								
TSS	mg/L	2241 (893)	2403 (521)	2518 (526)	1880 (250)	2358 (258)	1992 (271)	2431 (393)
Granular TSS	mg/L	247	793 (390)	862	262	571	454	313
Percent granules	%	16	30 (10)	25	16	21	20	14
TSS effluent rate in overflow	kg/d	36.6 (14.6)	37.2 (7.4)	38.4 (8.0)	28.7 (3.8)	36.0 (3.9)	29.5 (5.4)	31.8 (5.1)
Granule effluent rate in overflow	kg/d	4.0	12.3 (5.8)	13.2	4.0	8.7	6.9	4.1
Separator Underflow								
TSS	mg/L	5770 (492)	8194 (1128)	7914 (396)	6640 (515)	7535 (258)	7651 (279)	6322 (1038)
Granular TSS	mg/L	701	2557 (1030)	2594	1454	1679 (126)	1719	1236
Percent granules	%	13	30 (8)	31	20	22 (2)	21	17
TSS effluent rate in underflow	kg/d	23.6 (2.0)	33.4 (4.6)	32.4 (1.6)	27.1 (2.1)	27.3 (4.4)	24.2 (4.4)	25.8 (4.2)
Granule effluent rate in underflow	kg/d	2.9	10.5 (4.2)	10.6	5.9	6.1 (1.2)	4.7	5.1
Separator Performance								
Removal efficiency of solids	%	42 (12)	47 (5)	47 (4)	47 (5)	44 (7)	43 (7)	45 (8)
Removal efficiency of feed granules	%	30	49 (6)	42	52	38 (2)	41	53

Figure 4-23 shows the amount of granules leaving the separator in the underflow and overflow, the weekly average superficial upflow velocity, and the weekly average separator granule removal efficiency. The superficial upflow velocity, which varied from 3.6 to 10.5 m/h, had no effect on the separator granule removal efficiency. The separator granule removal efficiency was below 50% except for the weeks of February 21st and March 13th, which corresponds to the weeks where there were more granules leaving the separator in the underflow than the overflow. These two weeks also had the highest average SVI_{30} (106 and 161 mL/g, respectively), implying the flocculent sludge settleability has some effect on the difficulty of separator granules from flocs, but no correlations were able to be drawn.

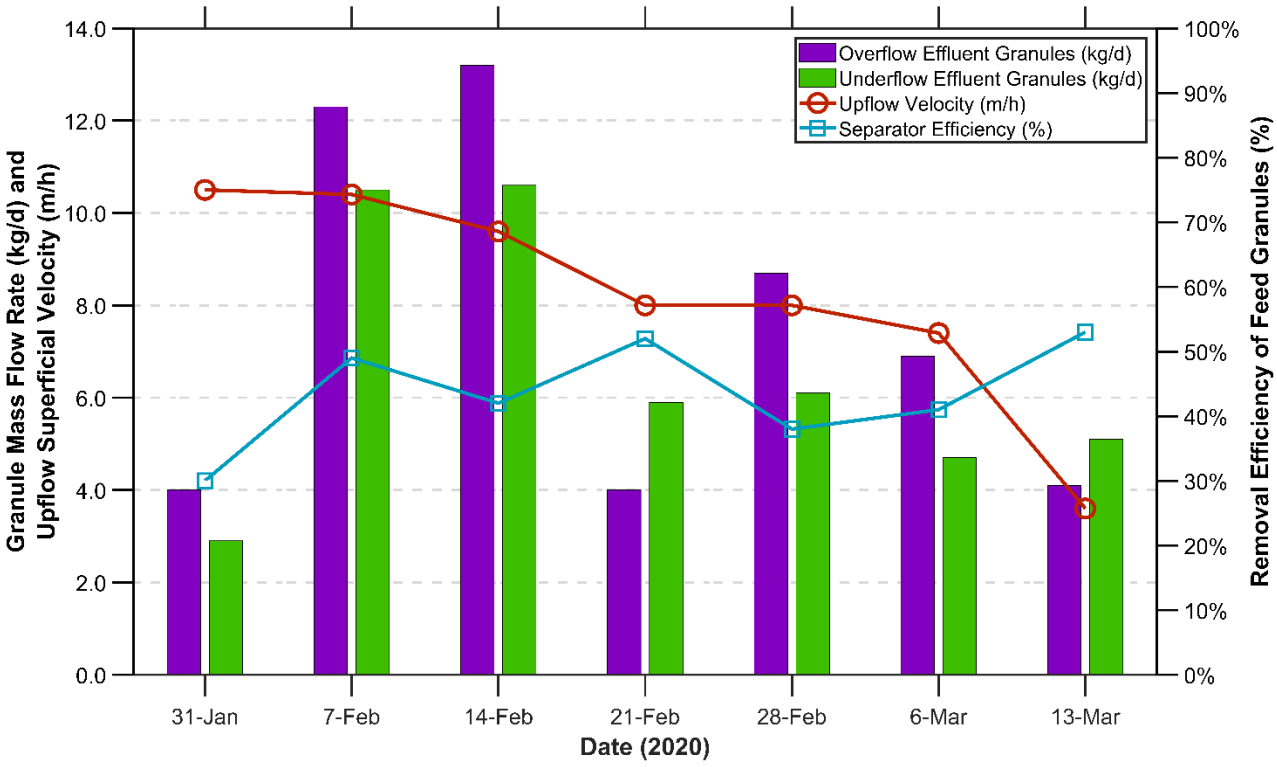

Figure 4-23. Comparison of separator granule removal efficiency, upflow superficial velocity, and amount of granular sludge in separator overflow and underflow for Phase 2.

4.3.4.1 Operating Conditions Affecting Separator Performance

Separator performance was expected to vary primarily based on the upflow superficial velocity, the granular MLSS, and the mixed liquor SRT. However, using the data from both Phases 1 and 2, no trends between separator efficiency and any of the above characteristics were able to be drawn (Figure 4-24). There was a slight trend between the mixed liquor percent granules and the granular removal efficiency, however it was not significant (R^2=0.01). Previous experiments done with the separator using sidestream granular sludge and WPTP flocculent sludge showed granule separation efficiencies between 91 and 94% at an upflow velocity of 10 m/h and a granule to floc ratio of 1.6. The discrepancy between previous tests and the results show during Phases 1 and 2 are likely a result of 1) the granule to floc ratio, 2) the inability of the granules to escape the floc matrix, 3) the good settling characteristics of the mixed liquor, and 4) the flow characteristics of the separator and distribution nozzle. Throughout Phases 1 and 2, the largest granule to floc ratio was 0.7, which is significantly lower than the ratio of 1.6 that the separator was tested at. Additionally, the low SRT flocculent sludge had a sticky nature, which caused fouling on probes, and likely helped to entrap the granules in the floc matrix. Because of SP's low SRT EBPR system, the seed sludge had good settling characteristics, SVI_{30} = 85 to 110 mL/g (Table 4-7, Table 4-12). This means discrete settling was more difficult to achieve because the floc and granules tended to settle as one unit (Figure 4-25). Finally, the separator influent flow had a rolling action which caused some flow to go under the nozzle, observed during clear water dye tests, which may have counteracted the selection pressure applied by the upflow velocity. Furthermore, because of the relatively small diameter of the separator, some flow from the nozzle hit the separator wall, which contributed to the rolling action described above.

Overall, the four factors described caused the separator overflow and underflow to exhibit near identical granule and floc ratio characteristics (Figure 4-26).

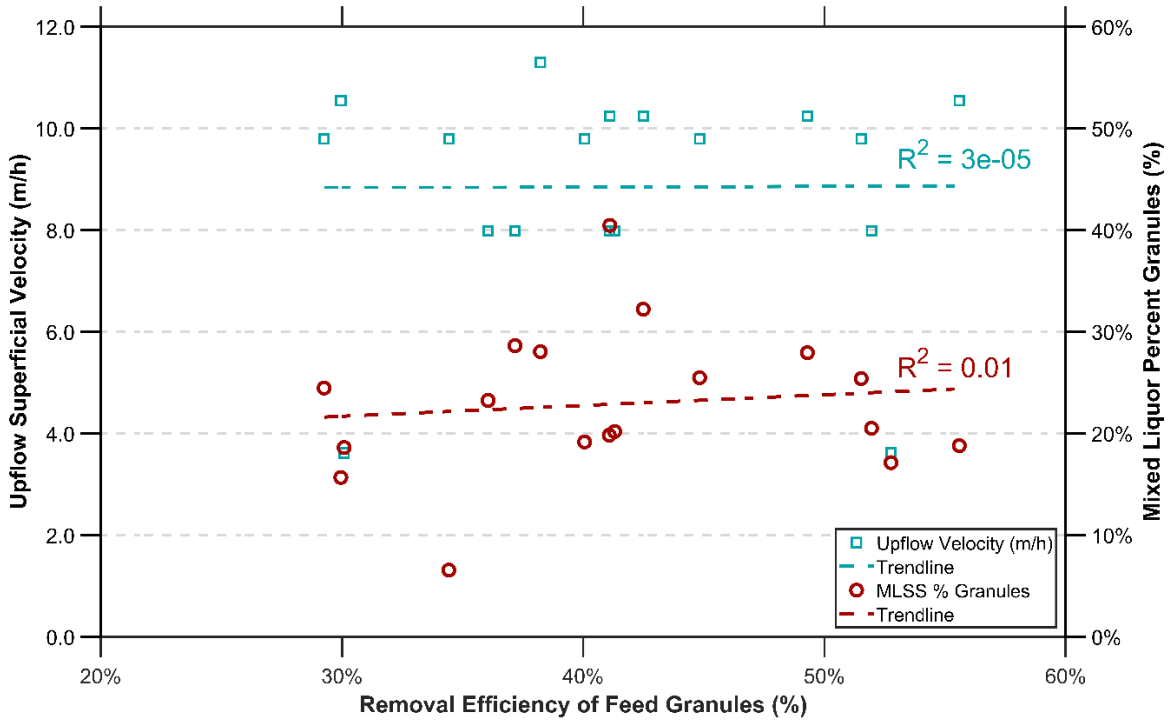

Figure 4-24. Removal efficiency of feed granules correlated to upflow velocity and mixed liquor percent granules, data from Phases 1 and 2 is used.

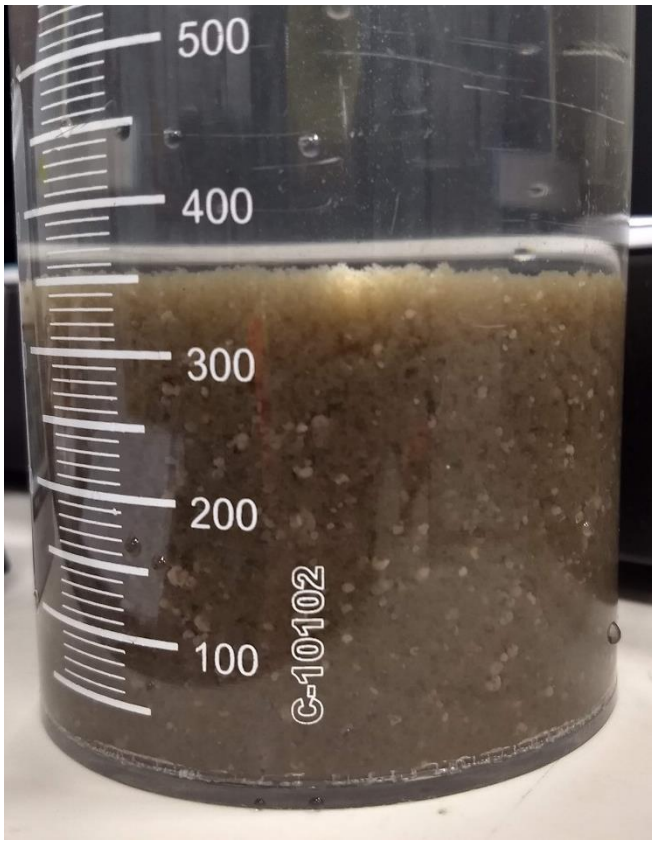

Figure 4-25. Settled mixed liquor from February 5, 2020, after the granule spike. Image was taken using a smartphone. The lack of discrete settling indicates the good settling characteristics of the flocculent sludge

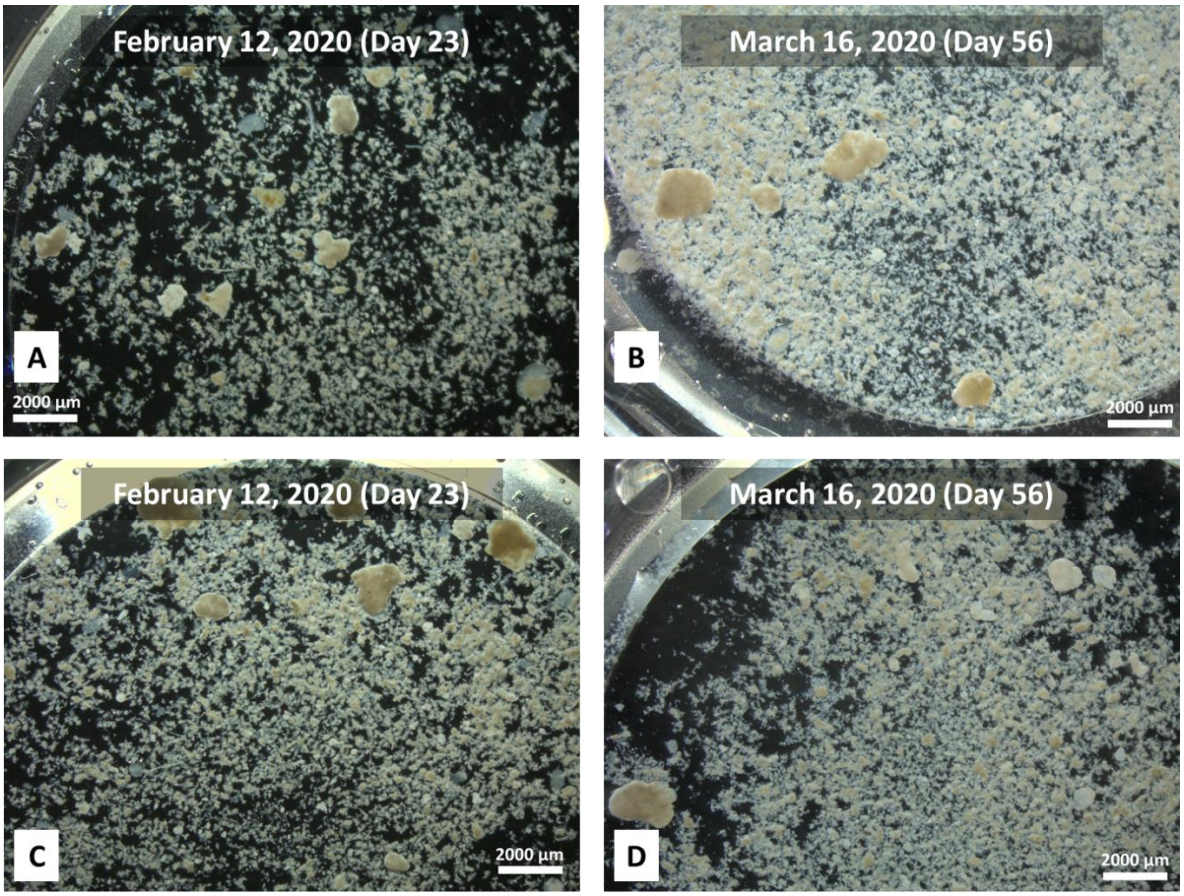

Figure 4-26. Images taken on separator overflow sludge (A, B) and separator underflow sludge (C, D) using a camera mounted to a stereo microscope. Sludges were diluted to 300-400 mg/L TSS for photographs.

4.3.5 Fate of Granules in the Mainstream Aeration Tank during Phase 2

The aeration tank mixed liquor was sampled weekly for sieve analysis to follow the fraction of granular sludge and the granular size distribution over time to determine if the size distribution of the sidestream bioaugmented granules changed in the mainstream system. Four sieve sizes were used: 212 µm, 425 µm, 850 µm, and 1700 µm.

A summary of the weekly mixed liquor granular sludge analysis is shown in Table 4-15. Granules accounted for 12.5% of the SP seed sludge MLSS concentration based on the definition of granular sludge being retained on a 212 µm sieve. Only 2.9% of the SP seed sludge was retained on the 425 µm sieve and there was no retention on the 850 µm sieve. At the end of the first week of operation without bioaugmentation, the amount of granular sludge in the mixed liquor increased slightly to 15.7%, with 2.1% being retained on the 425 µm sieve.

Table 4-15. Summary of weekly granule sludge analyses for the mainstream aeration tank mixed liquor during Phase 2.

		Sample Date							
Parameter	Units	27-Jan	5-Feb	10-Feb	18-Feb	24-Feb	2-Mar	9-Mar	16-Mar
Daily Bioaugmentation	Yes/No	N	Spike	N	N	Y	Y	Y	Y
MLSS	mg/L	2989	4929	4004	2885	3836.5	3201	3260	4084
Granule MLSS	mg/L	468	1994	1290	591	892	634	558	760
	%	15.7	40.5	32.2	20.5	23.2	19.8	17.1	18.6
MLSS >212 <425 um	mg/L	405.5	715	493	326.3	556.5	352	375.6	493
	%	13.6	14.5	12.3	11.3	14.5	11	11.5	12.1
MLSS >425 <850 um	mg/L	62.5	391.5	398	175.8	192.5	137	116.8	122
	%	2.1	7.9	9.9	6.1	5	4.3	3.6	3.0
MLSS >850 <1700 um	mg/L	0	665	364.5	89.2	142.5	145	65.6	128
	%	0	13.5	9.1	3.1	3.7	4.5	2	3.1
MLSS >1700 um	mg/L	0	222.5	34	0	0	0	0	17
	%	0	4.5	0.8	0	0	0	0	0.4

The data for the February 5, 2020 sample shows that after the spike of stored granules to the mainstream on February 4th, the percent granules in the mixed liquor increased to 40.5% and 62.5% of the granules present were within the size range covered by the 4 sieves. The faction of mixed liquor in the >850 and <1700 µm size range was 13.5%. A week later the granular fraction in that size range had decreased to 9.1% and the granule fraction of the mixed liquor had decreased to 32.3%. For sizes greater than 1700 µm, the granule fraction decreased from 4.5% to 0.8% of the mixed liquor, but for the size range between 425 and 850 µm it had increased from 7.9% to 9.9%. These results suggest that some of the larger granules broke up and there was loss of granules from the system, presumably due to the unexpected low efficiency of the separator and thus loss of granules of all sizes in the sludge wasting from the clarifier return line.

Two weeks after the granular spike, on February 18th, the granular TSS was only 20% of the MLSS. Some deterioration of larger size granules is also indicated by a reduction in the fraction of granules for sizes above 425 µm and an increase in the fraction of granules for sizes >212 µm and >425 µm. In the two weeks after February 25th with sidestream bioaugmentation, there was no buildup of granules and no significant change in the fraction of granules in the mixed liquor (19.8% and 17.1%, respectively). During those two weeks of continual bioaugmentation, there was a steady decrease at all granule sizes. For the last week of operation, the fraction of granular sludge was 4.6% lower than for the sample on February 24th, but there was an increase in the granules >850 µm, likely indicating a slight buildup from continual bioaugmentation. The change in granular size in the mixed liquor can be seen in the stereo microscope photos shown in Figure 4-27. Reduction in the size of granules bioaugmented from the sidestream reactor may

have been due to agitation from the anaerobic tank mixing intensity, recycle pumping, and/or its feeding regime.

It is possible that the integrity of the granules was affected by the different substrate feed regime in the anaerobic phase of the sidestream and mainstream reactors. The bulk liquid acetate COD concentration in the sidestream reactor anaerobic phase was more than 200 mg/L, whereas the bulk liquid acetate COD concentration in the mainstream anaerobic zone averaged 7 mg/L during Phase 2. A higher bulk liquid concentration allows for deeper penetration of growth substrate and thus would encourage a deeper biofilm or larger granule.

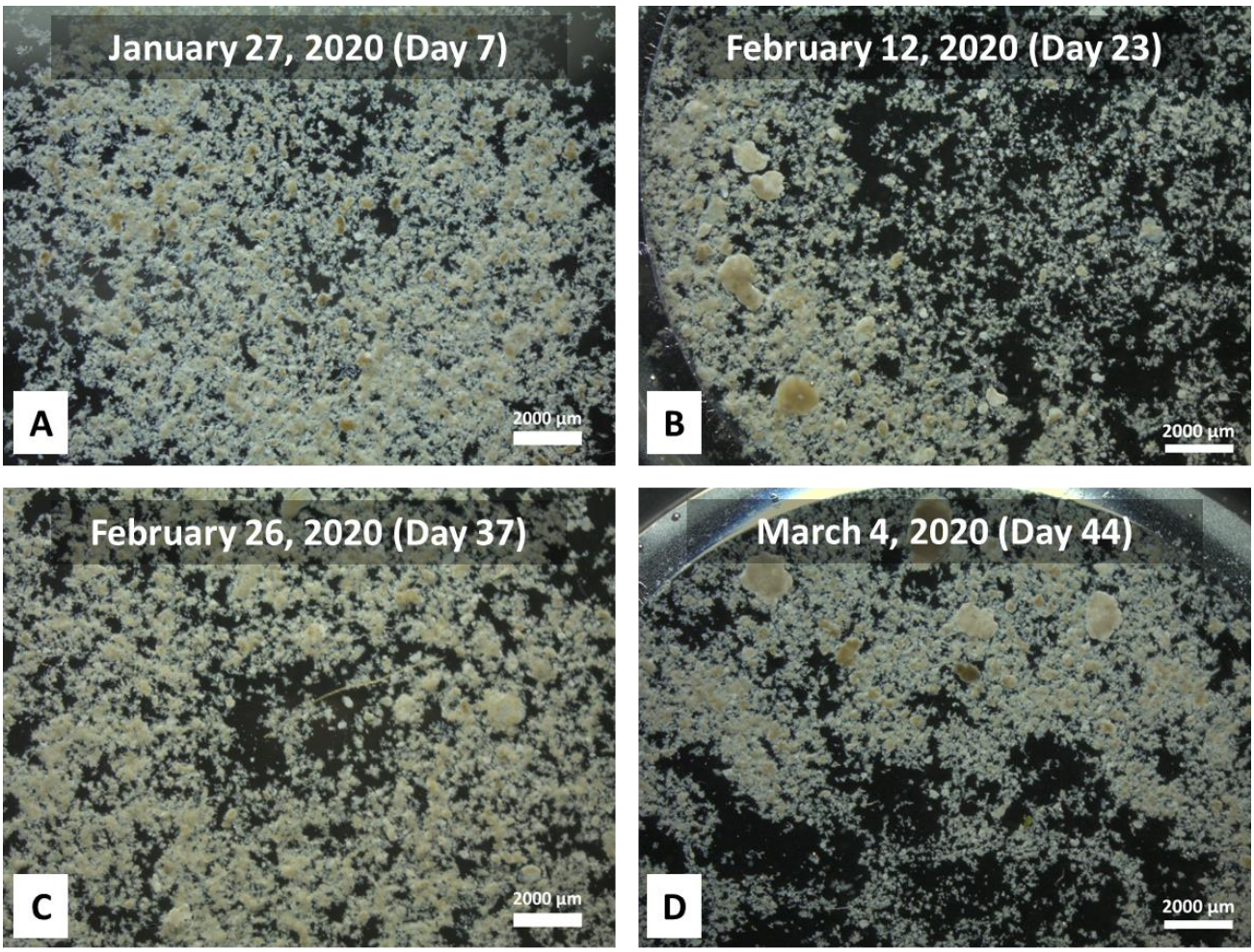

Figure 4-27. Image of Phase 2 mainstream aeration mixed liquor taken with a camera mounted to a stereo microscope. A) flocculent sludge before bioaugmentation B) mixed liquor a week after the granule spike C) mixed liquor the day after continuous bioaugmentation began D) mixed liquor 8 days after continuous bioaugmentation began.

5 Summary and Conclusion

A mainstream CFAS pilot plant was operated with a hydraulic separator to treat WPTP primary effluent alongside a pilot sidestream AGS SBR, which produced nitrifying granular sludge for bioaugmentation of the mainstream system. The sidestream reactor was maintained for the 6.5-month research period and it was fed acetate in an anerobic phase and centrate diluted with WPTP final effluent at the start of the aerobic phase to produce a mixed liquor dominated by PAO-NDN granules for bioaugmentation. The average diameter of the sidestream granular sludge ranged from 1.25 to 1.9 mm and over 90% simultaneous nitrification and denitrification occurred during the aerobic phase. The sidestream system processed anaerobic digestion centrate that contained an average of 21% of the nitrogen load to the mainstream treatment, which is within a typical range for municipal full-scale facilities with anaerobic digestion and sludge dewatering.

The mainstream pilot plant system had two operating phases: the first lasting 40 days with only flocculent sludge mixed liquor, and the second lasting 56 days, with about two weeks of flocculent sludge operation, a granular sludge spike which was monitored for 20 days, and 20 days of continual sidestream bioaugmentation. During phase 2, nitrification efficiency increased from 10 to 30%. Sidestream bioaugmented granules in the mainstream were maintained at a lower level than expected and at an SRT of only 50% higher than that of the mixed liquor due to a hydraulic granular/floc separator efficiency of less than 55%. There was also some deterioration in the granular size fed form the sidestream reactor. The following conclusions result from this pilot plant study:

1. The sidestream reactor operation was maintained at a NH_3-N loading of 0.30 to 0.35 g/L-d and produced a mixed liquor with over 95% granules at an average size of 1.25 to 1.9 mm.
2. Shortcut nitrogen removal and NOB suppression was achieved in the sidestream SBR as evidenced by a high NO_2^--N/NO_3^--N effluent ratio, a high NO_2^--N/NO_3^--N production rate ratio in batch tests, and a mixed liquor AOB:NOB abundance ratio of 3 to 4 from qPCR analyses.
3. The shortcut nitrogen removal was enabled by operation of the sidestream SBR with a final aeration DO:NH_3-N ratio of 0.02 – 0.58 mg/mg.
4. The Michaelis-Menten kinetic model fit for acetate uptake by the sidestream granules had a maximum specific acetate uptake rate of 2.7 gCOD/gVSS-day and an acetate half-saturation coefficient of 9.7 mg/L.
5. The sidestream reactor SNR were from 1.2 to 1.4 mg/gVSS-h.
6. The operation had a higher COD:N feed ratio than needed to have just enough stored carbon by PAOs and GAOs after anaerobic feeding to use the NO_2/NO_3 produced during aeration, which resulted in PAO growth in the aerobic outer layers of the granule to impede the nitrification efficiency.
7. The sidestream reactor denitrification efficiency ranged from 89 to 96% at average aeration phase DO concentrations from 2.2 to 2.6 mg/L.
8. Significant growth of small granules was shown in the mainstream during Phase 1, with up to 25% of the MLSS being retained on a 212 µm sieve.
9. Larger size granules from the sidestream reactor deteriorated within the mainstream system, which had more granule agitation due to pumping and mixing and also had a

lower substrate concentration feeding regime in the anaerobic phase compared to the sidestream SBR.

10. The granule separation efficiency ranged from 30 to 53% with upflow superficial velocities from 3.6 to 10.5 m/h and a granule content of 16 to 41% in the MLSS feed.
11. The mainstream nitrification efficiency was shown to increase from 10% to 30% with sidestream bioaugmentation.
12. During Phase 2 bioaugmentation the average aerobic SRT of the granular and flocculant sludges were 4.4 and 2.5 days, respectively, and the granule to mixed liquor SRT ratio averaged 1.5, showing marginal uncoupling of granule and floc SRTs.
13. Granules maintained their nitrification capability once added to the mainstream, based on batch nitrification tests.

6 Future Research

Additional research should be focused on developing an understanding of the potential and possible applications for bioaugmentation with sidestream AGS by evaluating the cause of the granule size reduction, startup procedure, methods to improve uncoupling of the granular and flocculent sludge SRTs, and performance with long-term continual bioaugmentation. Because both phases of this study were cut short, future research is needed to understand the treatment performance of long-term sidestream bioaugmentation with AGS. Furthermore, additional research is needed to determine the shear strength of granules and their potential to survive the pumping and mixing stresses associated with a mainstream system.

Various methods should be considered to improve decoupling of granular and flocculent sludge SRTs. Based on the testing done with the hydraulic upflow separator used in this study the granule to floc MLSS ratio is crucial for granule and floc separation. However, more research is needed to determine the optimal granule to floc ratio and the operating performance of various ratios. Additional suggestions for improving SRT decoupling between granule and flocculent sludges are as follows:

- Improving the hydraulic upflow separator with the use of computational fluid dynamics, taking into account the sludge solids, to better understand the hydraulics of the separator to enable optimization of design for granule/floc separation by minimizing any rolling actions to turbulent flows.

- Feeding secondary clarifier waste activated sludge from the mainstream to the sidestream SBR during continual bioaugmentation. This would allow for selective wasting of flocculent sludge using the selection pressures present in a sidestream SBR while supplementing continual bioaugmentation with additional granules.
- Modifying the mainstream secondary clarifier to allow for the selective wasting of lighter mixed liquor. For example, wasting could be done solely from sludge settling on the outer parts of the clarifier where lighter sludges are more likely to settle.
- Evaluate the effect of granule starvation and different bulk liquid substrate feeding conditions on the effect of granular integrity and size.

7 References

Ahn, J., Schroeder, S., Beer, M., McIlroy, S., Bayly, R. C., May, J. W., … Seviour, R. J. (2007). Ecology of the microbial community removing phosphate from wastewater under continuously aerobic conditions in a sequencing batch reactor. *Applied and Environmental Microbiology*, *73*(7), 2257–2270. https://doi.org/10.1128/AEM.02080-06

Anthonisen, A. C., Loehr, R. C., Prakasam, T. B. S., & Srinath, E. G. (1976). Inhibition of nitrification by ammonia and nitrous acid. *Journal of the Water Pollution Control Federation*, *48*(5), 835–852. https://doi.org/10.1016/0168-6496(92)90072-2

Armenta, M. (2019). Operation and Performance of a Sidestream Aerobic Granular Sludge (University of Washington). https://doi.org/10.1017/CBO9781107415324.004

Bartrolí, A., Pérez, J., & Carrera, J. (2010). Applying ratio control in a continuous granular reactor to achieve full nitritation under stable operating conditions. *Environmental Science and Technology*, *44*(23), 8930–8935. https://doi.org/10.1021/es1019405

Bassin, J. P., Kleerebezem, R., Dezotti, M., & van Loosdrecht, M. C. M. (2012). Simultaneous nitrogen and phosphate removal in aerobic granular sludge reactors operated at different temperatures. *Water Research*, *46*(12), 3805–3816. https://doi.org/10.1016/j.watres.2012.04.015

Bertanza, G. (1997). Simultaneous Nitrification-Denitrification Process in Extended Aeration Plants: Pilot and Real Scale Experiences. *Water Science and Technology*, *35*(6), 53–61.

Blackburne, R., Vadivelu, V. M., Yuan, Z., & Keller, J. (2007). Kinetic characterisation of an enriched Nitrospira culture with comparison to Nitrobacter. *Water Research*, *41*(14), 3033–3042. https://doi.org/10.1016/j.watres.2007.01.043

Boncescu, C., & Robescu, L. D. (2018). Modeling efficiency of biological process with aerobic granular sludge. *International Multidisciplinary Scientific GeoConference Surveying Geology and Mining Ecology Management, SGEM*, *18*(5.2), 649–654. https://doi.org/10.5593/sgem2018/5.2/S20.084

Bowden, G., Tsuchihashi, R., & Stensel, H. D. (2016). Technologies for Sidestream Nitrogen Removal. In *Water Intelligence Online* (Vol. 15). https://doi.org/10.2166/9781780407890

Bumbac, C., Ionescu, I. A., Tiron, O., & Badescu, V. R. (2015). Continuous flow aerobic granular sludge reactor for dairy wastewater treatment. *Water Science and Technology*, *71*(3), 440–445. https://doi.org/10.2166/wst.2015.007

Camejo, P. Y., Owen, B. R., Martirano, J., Ma, J., Kapoor, V., Santo Domingo, J., … Noguera, D. R. (2016). Candidatus Accumulibacter phosphatis clades enriched under cyclic anaerobic

and microaerobic conditions simultaneously use different electron acceptors. *Water Research*, *102*, 125–137. https://doi.org/10.1016/j.watres.2016.06.033

Carvalho, G., Lemos, P. C., Oehmen, A., & Reis, M. A. M. (2007). Denitrifying phosphorus removal: Linking the process performance with the microbial community structure. *Water Research*, *41*(19), 4383–4396. https://doi.org/10.1016/j.watres.2007.06.065

Chen, X., Yuan, L., Lu, W., Li, Y., Liu, P., & Nie, K. (2015). Cultivation of aerobic granular sludge in a conventional, continuous flow, completely mixed activated sludge system. *Frontiers of Environmental Science and Engineering*, *9*(2), 324–333. https://doi.org/10.1007/s11783-014-0627-3

Cofré, C., Campos, J. L., Valenzuela-Heredia, D., Pavissich, J. P., Camus, N., Belmonte, M., … Val del Río, A. (2018). Novel system configuration with activated sludge like-geometry to develop aerobic granular biomass under continuous flow. *Bioresource Technology*, *267*(May), 778–781. https://doi.org/10.1016/j.biortech.2018.07.146

de Kreuk, M. K., Kishida, N., & van Loosdrecht, M. C. M. (2007). Aerobic granular sludge - State of the art. *Water Science and Technology*, *55*(8–9), 75–81. https://doi.org/10.2166/wst.2007.244

De Kreuk, M. K., Picioreanu, C., Hosseini, M., Xavier, J. B., & Van Loosdrecht, M. C. M. (2007). Kinetic model of a granular sludge SBR: Influences on nutrient removal. *Biotechnology and Bioengineering*, *97*(4), 801–815. https://doi.org/10.1002/bit.21196

De Kreuk, M. K., Heijnen, J. J., & Van Loosdrecht, M. C. M. (2005). Simultaneous COD, nitrogen, and phosphate removal by aerobic granular sludge. *Biotechnology and Bioengineering*, *90*(6), 761–769. https://doi.org/10.1002/bit.20470

de Sousa Rollemberg, S. L., Mendes Barros, A. R., Milen Firmino, P. I., & Bezerra dos Santos, A. (2018). Aerobic granular sludge: Cultivation parameters and removal mechanisms. *Bioresource Technology*, *270*(July), 678–688. https://doi.org/10.1016/j.biortech.2018.08.130

Devlin, T. R., di Biase, A., Kowalski, M., & Oleszkiewicz, J. A. (2017). Granulation of activated sludge under low hydrodynamic shear and different wastewater characteristics. *Bioresource Technology*, *224*, 229–235. https://doi.org/10.1016/j.biortech.2016.11.005

Devlin, T. R., & Oleszkiewicz, J. A. (2018). Cultivation of aerobic granular sludge in continuous flow under various selective pressure. *Bioresource Technology*, *253*(November 2017), 281–287. https://doi.org/10.1016/j.biortech.2018.01.056

Downing, L., Redmond, E., Klopping, P., & Young, M. (2017). Selective pressures for granulation in full-scale, flow through activated sludge system. *Water Environment Federation Technical Exhibition and Conference 2017, WEFTEC 2017*, *7*(Figure 1), 4479–4483. https://doi.org/10.2175/193864717822155849

Fang, F., Ni, B. J., Li, X. Y., Sheng, G. P., & Yu, H. Q. (2009). Kinetic analysis on the two-step processes of AOB and NOB in aerobic nitrifying granules. *Applied Microbiology and Biotechnology*, *83*(6), 1159–1169. https://doi.org/10.1007/s00253-009-2011-y

Figdore, B. A., David Stensel, H., & Winkler, M. K. H. (2018a). Bioaugmentation of sidestream nitrifying-denitrifying phosphorus-accumulating granules in a low-SRT activated sludge system at low temperature. *Water Research*, *135*, 241–250. https://doi.org/10.1016/j.watres.2018.02.035

Figdore, B. A., Stensel, H. D., & Winkler, M. K. H. (2018b). Comparison of different aerobic granular sludge types for activated sludge nitrification bioaugmentation potential. *Bioresource Technology*, *251*(August 2017), 189–196. https://doi.org/10.1016/j.biortech.2017.11.004

Figdore, B. A., Winkler, M.-K. H., & Stensel, H. D. (2018c). Bioaugmentation with Nitrifying Granules in Low-SRT Flocculent Activated Sludge at Low Temperature. *Water Environment Research*, *90*(4), 343–354. https://doi.org/10.2175/106143017x15054988926488

Flowers, J. J., He, S., Yilmaz, S., Noguera, D. R., & McMahon, K. D. (2009). Denitrification capabilities of two biological phosphorus removal sludges dominated by different "Candidatus Accumulibacter" clades. *Environmental Microbiology Reports*, *1*(6), 583–588. https://doi.org/10.1111/j.1758-2229.2009.00090.x

Franca, R. D. G., Pinheiro, H. M., van Loosdrecht, M. C. M., & Lourenço, N. D. (2018). Stability of aerobic granules during long-term bioreactor operation. *Biotechnology Advances*, *36*(1), 228–246. https://doi.org/10.1016/j.biotechadv.2017.11.005

Gao, D., Liu, L., Liang, H., & Wu, W. M. (2011). Aerobic granular sludge: Characterization, mechanism of granulation and application to wastewater treatment. *Critical Reviews in Biotechnology*, *31*(2), 137–152. https://doi.org/10.3109/07388551.2010.497961

Guo, J., Peng, Y., Wang, S., Zheng, Y., Huang, H., & Wang, Z. (2009). Long-term effect of dissolved oxygen on partial nitrification performance and microbial community structure. *Bioresource Technology*, *100*(11), 2796–2802. https://doi.org/10.1016/j.biortech.2008.12.036

He, Q., Zhou, J., Song, Q., Zhang, W., Wang, H., & Liu, L. (2017). Elucidation of microbial characterization of aerobic granules in a sequencing batch reactor performing simultaneous nitrification, denitrification and phosphorus removal at varying carbon to phosphorus ratios. *Bioresource Technology*, *241*, 127–133. https://doi.org/10.1016/j.biortech.2017.05.093

He, S., Gall, D. L., & McMahon, K. D. (2007). "Candidatus accumulibacter" population structure in enhanced biological phosphorus removal sludges as revealed by polyphosphate kinase genes. *Applied and Environmental Microbiology*, *73*(18), 5865–5874. https://doi.org/10.1128/AEM.01207-07

Helmer, C., & Kunst, S. (1998). Simultaneous Nitrification/Denitrification in an Aerobic Biofilm System. *Water Science and Technology*, *37*(4–5), 183–187.

Isanta, E., Reino, C., Carrera, J., & Pérez, J. (2015). Stable partial nitritation for low-strength wastewater at low temperature in an aerobic granular reactor. *Water Research*, *80*, 149–158. https://doi.org/10.1016/j.watres.2015.04.028

Jahn, L., Svardal, K., & Krampe, J. (2019). Comparison of aerobic granulation in SBR and continuous-flow plants. *Journal of Environmental Management*, *231*(October 2018), 953–961. https://doi.org/10.1016/j.jenvman.2018.10.101

Kent, T. R., Bott, C. B., & Wang, Z. W. (2018). State of the art of aerobic granulation in continuous flow bioreactors. *Biotechnology Advances*, *36*(4), 1139–1166. https://doi.org/10.1016/j.biotechadv.2018.03.015

Kent, T. R., Sun, Y., An, Z., Bott, C. B., & Wang, Z. W. (2019). Mechanistic understanding of the NOB suppression by free ammonia inhibition in continuous flow aerobic granulation bioreactors. *Environment International*, *131*(July), 105005. https://doi.org/10.1016/j.envint.2019.105005

Kim, J. M., Lee, H. J., Lee, D. S., & Jeon, C. O. (2013). Characterization of the denitrification-associated phosphorus uptake properties of "Candidatusaccumulibacter phosphatis" clades in sludge subjected to enhanced biological phosphorus removal. *Applied and Environmental Microbiology*, *79*(6), 1969–1979. https://doi.org/10.1128/AEM.03464-12

Kong, Y., Xia, Y., Nielsen, J. L., & Nielsen, P. H. (2007). Structure and function of the microbial community in a full-scale enhanced biological phosphorus removal plant. *Microbiology*, *153*(12), 4061–4073. https://doi.org/10.1099/mic.0.2007/007245-0

Kouba, V., Catrysse, M., Stryjova, H., Jonatova, I., Volcke, E. I. P., Svehla, P., & Bartacek, J. (2014). The impact of influent total ammonium nitrogen concentration on nitrite-oxidizing bacteria inhibition in moving bed biofilm reactor. *Water Science and Technology*, *69*(6), 1227–1233. https://doi.org/10.2166/wst.2013.757

Krasnits, E., Beliavsky, M., Tarre, S., & Green, M. (2013). PHA based denitrification: Municipal wastewater vs. acetate. *Bioresource Technology*, *132*, 28–37. https://doi.org/10.1016/j.biortech.2012.11.074

Lanham, A. B., Moita, R., Lemos, P. C., & Reis, M. A. M. (2011). Long-term operation of a reactor enriched in Accumulibacter clade I DPAOs: Performance with nitrate, nitrite and oxygen. *Water Science and Technology*, *63*(2), 352–359. https://doi.org/10.2166/wst.2011.063

Li, D., Lv, Y., Zeng, H., & Zhang, J. (2016). Startup and long term operation of enhanced biological phosphorus removal in continuous-flow reactor with granules. *Bioresource Technology*, *212*, 92–99. https://doi.org/10.1016/j.biortech.2016.04.008

Li, J., Cai, A., Wang, M., Ding, L., & Ni, Y. (2014). Aerobic granulation in a modified oxidation ditch with an adjustable volume intraclarifier. *Bioresource Technology*, *157*, 351–354. https://doi.org/10.1016/j.biortech.2014.01.130

Li, J., Ding, L. Bin, Cai, A., Huang, G. X., & Horn, H. (2014). Aerobic sludge granulation in a full-scale sequencing batch reactor. *BioMed Research International*, *2014*. https://doi.org/10.1155/2014/268789

Liu, H., Li, Y., Yang, C., Pu, W., He, L., & Bo, F. (2012). Stable aerobic granules in continuous-flow bioreactor with self-forming dynamic membrane. *Bioresource Technology*, *121*, 111–118. https://doi.org/10.1016/j.biortech.2012.07.016

Liu, H., Xiao, H., Huang, S., Ma, H., & Liu, H. (2014). Aerobic granules cultivated and operated in continuous-flow bioreactor under particle-size selective pressure. *Journal of Environmental Sciences (China)*, *26*(11), 2215–2221. https://doi.org/10.1016/j.jes.2014.09.004

Long, B., Yang, C. Z., Pu, W. H., Yang, J. K., Liu, F. B., Zhang, L., & Cheng, K. (2015). Rapid cultivation of aerobic granular sludge in a continuous flow reactor. *Journal of Environmental Chemical Engineering*, *3*(4), 2966–2973. https://doi.org/10.1016/j.jece.2015.10.001

Meinhold, J., Filipe, C. D. M., Daigger, G. T., & Isaacs, S. (1999). *1999. Meinhold et al. Characterization of denitrifying fraction of PAO in BioP removal.pdf* (pp. 31–42). pp. 31–42. Water Science Technology.

Melcer, H., Dold, P. L., Jones, R. M., Bye, C. M., Takács, I., Stensel, H. D., … Bury, S. (2003). *Methods for Wastewater Characterization in Activated Sludge Modeling*. Retrieved from https://books.google.com.sg/books?id=JbtuFC3QHecC

Metcalf & Eddy. (2014). *Wastewater Engineering: Treatment and Resource Recovery* (5th ed.; G. Tchobanoglous, H. D. Stensel, R. Tsuchihashi, & F. L. Burton, Eds.). Retrieved from https://books.google.com.cu/books?id=6KVKMAEACAAJ

Münch, E. V., Lant, P., & Keller, J. (1996). Simultaneous nitrification and denitrification in bench-scale sequencing batch reactors. *Water Research*, *30*(2), 277–284. https://doi.org/10.1016/0043-1354(95)00174-3

Nielsen, P. H., McIlroy, S. J., Albertsen, M., & Nierychlo, M. (2019). Re-evaluating the microbiology of the enhanced biological phosphorus removal process. *Current Opinion in Biotechnology*, *57*(Figure 1), 111–118. https://doi.org/10.1016/j.copbio.2019.03.008

Oehmen, A., Carvalho, G., Lopez-Vazquez, C. M., van Loosdrecht, M. C. M., & Reis, M. A. M. (2010). Incorporating microbial ecology into the metabolic modelling of polyphosphate accumulating organisms and glycogen accumulating organisms. *Water Research*, *44*(17), 4992–5004. https://doi.org/10.1016/j.watres.2010.06.071

Oehmen, A., Carvalho, G., Freitas, F., & Reis, M. A. M. (2010). Assessing the abundance and activity of denitrifying polyphosphate accumulating organisms through molecular and chemical techniques. *Water Science and Technology*, *61*(8), 2061–2068. https://doi.org/10.2166/wst.2010.976

Plunkett, R. L., & Gemmill, C. L. (1951). The kinetics of invertase action. *The Bulletin of Mathematical Biophysics*, *13*(4), 303–312. https://doi.org/10.1007/BF02477924

Pochana, K., & Keller, J. (1999). Study of Factors Affecting Simultaneous Nitrification and Denitrification (SND). *Water Science and Technology*, *39*(6), 61–68.

Poot, V., Hoekstra, M., Geleijnse, M. A. A., van Loosdrecht, M. C. M., & Pérez, J. (2016). Effects of the residual ammonium concentration on NOB repression during partial nitritation with granular sludge. *Water Research*, *106*, 518–530. https://doi.org/10.1016/j.watres.2016.10.028

Pronk, M., de Kreuk, M. K., de Bruin, B., Kamminga, P., Kleerebezem, R., & van Loosdrecht, M. C. M. (2015). Full scale performance of the aerobic granular sludge process for sewage treatment. *Water Research*, *84*, 207–217. https://doi.org/10.1016/j.watres.2015.07.011

Qian, F., Wang, J., Shen, Y., Wang, Y., Wang, S., & Chen, X. (2017). Achieving high performance completely autotrophic nitrogen removal in a continuous granular sludge reactor. *Biochemical Engineering Journal*, *118*, 97–104. https://doi.org/10.1016/j.bej.2016.11.017

Reino, C., Suárez-Ojeda, M. E., Pérez, J., & Carrera, J. (2016). Kinetic and microbiological characterization of aerobic granules performing partial nitritation of a low-strength wastewater at 10 °C. *Water Research*, *101*, 147–156. https://doi.org/10.1016/j.watres.2016.05.059

Rubio-Rincón, F. J., Lopez-Vazquez, C. M., Welles, L., van Loosdrecht, M. C. M., & Brdjanovic, D. (2017). Cooperation between Candidatus Competibacter and Candidatus Accumulibacter clade I, in denitrification and phosphate removal processes. *Water Research*, *120*, 156–164. https://doi.org/10.1016/j.watres.2017.05.001

Saad, S. A., Welles, L., Abbas, B., Lopez-Vazquez, C. M., van Loosdrecht, M. C. M., & Brdjanovic, D. (2016). Denitrification of nitrate and nitrite by 'Candidatus Accumulibacter phosphatis' clade IC. *Water Research*, *105*, 97–109. https://doi.org/10.1016/j.watres.2016.08.061

Sajjad, M., Kim, I. S., & Kim, K. S. (2016). Development of a novel process to mitigate membrane fouling in a continuous sludge system by seeding aerobic granules at pilot plant. *Journal of Membrane Science*, *497*, 90–98. https://doi.org/10.1016/j.memsci.2015.09.021

Smolders, G. J. F., van Loosdretch, M. C. M., & Heijnen, J. J. (1995). *bio P model-smolders 1995.pdf* (pp. 79–93). pp. 79–93. Water Science Technology.

Smolders, G. J. F., van der Meij, J., van Loosdrecht, M. C. M., & Heijnen, J. J. (1994). Stoichiometric model of the aerobic metabolism of the biological phosphorus removal process. *Biotechnology and Bioengineering*, *44*(7), 837–848. https://doi.org/10.1002/bit.260440709

Stokholm-Bjerregaard, M., McIlroy, S. J., Nierychlo, M., Karst, S. M., Albertsen, M., & Nielsen, P. H. (2017). A critical assessment of the microorganisms proposed to be important to enhanced biological phosphorus removal in full-scale wastewater treatment systems. *Frontiers in Microbiology*, *8*(APR), 1–18. https://doi.org/10.3389/fmicb.2017.00718

Sun, Y., Angelotti, B., & Wang, Z. W. (2019). Continuous-flow aerobic granulation in plug-flow bioreactors fed with real domestic wastewater. *Science of the Total Environment*, *688*, 762–770. https://doi.org/10.1016/j.scitotenv.2019.06.291

WANG, J., PENG, Y., WANG, S., & GAO, Y. (2008). Nitrogen Removal by Simultaneous Nitrification and Denitrification via Nitrite in a Sequence Hybrid Biological Reactor. *Chinese Journal of Chemical Engineering*, *16*(5), 778–784. https://doi.org/10.1016/S1004-9541(08)60155-X

Wang, X., Chen, Z., Shen, J., Zhao, X., & Kang, J. (2019). Impact of carbon to nitrogen ratio on the performance of aerobic granular reactor and microbial population dynamics during aerobic sludge granulation. *Bioresource Technology*, *271*(September 2018), 258–265. https://doi.org/10.1016/j.biortech.2018.09.119

Wastewater, M., & District, R. (2017). *Weftec 2017*. *40*(4), 129–140. https://doi.org/https://doi.org/10.2175/193864717822156785

Wei, S., David Stensel, H., Quoc, B. N., Lee, P. H., Huang, X., & Winkler, M. K. H. (2019). What's in your sludge? Hunting for baby granules in full-scale activated sludge treatment plants. *WEFTEC 2019 - 92nd Annual Water Environment Federation's Technical Exhibition and Conference*, (2016), 1318–1323.

Weissbrodt, D. G., Neu, T. R., Kuhlicke, U., Rappaz, Y., & Holliger, C. (2013). Assessment of bacterial and structural dynamics in aerobic granular biofilms. *Frontiers in Microbiology*, *4*(JUL), 1–18. https://doi.org/10.3389/fmicb.2013.00175

Winkler, M. K. H., Bassin, J. P., Kleerebezem, R., de Bruin, L. M. M., van den Brand, T. P. H., & Van Loosdrecht, M. C. M. (2011). Selective sludge removal in a segregated aerobic granular biomass system as a strategy to control PAO-GAO competition at high temperatures. *Water Research*, *45*(11), 3291–3299. https://doi.org/10.1016/j.watres.2011.03.024

Winkler, M. K. H., Le, Q. H., & Volcke, E. I. P. (2015). Influence of Partial Denitrification and Mixotrophic Growth of NOB on Microbial Distribution in Aerobic Granular Sludge. *Environmental Science and Technology*, *49*(18), 11003–11010. https://doi.org/10.1021/acs.est.5b01952

Winkler, M. K. H., Meunier, C., Henriet, O., Mahillon, J., Suárez-Ojeda, M. E., Del Moro, G., … Weissbrodt, D. G. (2018). An integrative review of granular sludge for the biological removal of nutrients and recalcitrant organic matter from wastewater. *Chemical Engineering Journal*, *336*(December 2017), 489–502. https://doi.org/10.1016/j.cej.2017.12.026

Yuan, X., & Gao, D. (2010). Effect of dissolved oxygen on nitrogen removal and process control in aerobic granular sludge reactor. *Journal of Hazardous Materials*, *178*(1–3), 1041–1045. https://doi.org/10.1016/j.jhazmat.2010.02.045

Yulianto, A., Soewondo, P., Handajani, M., & Ariesyady, H. D. (2017). Preliminary study on aerobic granular biomass formation with aerobic continuous flow reactor. *AIP Conference Proceedings*, *1823*(March 2017). https://doi.org/10.1063/1.4978186

Zeng, R. J., Yuan, Z., & Keller, J. (2003). Enrichment of denitrifying glycogen-accumulating organisms in anaerobic/anoxic activated sludge system. *Biotechnology and Bioengineering*, *81*(4), 397–404. https://doi.org/10.1002/bit.10484

Zhang, Z., Yu, Z., Dong, J., Wang, Z., Ma, K., Xu, X., … Zhu, L. (2018). Stability of aerobic granular sludge under condition of low influent C/N ratio: Correlation of sludge property and functional microorganism. *Bioresource Technology*, *270*(866), 391–399. https://doi.org/10.1016/j.biortech.2018.09.045

Zhao, H. W., Mavinic, D. S., Oldham, W. K., & Koch, F. A. (1999). Controlling factors for simultaneous nitrification and denitrification in a two-stage intermittent aeration process treating domestic sewage. *Water Research*, *33*(4), 961–970. https://doi.org/10.1016/S0043-1354(98)00292-9

Zhou, D., Niu, S., Xiong, Y., Yang, Y., & Dong, S. (2014). Microbial selection pressure is not a prerequisite for granulation: Dynamic granulation and microbial community study in a complete mixing bioreactor. *Bioresource Technology*, *161*, 102–108. https://doi.org/10.1016/j.biortech.2014.03.001

Zou, J., Tao, Y., Li, J., Wu, S., & Ni, Y. (2018). Cultivating aerobic granular sludge in a developed continuous-flow reactor with two-zone sedimentation tank treating real and low-strength wastewater. *Bioresource Technology*, *247*(September 2017), 776–783. https://doi.org/10.1016/j.biortech.2017.09.088

Appendix A: Supplemental Pilot Facility Fabrication Information

Sidestream Sequencing Batch Reactor Pilot

- To ensure mechanical stability, the reactor tube was mounted to a stainless-steel pedestal with a PVC flange. Additionally, a Unistrut™ frame was built with two crossbars, one just above 4 ft and one just below 8 ft, to further stabilize the reactor.
- The stability of the end of the COD feed line was ensured by three stainless steel supports, which connected to a torus laid against the reactor bottom, around the diffuser (Figure 3-2).

Mainstream Continuous Flow Pilot

- The stainless-steel biological reactors were manufactured by KC employees from ASTM A312 type 316L, schedule 10s pipe.
- The granule/floc separator and upflow feed nozzle was designed and manufactured by Ovivo.
- The secondary clarifier was constructed by KC employees using a polyethylene plastic easy-drain tank from McMaster-Carr® and a custom fabricated metal frame using the McMaster-Carr tank stand as a base.

Aerobic Reactor

- The bottom of the pipe was rounded into a dome, consistent with the anaerobic and anoxic reactors.
- The four support legs and the top edge were constructed using 3-in x 3-in x ¼-in stainless-steel L-channel. Small 6-in square base plates were welded onto the bottom of

the support legs to create a stable platform for the reactor. Including the support legs, the reactor stood at a total height of 9 ft and ¼ in.

- The two fine bubble diffusers were attached together using two Unitstrut™ channels (Figure 3-6). The two diffusers were separated by about 6 in and lowered down into the center of the aeration tank for installation. The diffuser array was heavy enough to remain in position without additional securing methods.

Hydraulic Upflow Separator

- The first launder design was made using acrylic and was secured to the top of the separator by a flange which was attached to the separator body and supported with several triangular acrylic members. A rubber gasket was sandwiched between the launder flange and the flanged top of the separator. To keep the two sandwiched together, twelve holes for ½-in bolts were evenly distributed across the circumference, these were filled in by eight ½-in bolts and four sections of all thread. The four all thread bars secured the top of the launder flange to the steel base, keeping the gasket in compression, and ensuring the launder's stability. While the additional eight bolts functioned to keep the gasket and flanges sandwiched together.
- The influent diffuser was designed by Ovivo and 3D printed out of plastic.

Secondary Clarifier

- To modify the tank base to support the necessary equipment, four 6.5-ft sections of stainless-steel angle channel were attached to the corners of the base. These angle

channel sections became the mounting points for the Unistrut™ frame which supported the scraper, scraper motor, and the feed well.

- The scraper was made from 11-gauge stainless-steel sheet with openings in the center to avoid over torqueing the motor, while still providing mixing, ¼ in from the bottom, to move the settled sludge. The scraper motor at the top was connected to a ½-in diameter stainless-steel drive shaft.
- Four 0.5-inch-wide by 1.5-inch-tall rectangular slots were cut into the 6-inch PVC cap, separated by 90°. These rectangular slots were centered on the liquid level and directed the flow evenly into the clarifier. A second set of four rectangular slots, 0.5-inch-wide by 1-inch-tall, were cut into the 12-inch PVC pipe to prevent scum buildup. These slots were offset from the first set by 45°, to limit short-circuiting. The rectangular slots in the 12-inch pipe were cut so that the bottom of the slots would be at the liquid level.

Appendix B: West Point Treatment Plant Primary Effluent Data

Date	PE NH_3, mg/L	PE TKN, mg/L
7/29/2018	36.5	53.6
8/12/2018	38.1	55.3
8/19/2018	36.4	53.5
8/26/2018	38.7	54.8
9/3/2018	39.2	50.8
9/9/2018	34.6	51.4
9/16/2018	25.3	40.3
9/23/2018	40.5	56.3
9/30/2018	39.4	54.1
10/7/2018	38.2	60
10/14/2018	38.7	58.1
10/21/2018	39.1	60.2
10/28/2018	13.3	24.1
11/4/2018	29.3	44.8

11/12/2018	38.7	57.7
11/25/2018	32.1	48.2
12/2/2018	21.7	32.2
12/9/2018	26.4	38
12/30/2018	13.4	20.8
1/6/2019	15.4	24.7
1/20/2019	29.2	44.1
1/27/2019	30.9	42.9
2/4/2019	29.5	42.3
2/11/2019	28.8	40.4
2/18/2019	17.4	26.8
2/25/2019	27.4	38.8
3/4/2019	34.1	44.8
3/11/2019	32.5	47
3/18/2019	29.3	41.9
3/25/2019	33.5	44.6
4/1/2019	35.3	45.4
4/8/2019	34	47.2
4/15/2019	32.7	44.9
4/29/2019	35.2	47.7
5/6/2019	37.3	49.9
5/13/2019	37	52.9
5/28/2019	33.2	48.3
6/3/2019	35.3	51.1
6/10/2019	33.8	51.9
6/17/2019	34	50.9
6/24/2019	36.9	49.3
7/8/2019	28.1	41.4
7/15/2019	32.2	46.6
7/22/2019	41.8	59.6
7/29/2019	39	53.1
8/5/2019	37.7	52.7
8/12/2019	39.2	53.1
8/19/2019	36.9	52.6
8/26/2019	30.2	50
9/9/2019	34.3	49.8
9/16/2019	32.9	46.1
9/23/2019	25.6	42.1
9/30/2019	34.1	51.3
10/7/2019	39	54.4
10/14/2019	38.5	55.7
10/21/2019	25.6	37.3
10/28/2019	37.2	53

11/4/2019	38.3	54.8
11/12/2019	29.3	44.7
11/18/2019	26.2	34.8
12/2/2019	36.7	55.9
12/9/2019	36.1	52.8
12/16/2019	30.9	43.7
1/6/2020	19.9	28.4
1/13/2020	22.1	33.1
1/27/2020	15.4	23.3
2/3/2020	14.6	27
2/10/2020	15.4	26.2
2/24/2020	24.7	34.2
3/2/2020	25.6	40.1